

IN-02  
49059  
P-86

# Airfoil Modification Effects on Subsonic and Transonic Pressure Distributions and Performance for the EA-6B Airplane

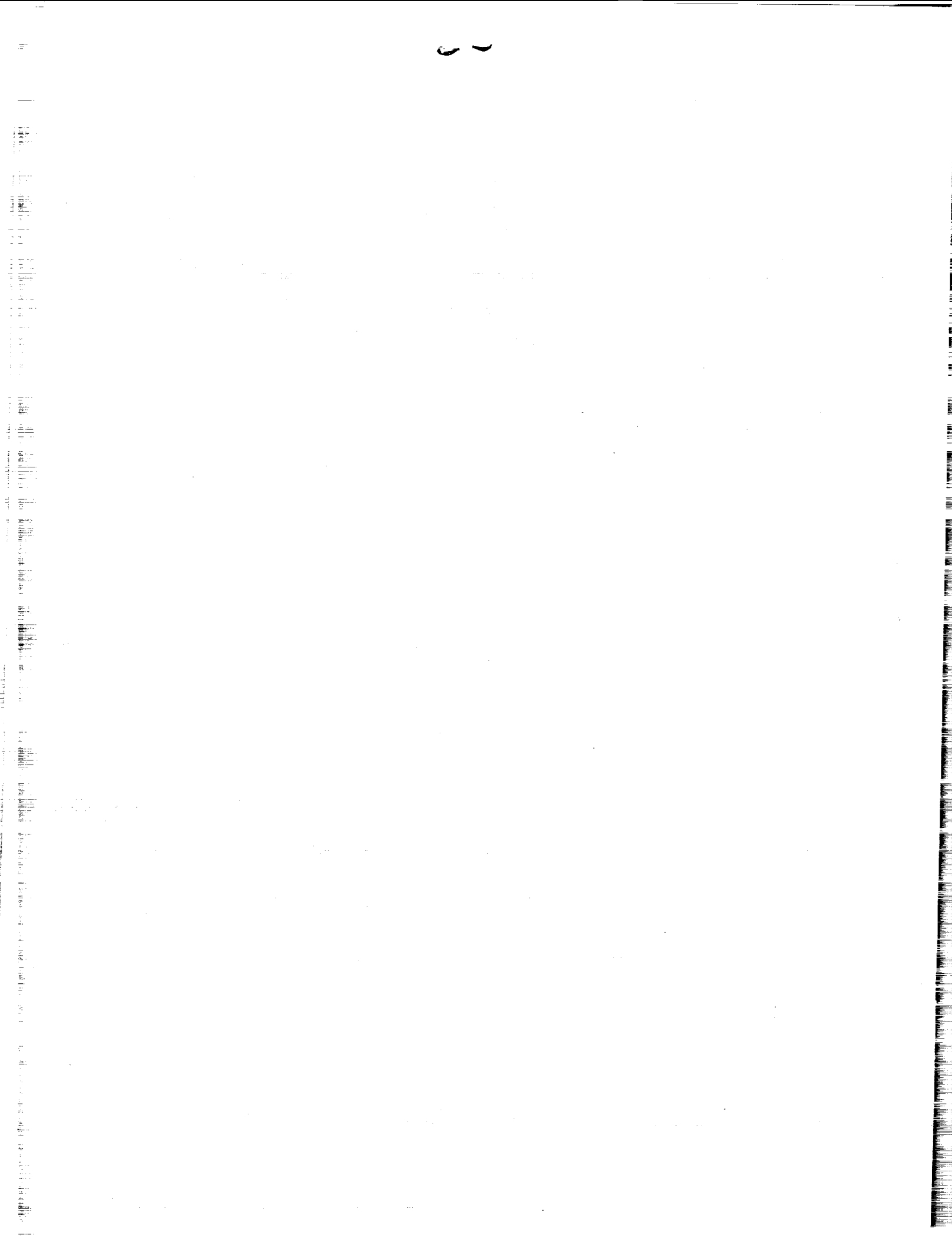
*Dennis O. Allison and William G. Sewall*

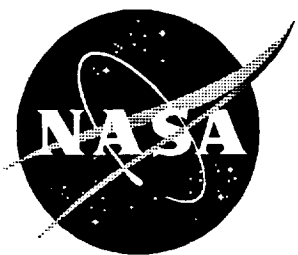
(NASA-TP-3516) AIRFOIL  
MODIFICATION EFFECTS ON SUBSONIC  
AND TRANSONIC PRESSURE  
DISTRIBUTIONS AND PERFORMANCE FOR  
THE EA-6B AIRPLANE (NASA, Langley  
Research Center) 86 p

N95-26382

Unclassified

H1/02 0049059





# Airfoil Modification Effects on Subsonic and Transonic Pressure Distributions and Performance for the EA-6B Airplane

---

*Dennis O. Allison and William G. Sewall  
Langley Research Center • Hampton, Virginia*

---

National Aeronautics and Space Administration  
Langley Research Center • Hampton, Virginia 23681-0001

---

May 1995

Available electronically at the following URL address: <http://techreports.larc.nasa.gov/ltrs/ltrs.html>

Printed copies available from the following:

NASA Center for AeroSpace Information  
800 Elkridge Landing Road  
Linthicum Heights, MD 21090-2934  
(301) 621-0390

National Technical Information Service (NTIS)  
5285 Port Royal Road  
Springfield, VA 22161-2171  
(703) 487-4650

## **Contents**

Summary . . . . .	1
Introduction . . . . .	1
Symbols . . . . .	2
Model and Procedure . . . . .	2
Wind Tunnel . . . . .	2
Wing Fuselage and Modifications . . . . .	3
Instrumentation . . . . .	3
Test Conditions . . . . .	3
Data Reduction . . . . .	4
Presentation of Data . . . . .	4
Results and Discussion . . . . .	4
Subsonic Performance . . . . .	4
Attached flow . . . . .	5
Onset of trailing-edge separation . . . . .	5
Established trailing-edge separation . . . . .	7
Transonic Performance . . . . .	7
Cruise . . . . .	8
Low-altitude cruise . . . . .	8
Climb and maneuver . . . . .	8
Conclusions . . . . .	9
References . . . . .	9
Tables . . . . .	11
Figures . . . . .	37



## Summary

Longitudinal characteristics and wing-section pressure distributions are compared for the EA-6B airplane with and without airfoil modifications. The airfoil modifications were designed to increase low-speed maximum lift for maneuvering, while having a minimal effect on transonic performance. Section contour changes were confined to the leading-edge slat and trailing-edge flap regions of the wing. Experimental data are analyzed from tests in the Langley 16-Foot Transonic Tunnel on a wing-fuselage model with the slats and flaps in their retracted positions. Stall characteristics are discussed for the baseline and modified-wing configurations. Wing modification effects on subsonic and transonic performance are seen in wing-section pressure distributions of various configurations at similar lift coefficients. The modified-wing configurations produced maximum lift coefficients which exceeded those of the baseline configuration at low-speed subsonic Mach numbers (0.300 and 0.400). This benefit was related to the pressurized aft region of the lower surface, the behavior of the wing upper surface leading-edge suction peak, and the behavior of the trailing-edge pressure. At transonic Mach numbers (0.725 to 0.900), the wing modifications produced a somewhat stronger nose-down pitching moment, a slightly higher drag at low-lift levels, and a lower drag at higher lift levels. These variations were related to changes in the chordwise lift distribution, the lower surface leading-edge suction peak, the upper surface pressure recovery to the trailing edge, and the relative extent of separation from the trailing edge.

## Introduction

The EA-6B is an electronics countermeasures airplane, which evolved from the A-6 attack airplane. The EA-6B airplane has an extended fuselage, a bulged housing atop the vertical tail, and several permanently mounted external pods along the lower surface of the wing. In addition, the EA-6B has 20 percent more sea-level engine thrust than the A-6 airplane, but also operates at a maximum 45 500-lb landing weight compared with a 36 000-lb landing-weight limit for the A-6. With virtually the same wing geometry, the higher wing loading significantly reduces stall margin during maneuver. In particular, several loss-of-control incidents have occurred during low-altitude turning maneuvers with  $2g$  accelerations at speeds near 250 knots (Mach numbers near 0.38).

The NASA Langley Research Center has been involved in a cooperative program with the Navy and Grumman Aerospace Corporation to improve the maneuvering capability of the EA-6B airplane (refs. 1

to 7). This program supported the Navy's plan to incorporate an advanced capability (ADVCAP) into the EA-6B. The ADVCAP version will result in additional electronic weight growth which will further reduce stall margin. One objective of the maneuver improvement program was to improve the low-speed capability of the EA-6B by designing relatively simple wing modifications which would not degrade high-speed cruise performance, particularly at the design point  $M_\infty = 0.800$  and  $C_L = 0.32$  (ref. 3). Modifications were defined which significantly increased maximum lift at low speeds with minimal impact on transonic performance. To avoid major modifications to the main wing structure, these wing modifications were constrained to changes of the leading-edge slat and trailing-edge flap regions of the wing. This effort focused on computational design and experimental verification of the wing-section (airfoil) modifications. Two- and three-dimensional low-speed and transonic computational techniques were used during the design effort. The modifications were evaluated experimentally during extensive airfoil (two-dimensional) and wing-fuselage (three-dimensional) testing in several NASA Langley wind tunnels. The airfoil testing (ref. 2) was performed in the Langley Low-Turbulence Pressure Tunnel and the Langley 6- × 28-Inch Transonic Tunnel. The wing-fuselage testing was performed in the Langley 7- × 10-Foot High-Speed Tunnel and the National Transonic Facility (refs. 3 and 6), and subsequently, in the Langley 16-Foot Transonic Tunnel (16-Foot TT); see reference 8. Model forces and moments were measured in all five tunnels. Airfoil pressure measurements were made in the Langley 6- × 28-Inch Transonic Tunnel (ref. 2), and wing pressure measurements were made in the 16-Foot TT. (Ref. 8 reported only the force and moment data.)

This report presents selected data from the 16-Foot TT test for the wing-fuselage configurations with stores, tail, and external antennas removed and the baseline and modified slats and flaps retracted. Testing these simplified configurations could help validate the computer codes used to predict the performance increments of the wing-section modifications. Data are presented for free-stream Mach numbers of 0.300, 0.400, and 0.725 to 0.900. Wing pressure distributions are included as an aid in understanding the wing-section modification effects on subsonic and transonic lift, pitching moment, and drag coefficients for the EA-6B airplane. Results include detailed comparisons between baseline-wing and modified-wing pressure distributions at similar lift coefficients.

## Symbols

Force and moment data are presented in this paper in coefficient form. Longitudinal aerodynamic characteristics are referred to the stability axis system. Moments are referenced to the quarter chord of the mean aerodynamic chord. The symbols are defined as follows:

$AR$	aspect ratio, 5.31	$y$	spanwise distance from model symmetry plane, ft
$b$	wing span, 6.24 ft	$z$	local vertical distance from WL that bisects trailing edge of baseline airfoil, positive upward, ft
$C_D$	wing-fuselage drag coefficient, $\frac{\text{Drag}}{q_\infty S}$	$\alpha$	angle of attack between free-stream velocity and WL = 0.98 in model symmetry plane, deg
$C_L$	wing-fuselage lift coefficient, $\frac{\text{Lift}}{q_\infty S}$	$\eta$	semispan location, $\frac{2y}{b}$ (fig. 2(a))
$C_{L,\max}$	wing-fuselage maximum lift coefficient, $\frac{\text{Maximum lift}}{q_\infty S}$	$\Gamma$	dihedral angle between plane of each wing and WL = 0.98, $-1^\circ$ outboard of $\eta = 0.20$
$C_m$	wing-fuselage pitching-moment coefficient, $\frac{\text{Pitching moment}}{q_\infty S \bar{c}}$	$\rho_\infty$	free-stream air density, slugs/ft <sup>3</sup>
$C_p$	pressure coefficient, $\frac{p - p_\infty}{q_\infty}$	$\Lambda_{c/4}$	nominal quarter-chord sweep angle, $25^\circ$
$C_{p,te}$	trailing-edge pressure coefficient, $\frac{p_{te} - p_\infty}{q_\infty}$	$\Lambda_{le}$	nominal leading-edge sweep angle, $30^\circ$
$c$	local streamwise chord, ft	$\Lambda_{te}$	nominal trailing-edge sweep angle, $10^\circ$
$\bar{c}$	mean aerodynamic chord, 1.28 ft (fig. 2(a))	$\lambda$	taper ratio, 0.31
$g$	acceleration due to gravity ( $1g = 32.2 \text{ ft/sec}^2$ )	$\mu_\infty$	free-stream air viscosity, slugs/ft-sec
$M_\infty$	free-stream Mach number	Subscripts:	
$p$	local pressure, psf	$l$	lower surface
$p_{te}$	trailing-edge pressure, psf	$u$	upper surface
$p_\infty$	free-stream static pressure, psf	Abbreviations:	
$q_\infty$	free-stream dynamic pressure, $\frac{1}{2} \rho_\infty U_\infty^2$ , psf	ADVCAP	advanced capability
$R_{\bar{c}}$	free-stream Reynolds number based on $\bar{c}$ , $\frac{\rho_\infty U_\infty \bar{c}}{\mu_\infty}$	Basln	wing fuselage with baseline trailing edge and baseline leading edge
$S$	wing reference area, 7.32 ft <sup>2</sup> (fig. 2(a))	Fulmod	wing fuselage with trailing-edge and leading-edge modifications
$t$	airfoil thickness, ft	Temod	wing fuselage with trailing-edge modification and baseline leading edge
$U_\infty$	free-stream velocity, ft/sec	$le$	leading edge
$WL$	water line; vertical coordinate of model, ft (fig. 2(b))	$te$	trailing edge
$x$	local chordwise distance from wing leading edge, positive aft, ft		

## Model and Procedure

### Wind Tunnel

The test was conducted in the 16-Foot TT (refs. 9 to 11). This facility is a single-return, continuous-flow, atmospheric wind tunnel with continuous air exchange for cooling that has an octagonal test section of 47 ft with axial slots at the wall vertices and a throat cross-sectional area of  $199.15 \text{ ft}^2$ . The width of the eight slots near the model is about 3.7 percent of the test section perimeter. The wall divergence in the test section is adjusted as a function of the airstream

dew point and Mach number to minimize any longitudinal static pressure gradients. The free-stream Mach number is continuously variable to a maximum of 1.3 with an accuracy of  $\pm 0.005$ . The tunnel sting support system pivots so that the model remains on or near the centerline throughout the angle-of-attack range.

### Wing Fuselage and Modifications

The test was conducted using a sting-mounted 1/8.5-scale wing-fuselage (no tails) model with flow-through inlets. (See photographs in fig. 1.) For the present investigation, airfoil modification effects were measured with no control surface deflections or deployments. The model wing had interchangeable parts for the slat and flap regions.

Figure 2 shows details of the EA-6B wing-fuselage arrangement. The planform sketch in figure 2(a) shows the locations of the following: leading-edge slats, trailing-edge flaps, and the inboard ( $\eta = 0.28$ ) and outboard ( $\eta = 0.75$ ) airfoil design stations. Four wing stations were instrumented for pressure distribution measurements, two on the right wing ( $\eta = 0.50$  and  $0.82$ ) and two on the left wing ( $\eta = 0.33$  and  $0.67$ ). The trailing-edge pressures were located at  $x/c = 1.00$  and were measured using aft-facing orifices. The wing reference area  $S = 7.32 \text{ ft}^2$  is the area of the projected wings from the fuselage centerline, where  $c = 1.79 \text{ ft}$ , to the tips, where  $c = 0.56 \text{ ft}$ , as indicated by the dotted lines in figure 2(a). The wings have a dihedral angle of  $-1^\circ$  outboard of  $\eta = 0.20$ . The sketches in figure 2(b) of the fuselage show the inlet and engine cowling shape. The model solid blockage at an angle of attack of  $0^\circ$  was approximately 0.5 percent of the test sectional area, a value typical of full-span models tested in the 16-Foot TT.

Airfoil modifications reshaped the full span of the slat and flap regions. Spanwise discontinuities occur at the ends of the slat ( $\eta = 0.25$  and  $0.93$ ) and flap ( $\eta = 0.18$  and  $0.84$ ). Contour modifications were defined in the streamwise direction at  $\eta = 0.28$  (fig. 2(c)) and  $\eta = 0.75$  (fig. 2(d)), the inboard and outboard design stations. The other station modifications were determined later by interpolation or extrapolation of dimensional airfoil coordinates. The slat extended chordwise to  $x/c = 0.15$  on the upper surface and to  $x/c = 0.05$  on the lower surface, and the flap began at  $x/c = 0.82$  on the upper surface and at  $x/c = 0.70$  on the lower surface. The slat modification consisted of increases in both the leading-edge radius and camber. The slat modification was constrained to match the upper surface curvature of the main wing at the slat trailing edge,  $x/c = 0.15$ . Matching the curvature and contour at

the lower surface slat/wing juncture required adding extra wing thickness behind the slat in the  $x/c = 0.05$  to  $x/c = 0.15$  region. The trailing-edge modification increased the flap camber and thickened the flap base. The flap modification was constrained to match the wing curvature at  $x/c = 0.82$  on the upper surface and  $x/c = 0.70$  on the lower surface. The baseline airfoil coordinates (Basln) and the airfoil coordinates with both the leading-edge and trailing-edge modifications (Fulmod) are given in tables 1 ( $\eta = 0.28$ ) and 2 ( $\eta = 0.75$ ). Runs were also made with only the trailing-edge modification (Temod). The Basln, Temod, and Fulmod configurations correspond respectively to the "bl", "te", and "le and te" configurations in reference 6, where predicted effects were compared with data from the National Transonic Facility.

### Instrumentation

The model aerodynamic force and moment data were measured using an internally mounted six-component strain gauge balance. The balance had the following component load capacities:

Component	Capacity
Normal force, lb . . . . .	$\pm 6\,500$
Axial force, lb . . . . .	$\pm 700$
Side force, lb . . . . .	$\pm 4\,000$
Pitching moment, in-lb . . . . .	$\pm 13\,000$
Rolling moment, in-lb . . . . .	$\pm 9\,000$
Yawing moment, in-lb . . . . .	$\pm 6\,500$

An accelerometer mounted in the model nose measured angle of attack. Electrical strain gauge transducers measured sting cavity pressures which were used to correct the force coefficients for the difference between the cavity static pressure and the free-stream static pressure. Electronically scanning pressure devices measured model surface pressures. All instruments were calibrated to an accuracy of at least  $\pm 0.5$  percent of their maximum load.

### Test Conditions

The wing-fuselage configurations were tested at Mach numbers of 0.300, 0.400, 0.725, 0.800, 0.850, and 0.900 at angles of attack between  $0^\circ$  and  $20^\circ$  at  $0^\circ$  yaw. Free-stream Reynolds numbers based on mean aerodynamic chord for the subsonic conditions of  $M_\infty = 0.300$  and  $0.400$  were  $R_c = 2.4 \times 10^6$  and  $3.1 \times 10^6$ , respectively, and for the transonic conditions of  $M_\infty = 0.725$  to  $0.900$  they were

$R_c = 4.3 \times 10^6$  to  $5.0 \times 10^6$ . Boundary-layer transition was fixed with 0.10-in.-wide strips of No. 120 Carborundum on the wing and fuselage. Fuselage transition was fixed at 1.00 in. aft of both the nose tip and the inlet leading edge (inside and outside). Wing transition was fixed 0.60 in. aft of the leading edge in the streamwise direction on both surfaces. The location of 0.60 in. aft of the leading edge corresponds to approximately 4 to 6 percent of the local chord in the region where the pressure distributions were measured ( $\eta = 0.33$  to 0.82).

### Data Reduction

All data were recorded simultaneously on magnetic tape with 50 frames of data comprising each data point; average values were used in computations. The model angle of attack was corrected for tunnel upflow. Angle of attack was defined as the angle between the free-stream velocity and  $WL = 0.98$  in the model symmetry plane. Sting cavity pressures were used to correct the longitudinal balance components for pressure forces in the sting cavity. No corrections were made to balance and pressure data for test section wall interference effects. A more complete description of the data reduction procedure is presented in reference 11.

### Presentation of Data

Three configurations were tested to determine the effects of airfoil section modifications: a baseline configuration (Basln), a configuration with a wing trailing-edge modification (Temod), and a configuration with a wing leading-edge modification in addition to the Temod trailing-edge modification (Fulmod). Selected wing chordwise pressure distributions and variations of the trailing-edge pressure coefficient with  $\alpha$  are given at four spanwise wing stations:  $\eta = 0.33$  and 0.67 on the left wing and  $\eta = 0.50$  and 0.82 on the right wing (fig. 2(a)). Asymmetric flow occurred at stall onset when one wing stalled at a lower angle of attack than the other. Because the wing-pressure distributions used in analyzing the force data combined pressures from both wings (i.e., assumed symmetric flow), pressure distributions for these asymmetric flow cases were not selected for presentation.

The data are presented in both tabulated and plotted form. For  $M_\infty = 0.300$  to 0.900, longitudinal characteristics and wing trailing-edge pressure coefficients are presented in tables 3 to 8, and wing pressure distributions are shown in tables 9 to 26. The low-speed subsonic data ( $M_\infty = 0.300$  and 0.400) and the transonic data ( $M_\infty = 0.725$  to 0.900) are presented in the figures as follows:

Figure	Data type	$M_\infty$	Conditions
Subsonic data			
3	Force	0.300	
4	Force	.400	
5	Pressure	.300	$\alpha = 8.1^\circ$
6	Pressure	.400	$\alpha = 8.1^\circ$
7	Pressure	.300	$C_L \approx 0.87$
8	Pressure	.400	$C_L \approx 0.87$
9	Pressure	.300	$C_L \approx 0.91$
10	Pressure	.400	$C_L \approx 0.91$
11	Pressure	.300	$\alpha = 15.1^\circ$
12	Pressure	.400	$\alpha = 15.1^\circ$
13	te pressure	.300	
14	te pressure	.400	
Transonic data			
15	Force	0.725	
16	Force	.800	
17	Force	.850	
18	Force	.900	
19	Drag	Varying	$C_L = 0.10$
20	Pressure (design)	.800	$C_L \approx 0.32$
21	Pressure	.725	$C_L \approx 0.20$
22	Pressure	.800	$C_L \approx 0.20$
23	Pressure	.850	$C_L \approx 0.10$
24	Pressure	.900	$C_L \approx 0.10$
25	Pressure	.725	$C_L \approx 0.70$
26	Pressure	.800	$C_L \approx 0.70$
27	Pressure	.850	$C_L \approx 0.40$
28	Pressure	.900	$C_L \approx 0.40$
29	Pressure	.725	$C_L \approx 0.80$
30	Pressure	.800	$C_L \approx 0.80$
31	Pressure	.850	$C_L \approx 0.70$
32	Pressure	.900	$C_L \approx 0.70$
33	te pressure	.725	
34	te pressure	.800	
35	te pressure	.850	
36	te pressure	.900	

### Results and Discussion

#### Subsonic Performance

Low-speed subsonic characteristics of the three configurations are presented in figures 3 to 14 for Mach numbers of 0.300 and 0.400. Longitudinal force and moment characteristics are shown in figures 3 and 4, chordwise pressure distributions in figures 5 to 12, and trailing-edge pressure coefficients as a function of angle of attack in figures 13 and 14. The primary impetus of this investigation was to improve low-speed, high-lift performance, particularly at maneuvering flight accelerations of 2g to 2.5g at speeds

near 250 knots ( $M_{\infty} \approx 0.38$ ). These conditions correspond to lift coefficients between 0.75 and 1.05 for the EA-6B airplane. The maximum lift coefficients for the three configurations fell within this range (figs. 3(a) and 4(a)).

**Attached flow.** Wing modification effects on longitudinal characteristics can be determined by comparing the results for the three configurations at a constant angle of attack (figs. 3 and 4). (Note that  $C_L$  versus  $\alpha$  curves have been truncated below  $\alpha = 4^\circ$  in figs. 3(a) and 4(a).) At a constant angle of attack, the Temod and Fulmod configurations have higher lift coefficients and more negative pitching-moment coefficients than the Basln configuration. The additional camber afforded by both the leading-edge and trailing-edge modifications contributes to these increments in lift coefficient and pitching-moment coefficient. Comparison of these increments for the Temod and Fulmod configurations indicates that the main cause of the lift and pitching-moment increments is the trailing-edge modification. At constant lift coefficients of 0.6 and above, the Temod and Fulmod configurations clearly have lower drag coefficients than the Basln configuration (figs. 3(b) and 4(b)). (For a constant lift coefficient, the drag coefficient differences include not only increments caused by the wing modifications, but also wing and fuselage drag increments associated with the resulting differences in angle of attack.) Above  $C_L = 0.7$  ( $\alpha \approx 8^\circ$ ), the Fulmod configuration has lower drag coefficients than the Temod configuration.

The effects of leading-edge and trailing-edge wing modifications can be understood better by analyzing wing pressure-coefficient distributions. Wing chordwise pressure-coefficient distributions at four span stations for  $\alpha = 8.1^\circ$  are presented in figures 5 and 6. The dominant effect of the trailing-edge modification is the more positive pressure coefficients for the lower surface between  $x/c = 0.8$  and 1.0 and results in an aft loading that contributes to the increments in lift, nose-down pitching moment, and drag. (The drag increment caused by the aft region of the lower surface results from higher viscous drag and higher pressure drag caused by the adverse pressure gradient, which both thickens the boundary layer and produces more positive pressure coefficients in this region, which is mostly forward facing at  $\alpha = 8.1^\circ$ .)

The leading-edge modification effects are less discernible because of the scarcity of pressure instrumentation where large pressure gradients occur in the upper surface leading-edge region. The leading-edge suction peak covers approximately the forward 20 percent of the chord. Any differences between the Temod and Basln configurations would indicate that

the trailing-edge modification can affect the leading-edge suction peak by increasing the wing circulation. More negative upper surface pressures would contribute to greater lift but to a more adverse pressure gradient, which would promote boundary-layer thickening and higher viscous drag. At  $\alpha = 8.1^\circ$  there is evidently little difference in the leading-edge portion of the pressure distributions of the three configurations, and the Temod and Fulmod configurations have nearly the same lift and pitching-moment coefficients, and relatively the same drag coefficient.

**Onset of trailing-edge separation.** For the three configurations,  $C_L = 0.87$  corresponds to pre-stall conditions with some trailing-edge boundary-layer separation, as shown by the local reductions in the lift-curve slopes from those at lower angles of attack. Trailing-edge pressure coefficients provide an indication of the onset and relative extent of trailing-edge boundary-layer separation as a function of angle of attack (figs. 13 and 14). (Curves for  $C_L$  as a function of  $\alpha$  are repeated in figs. 13 and 14 for easy reference.) Each  $C_{p,te}$  curve has a relatively low-gradient region at lower angles of attack. (See, for example,  $\alpha = 4^\circ$  to  $\alpha \approx 10^\circ$  at  $\eta = 0.33$  for Temod in fig. 13.) At higher angles of attack, each curve has a significantly stronger gradient (toward more negative pressure coefficients). The stronger gradient beginning indicates the onset of significant trailing-edge separation. The extent of separation increases as the trailing-edge pressure becomes more negative with increasing  $\alpha$ .

Whereas comparisons at a constant angle of attack directly show the wing modification effects, comparisons at a constant lift coefficient give the differences between configurations (including different angles of attack) that correspond to a given aircraft maneuver at a constant weight and altitude. As occurred for attached flow, at a given value of  $\alpha$  in the range for flow-separation onset, the Temod and Fulmod configurations generate more lift than the Basln configuration, with the Fulmod configuration generating the most lift (figs. 3(a) and 4(a)). Consequently, for both Mach numbers at  $C_L = 0.87$ , the Fulmod configuration has the lowest angle of attack and the Basln configuration has the highest. Similarly, the Fulmod configuration has the lowest drag coefficient and the Basln configuration has the highest (figs. 3(b) and 4(b)). Both the Temod and Fulmod configurations produce a nose-down pitching-moment coefficient increment compared to the Basln configuration. The Fulmod configuration has a slightly more negative pitching-moment coefficient than the Temod configuration has.

Chordwise pressure coefficient distributions for the three configurations at similar lift coefficients of  $C_L \approx 0.87$  are presented in figures 7 and 8. Since test data are not available at constant lift coefficients, corresponding pressure coefficient distribution comparisons are made at similar lift coefficients (within a range of  $\pm 0.02$  in lift coefficient). The pressure coefficient distributions for  $C_L \approx 0.87$  (figs. 7 and 8) have features similar to those at  $\alpha = 8.1^\circ$  (figs. 5 and 6). The dominant features are the aft loading on the lower surface near the trailing edge caused by the trailing-edge modification and the leading-edge suction peak variations on the upper surface caused by the leading-edge modification and angle-of-attack differences corresponding to a constant lift coefficient. (Unfortunately, the  $\pm 0.02$  lift coefficient range results in noticeable leading-edge suction peak variations also.) Comparing pressure coefficient distributions in figures 5 to 8 shows that the leading-edge suction peak generally becomes higher (has a more negative peak value) and is followed by a more adverse pressure gradient as angle of attack increases, eventually collapsing after trailing-edge separation develops. (See, for example, the lower leading-edge suction peak at  $\alpha = 11.1^\circ$  for the Temod configuration at  $\eta = 0.67$  in fig. 7 compared with the more negative peak at  $\alpha = 8.1^\circ$  in fig. 5.) Trailing-edge separation results in more negative trailing-edge pressure coefficients.

The leading-edge modification has both outboard leading-edge droop to delay outboard separation (for aileron effectiveness) and increased leading-edge radius to lower inboard suction peaks. The lower inboard peaks delay separation and thereby increase the maximum lift potential. At the inboard stations ( $\eta = 0.33$  and  $\eta = 0.50$ ), the Temod and Basln configurations have high leading-edge suction peaks (figs. 7 and 8), whereas the Fulmod configuration appears to have lower peaks. At the outboard station  $\eta = 0.67$ , the Fulmod configuration has the highest suction peak, especially at  $M_\infty = 0.300$ . The leading-edge suction peak of the Fulmod configuration has not yet collapsed, and trailing-edge separation has not yet occurred because of the increased leading-edge camber and lower angle of attack. At  $\eta = 0.82$ , the leading-edge modification again has the highest suction peak and usually eliminates the outboard stall at  $M_\infty = 0.300$ ; however, the suction peak collapses and separation is apparently not reduced at  $M_\infty = 0.400$ . The Basln configuration at  $M_\infty = 0.300$  and 0.400 and the Temod configuration at  $M_\infty = 0.400$  redevelop leading-edge suction peaks (under the assumption that the right and left wings have symmetric flow; recall that the  $\eta = 0.67$  and  $\eta = 0.82$  orifice

rows are on opposite wings). These suction peaks are a three-dimensional effect probably caused by less induced upwash being generated by the portions of the wing inboard of  $\eta = 0.82$ . Pressure distributions at station  $\eta = 0.67$  show that the Basln and Temod configurations have more flow separation than the Fulmod configuration (e.g., by more negative values of  $C_{p,te}$ ) and therefore have lower lift and circulation than the Fulmod configuration. Thus, the induced upwashes from station  $\eta = 0.67$  for the Basln and Temod configurations are lower than those for the Fulmod configuration. The resulting lower local  $\alpha$ 's at station  $\eta = 0.82$  are reduced enough to preserve the leading-edge suction peaks. All three configurations have significant trailing-edge separation at  $\eta = 0.82$  (fig. 8), as shown by the negative values of  $C_{p,te}$ . Deviations from these trends, seen in comparisons involving the Temod configuration, are probably caused by the poor lift coefficient match between the Temod configuration and the other two configurations, especially at  $M_\infty = 0.400$  (fig. 8). The inboard leading-edge suction peaks for the Fulmod configuration could be much lower than they actually are in order to integrate with the larger outboard peaks to obtain the same lift coefficient; however, the inboard pressures act on a larger wing area, and differences exist in fuselage lift associated with lower Fulmod configuration angles of attack.

Wing-lift distribution changes are also shown in figures 7 and 8. Since comparisons are at a nearly constant lift coefficient and the trailing-edge modification adds aft lift, the Basln configuration should compensate with higher leading-edge suction peaks. This effect should be lessened somewhat by the higher fuselage lift of the Basln configuration with its higher angle of attack. Allowing for the lift coefficient differences for the pressure coefficient distributions of the Temod configuration, the Basln configuration has higher suction peaks at the inboard stations, which account for the majority of the wing planform area. The Fulmod configuration generally has higher suction peaks at the outboard stations because of the leading-edge modification. As in the comparison at  $\alpha = 8.1^\circ$ , the nose-down pitching-moment coefficient increments are mainly caused by the trailing-edge modification. The generally lower leading-edge suction peaks of the Temod and Fulmod configurations also add to this nose-down increment.

The pressure coefficient distributions in figures 7 and 8 show several counteracting effects for drag comparisons between the modified and baseline configurations. As discussed previously, the trailing-edge modification adds drag. At the inboard wing stations  $\eta = 0.33$  and 0.50, the lower leading-edge

suction peaks of the modified configurations, especially the Fulmod configuration, produce higher pressure drag, but their reduced adverse pressure gradients do not thicken the boundary layer as much, and thinner boundary layers produce less drag. At the outboard wing stations  $\eta = 0.67$  and  $0.82$ , the Basln configuration clearly shows severe flow separation compared with the Fulmod configuration (and thus more drag), as shown by the more negative trailing-edge pressure coefficients. In some cases the leading-edge suction peaks are collapsed, indicating major loss in circulation. The Temod configuration has pressure coefficient distributions similar to those of the Basln configuration and thus also has more drag than the Fulmod configuration. Another factor in drag comparisons is the angle of attack. The Basln configuration should have the most fuselage drag because it has the highest angle of attack, and the Fulmod configuration should have the least fuselage drag because it has the lowest angle of attack.

**Established trailing-edge separation.** The lift curves of the three configurations all have a large angle-of-attack range (at least  $5^\circ$ ), over which the lift coefficients are close to  $C_{L,\max}$  (figs. 3 and 4). At these lift coefficients, the configurations have extensive trailing-edge separation (figs. 13 and 14). The maximum lift coefficient for the Basln configuration is approximately  $C_L = 0.91$ . At  $C_L = 0.91$ , performance comparisons between the configurations are similar to those at  $C_L = 0.87$ . Again, the wing modifications result in reduced drag, with the Fulmod configuration having the least drag. Wing-pressure coefficient distributions for  $C_L \approx 0.91$  are presented in figures 9 and 10. The pressure coefficient distribution trends are also similar to those for  $C_L \approx 0.87$ . In general leading-edge suction peaks are collapsed at more spanwise stations and trailing-edge pressure coefficients are more negative, indicating more extensive separation. Poor lift coefficient matches occurred for the Basln configuration at  $M_\infty = 0.300$  and the Temod configuration at  $M_\infty = 0.400$ .

The maximum lift coefficient for the Basln configuration occurred at  $\alpha = 15.1^\circ$  (figs. 3(a) and 4(a)). For both  $M_\infty = 0.300$  and  $M_\infty = 0.400$ , the wing modifications resulted in higher lift coefficients at  $\alpha = 15.1^\circ$ , with the Fulmod configuration having the highest lift coefficients. The overall increase in maximum lift coefficient (the difference between the Fulmod and Basln configurations) was about the same at the two Mach numbers: 0.064 at  $M_\infty = 0.300$ , and 0.061 at  $M_\infty = 0.400$ . However, the increment in lift coefficient caused by the leading-edge modification (the difference between the Fulmod and Temod configurations) was 0.031 at  $M_\infty = 0.300$

and only 0.017 at  $M_\infty = 0.400$ . This trend is consistent with the decrease in benefit with increasing Mach number from the leading-edge modification that was observed earlier in two-dimensional test results. (See ref. 2, fig. 9, where "Mod 2 T.E. with Mod 1 L.E." corresponds to the Fulmod configuration.) The characteristics of the pressure coefficient distributions at  $\alpha = 15.1^\circ$  (figs. 11 and 12) for the three configurations are similar to those at  $C_L \approx 0.91$ , with even more collapsed leading-edge suction peaks and more negative trailing-edge pressure coefficients.

### Transonic Performance

Transonic characteristics of the three configurations are presented in figures 15 to 36 for Mach numbers of 0.725, 0.800, 0.850, and 0.900. Longitudinal force and moment characteristics are shown in figures 15 to 19, chordwise pressure distributions are shown in figures 20 to 32, and trailing-edge pressure coefficients, plotted versus angle of attack are shown in figures 33 to 36. Pressure coefficient distributions for the three configurations (figs. 20 to 32) were compared at similar lift coefficients (within  $\pm 0.02$  of their average, with a  $\pm 0.04$  variation from a nominal value, an undesirably large lift-coefficient band). The primary concern in this speed range was to ensure that the wing modifications (designed to enhance low-speed maximum lift) had a minimum impact on transonic performance.

Wing modifications had similar effects at transonic speeds and at low speeds. The modifications reduced the angle of attack required to achieve a given lift coefficient of  $C_L = 0.8$  or less by amounts between  $0.5^\circ$  and  $2^\circ$  and increased the maximum lift coefficient by about 0.05 (figs. 15(a) to 18(a)). Pitching-moment coefficient increments, as much as 0.063 more negative (nose down), were considered minimal. Drag polars were rotated about lift coefficients which varied from about  $C_L = 0.45$  at  $M_\infty = 0.725$  (fig. 15(b)) to about  $C_L = 0.15$  at  $M_\infty = 0.900$  (fig. 18(b)). At lift coefficients below these crossover points, the Fulmod and Temod configurations had drag coefficient penalties up to 0.004 at a given lift coefficient, compared to the Basln configuration, with the Fulmod configuration having the highest drag. At lift coefficients above these crossover points, the Fulmod and Temod configurations had lower drag coefficients at a given lift coefficient than the Basln configuration. The Fulmod configuration had the lowest drag at Mach numbers above the design cruise  $M_\infty = 0.800$ , and the Temod configuration had the lowest drag at Mach numbers below  $M_\infty = 0.800$ .

**Cruise.** The lift coefficient range for cruise includes the lift coefficients near the drag polar crossover points (figs. 15(b) to 18(b)). At the cruise design point for the EA-6B airplane,  $M_\infty = 0.800$  with  $C_L = 0.32$ , the modifications had a minimal impact on performance (fig. 16). The trailing-edge modification generated added lift on the aft lower wing surface between  $x/c = 0.8$  and  $x/c = 1.0$  (fig. 20). The angle of attack required to achieve the design lift coefficient was reduced by  $0.7^\circ$ , and the pitching-moment coefficient was made 0.027 more negative. The drag coefficient stayed about the same as for the Basln configuration. The upper surface suction peaks for all three configurations extended much farther aft at transonic speeds than at low speeds. (See, for example, figs. 6 and 20.) A larger portion of the less negative Temod configuration suction pressures therefore acted on rearward-facing surfaces. This drag reduction on the forward portion of the wing counteracted the added drag from the flap region and fuselage drag increments (positive or negative) without a change in drag from the Basln configuration. The Fulmod configuration had essentially the same performance as the Temod configuration, indicating that the leading-edge modification had little effect at the cruise design point.

**Low-altitude cruise.** Lift coefficients of  $C_L = 0.20$  at  $M_\infty = 0.725$  and 0.800 and  $C_L = 0.10$  at  $M_\infty = 0.850$  and 0.900 are representative of low-altitude cruise, including the low-level dash regime. Drag coefficient variation with Mach number at  $C_L = 0.10$  (fig. 19) reveals that, for all three configurations, the EA-6B airplane has a drag-divergence Mach number of approximately 0.84 (slope of  $C_D$  versus  $M_\infty$  is 0.1). Consequently, the drag is very sensitive in the dash regime ( $M_\infty > 0.800$ ), especially at  $M_\infty = 0.900$ , where small differences in Mach number cause wiggles in the drag polars (fig. 18(b)). Drag polar comparisons of the three configurations at transonic Mach numbers (figs. 15(b) to 18(b)) indicate that the wing modifications caused drag coefficient penalties up to 0.003. Drag penalties associated with the wing leading-edge modification were larger than those associated with the wing trailing-edge modification.

Some drag penalty sources are revealed in the wing-pressure coefficient distributions (figs. 21 to 24). In addition to the higher pressures in the wing lower surface flap region, both the Fulmod and Temod configurations had higher leading-edge suction peaks from  $\eta = 0.33$  to 0.67 on the wing lower surface than the Basln configuration had. (This assessment is supported by the more detailed measurements in this region for two-dimensional airfoils shown in ref. 2.)

Two reasons are given for these higher leading-edge suction peaks on the lower surface. One is that the lower angle of attack required to match the lift coefficient of the Basln configuration causes the leading-edge stagnation point to move toward the upper surface and results in a stronger expansion on the lower surface. Thus, the Temod configuration (which has the same baseline leading edge) has a stronger lower surface suction peak than the Basln configuration. The other reason for stronger peaks for the Fulmod configuration is its modified leading edge. The increased leading-edge camber and thickness caused the Fulmod configuration to have stronger peaks than the Temod configuration, even though the configurations were at similar angles of attack (figs. 21 to 24).

The wing modifications had counteracting effects on drag at low-lift coefficients ( $C_L = 0.20$  and 0.10). The wing trailing-edge modification produced high pressures which acted on both forward- and rearward-facing surfaces, making little if any net pressure drag increment. Some drag increment occurs because of the thicker boundary layer in that region. For the Temod configuration, the suction peak on the lower surface near the leading edge acted on forward-facing surfaces and exceeded that of the Basln configuration. This stronger peak helped reduce pressure drag for the Temod configuration. For the Fulmod configuration, however, much of this peak occurred on a rearward-facing portion of the leading-edge modification, resulting in the Fulmod configuration having higher pressure drag compared with the Temod configuration. At  $M_\infty = 0.850$  and 0.900, the high suction peaks for the Temod and Fulmod configurations contribute to wave drag by generating supersonic bubbles which, particularly for the Fulmod configuration, are followed by strong shock waves (figs. 23 and 24).

Another source of drag increment can also be attributed to the different flows at the fuselage caused by slightly different angles of attack. All three configurations were probably at angles of attack below that for minimum fuselage drag.

**Climb and maneuver.** Lift coefficients above the crossover points on the drag polars are representative of climb and maneuver where both the Temod and Fulmod configurations have lower drag than the Basln configuration has at a constant lift coefficient. Configuration performance comparisons in this lift-coefficient region are very similar to those at high-lift coefficients at low speeds. Pressure coefficient distributions are presented at two representative lift coefficients at each Mach number in figures 25

to 32. The lower lift coefficients at each Mach number are  $C_L \approx 0.70$  for  $M_\infty = 0.725$  and  $M_\infty = 0.800$  and  $C_L \approx 0.40$  for  $M_\infty = 0.850$  and  $M_\infty = 0.900$ . The higher lift coefficients at each Mach number are  $C_L \approx 0.80$  for  $M_\infty = 0.725$  and  $0.800$  and  $C_L \approx 0.70$  for  $M_\infty = 0.850$  and  $0.900$ .

Wing modification effects on the wing pressure distributions for the lower representative lift coefficients are shown in figures 25 to 28. At  $M_\infty = 0.725$  the baseline airfoil has the most positive pressure recovery from the suction peak to the trailing-edge pressure, resulting in more boundary-layer thickening and more drag (fig. 25). The baseline recovery is also most positive at  $M_\infty = 0.800$  and  $0.850$ , except at  $\eta = 0.67$  (figs. 26 and 27). At  $\eta = 0.67$ , at  $M_\infty = 0.800$  and  $0.850$ , and over most of the wing span at  $M_\infty = 0.900$  (fig. 28), the baseline airfoil has a more forward shock location, indicating that shock-wave-boundary-layer interaction is the primary mechanism for higher drag. This interaction occurs when a shock thickens or separates a boundary layer and usually causes the shock to move forward.

Wing modification effects on the wing-pressure distributions for the higher representative lift coefficients are shown in figures 29 to 32. Trailing-edge pressure coefficient variations with angle of attack (figs. 33 to 36) indicate that boundary-layer separation is generally a stronger drag contributor for the baseline airfoil than for the modified airfoils. Except for  $\eta = 0.33$  at  $M_\infty = 0.725$  (fig. 29), all chordwise pressure coefficient distributions (figs. 29 to 32) show that the Basln configuration has a negative trailing-edge pressure coefficient and a larger extent of trailing-edge separation than the modified configurations. The trailing-edge pressure coefficient plots (fig. 33) also indicate that the Basln configuration has little separation at  $\eta = 0.33$  for this case. At a higher lift coefficient of  $C_L \approx 0.86$ , however, the trailing-edge pressures indicate that the Basln configuration does have more separation than the modified configurations at all four span stations.

For  $M_\infty = 0.800$ , figure 34 shows a large dip in trailing-edge pressures at  $\eta = 0.67$  for the Basln configuration between  $\alpha = 8^\circ$  and  $11^\circ$ . However, no significant effect on the corresponding lift coefficients occurs. The exact cause for this dip is unknown; however, yaw oscillations were observed for the Basln configuration at these conditions.

## Conclusions

Airfoil contour modifications consisting of shape changes to the leading- and trailing-edge regions were investigated on a baseline wing-fuselage model in

the Langley 16-Foot Transonic Tunnel. The airfoil leading-edge modification was investigated as an incremental change to the model that already had the trailing-edge modification. The following conclusions are based on an analysis of the longitudinal characteristics and wing-pressure distributions:

1. Significant gains occur in low-speed maximum lift for both modifications. The modification effects were analyzed at two nominal lift coefficients of 0.87 and 0.91, which were near stall for the baseline configuration. The primary benefit was delayed separation from the trailing edge.
2. The trailing-edge modification resulted in a very significant increase in the maximum lift coefficient.
3. Adding the leading-edge modification resulted in an appreciable increase in the maximum lift coefficient at  $M_\infty = 0.300$ . This lift benefit was reduced at  $M_\infty = 0.400$ .
4. The increased aft lift from the additional camber in the trailing-edge modification reduced the angle of attack required for the same lift coefficient, and it produced stronger nose-down pitching moments for all Mach numbers.
5. Overall effects on transonic performance were minimal, in spite of significant effects on transonic pressure distributions.
6. At the transonic Mach numbers, the modifications slightly increased the drag coefficient for the low-altitude cruise conditions. These increases were partly caused by added viscous and wave drag resulting from the strengthening of a suction peak on the wing lower surface near the leading edge.
7. At the transonic Mach numbers, the modifications decreased the drag coefficient for the climb and maneuver conditions.

NASA Langley Research Center  
Hampton, VA 23681-0001  
February 14, 1995

## References

1. Hanley, Robert J.: Development of an Airframe Modification To Improve the Mission Effectiveness of the EA-6B Airplane. *A Collection of Technical Papers—AIAA 5th Applied Aerodynamics Conference*, Aug. 1987, pp. 241-247. (Available as AIAA-87-2358.)
2. Sewall, W. G.; McGhee, R. J.; and Ferris, J. C.: Wind-Tunnel Test Results of Airfoil Modifications for the EA-6B. *A Collection of Technical Papers—AIAA 5th Applied Aerodynamics Conference*, Aug. 1987, pp. 248-256. (Available as AIAA-87-2359.)

3. Waggoner, E. G.; and Allison, D. O.: EA-6B High-Lift Wing Modifications. *A Collection of Technical Papers—AIAA 5th Applied Aerodynamics Conference*, Aug. 1987, pp. 257–269. (Available as AIAA-87-2360.)
4. Jordan, Frank L., Jr.; Hahne, David E.; Masiello, Matthew F.; and Gato, William: High-Angle-of-Attack Stability and Control Improvements for the EA-6B Prowler. *A Collection of Technical Papers—AIAA 5th Applied Aerodynamics Conference*, Aug. 1987, pp. 270–285. (Available as AIAA-87-2361.)
5. Gato, W.; and Masiello, M. F.: Innovative Aerodynamics: The Sensible Way of Restoring Growth Capability to the EA-6B Prowler. *A Collection of Technical Papers—AIAA 5th Applied Aerodynamics Conference*, Aug. 1987, pp. 286–299. (Available as AIAA-87-2362.)
6. Allison, Dennis O.; and Waggoner, E. G.: *Prediction of Effects of Wing Contour Modifications on Low-Speed Maximum Lift and Transonic Performance for the EA-6B Aircraft*. NASA TP-3046, 1990.
7. Jordan, Frank L., Jr.; and Hahne, David E.: *Wind-Tunnel Static and Free-Flight Investigation of High-Angle-of-Attack Stability and Control Characteristics of a Model of the EA-6B Airplane*. NASA TP-3194, 1992.
8. Morgan, M. D.; and Masiello, M. F.: *Tabulated Data Report 1/8.5-Scale EA-6B Model in the NASA Langley Research Center 16-Foot Transonic Tunnel*. XA1128-121-2, Grumman Aerospace Corp., June 1988.
9. Peddrew, Kathryn, compl.: *A User's Guide to the Langley 16-Foot Transonic Tunnel*. NASA TM-83186, 1981.
10. Corson, Blake W., Jr.; Runkel, Jack F.; and Igoe, William B.: *Calibration of the Langley 16-Foot Transonic Tunnel With Test Section Air Removal*. NASA TR R-423, 1974.
11. Mercer, Charles E.; Berrier, Bobby L.; Capone, Francis J.; Grayston, Alan M.; and Sherman, C. D.: *Computations for the 16-Foot Transonic Tunnel—NASA, Langley Research Center, Revision 1*. NASA TM-86319, 1987. (Supersedes NASA TM-86319, 1984.)

Table 1. Streamwise Airfoil Coordinates for Inboard Design Station

 $[\eta = 0.28; t/c = 0.087]$ 

$x/c$	Basln		Fulmod	
	$(z/c)_u$	$(z/c)_l$	$(z/c)_u$	$(z/c)_l$
0.00000	0.00041	0.00041	0.00049	0.00049
.00100	.00380	-.00240	.00497	-.00378
.00300	.00661	-.00433	.00828	-.00657
.00500	.00847	-.00562	.01053	-.00821
.00700	.00995	-.00659	.01229	-.00931
.01000	.01184	-.00774	.01441	-.01046
.02000	.01673	-.01010	.01952	-.01251
.03000	.02065	-.01160	.02335	-.01362
.04000	.02403	-.01281	.02652	-.01442
.05000	.02702	-.01384	.02924	-.01508
.06000	.02973	-.01473	.03162	-.01565
.08000	.03443	-.01627	.03569	-.01672
.10000	.03839	-.01763	.03912	-.01782
.12000	.04179	-.01890	.04212	-.01896
.14000	.04471	-.02011	.04480	-.02013
.16000	.04721	-.02129	.04721	-.02129
.18000	.04933	-.02243	.04933	-.02243
.20000	.05119	-.02353	.05119	-.02353
.25000	.05451	-.02613	.05451	-.02613
.30000	.05633	-.02834	.05633	-.02834
.35000	.05688	-.02999	.05688	-.02999
.40000	.05623	-.03088	.05623	-.03088
.45000	.05453	-.03091	.05453	-.03091
.50000	.05186	-.03014	.05186	-.03014
.55000	.04830	-.02866	.04830	-.02866
.60000	.04406	-.02661	.04406	-.02661
.65000	.03926	-.02397	.03926	-.02397
.70000	.03400	-.02090	.03400	-.02088
.75000	.02843	-.01749	.02843	-.01695
.80000	.02283	-.01408	.02283	-.01162
.82000	.02059	-.01271	.02063	-.00900
.84000	.01835	-.01135	.01846	-.00614
.86000	.01611	-.00998	.01635	-.00324
.88000	.01387	-.00862	.01440	-.00062
.90000	.01163	-.00725	.01248	.00151
.92000	.00939	-.00588	.01054	.00298
.94000	.00715	-.00452	.00859	.00358
.95000	.00603	-.00384	.00762	.00345
.96000	.00490	-.00315	.00665	.00296
.97000	.00378	-.00247	.00568	.00209
.98000	.00266	-.00179	.00471	.00078
.99000	.00154	-.00111	.00374	-.00103
1.00000	.00042	-.00042	.00277	-.00338

Table 2. Streamwise Airfoil Coordinates for Outboard Design Station

$[\eta = 0.75; t/c = 0.074]$

$x/c$	Basln		Fulmod	
	$(z/c)_u$	$(z/c)_l$	$(z/c)_u$	$(z/c)_l$
0.00000	-0.00263	-0.00263	-0.00600	-0.00600
.00100	.00101	-.00464	-.00193	-.00959
.00300	.00320	-.00621	.00114	-.01168
.00500	.00483	-.00720	.00323	-.01283
.00700	.00613	-.00796	.00488	-.01356
.01000	.00785	-.00882	.00695	-.01427
.02000	.01252	-.01052	.01218	-.01526
.03000	.01627	-.01135	.01621	-.01545
.04000	.01948	-.01199	.01959	-.01539
.05000	.02227	-.01251	.02252	-.01522
.06000	.02481	-.01295	.02512	-.01504
.08000	.02933	-.01363	.02959	-.01483
.10000	.03315	-.01430	.03334	-.01490
.12000	.03645	-.01499	.03654	-.01522
.14000	.03925	-.01568	.03928	-.01574
.16000	.04161	-.01640	.04162	-.01640
.18000	.04360	-.01712	.04360	-.01712
.20000	.04527	-.01787	.04527	-.01787
.25000	.04834	-.01979	.04834	-.01979
.30000	.05005	-.02158	.05005	-.02158
.35000	.05053	-.02303	.05053	-.02303
.40000	.04992	-.02403	.04992	-.02403
.45000	.04834	-.02436	.04834	-.02436
.50000	.04588	-.02380	.04588	-.02380
.55000	.04265	-.02268	.04265	-.02268
.60000	.03882	-.02118	.03882	-.02118
.65000	.03455	-.01924	.03455	-.01924
.70000	.02999	-.01686	.02999	-.01689
.75000	.02529	-.01432	.02529	-.01384
.80000	.02051	-.01172	.02051	-.00961
.82000	.01858	-.01066	.01861	-.00750
.84000	.01663	-.00960	.01673	-.00516
.86000	.01469	-.00853	.01490	-.00279
.88000	.01274	-.00746	.01319	-.00065
.90000	.01079	-.00639	.01151	.00107
.92000	.00884	-.00532	.00982	.00223
.94000	.00689	-.00425	.00812	.00265
.95000	.00591	-.00372	.00728	.00249
.96000	.00494	-.00318	.00643	.00203
.97000	.00397	-.00265	.00558	.00124
.98000	.00300	-.00212	.00474	.00007
.99000	.00203	-.00159	.00389	-.00152
1.00000	.00107	-.00107	.00304	-.00359

Table 3. Longitudinal Characteristics and Trailing-Edge Pressure Coefficients at  $M_\infty = 0.300$ 

$M_\infty$	$\alpha$ , deg	$C_L$	$C_m$	$C_D$	$C_{p,te}$ for $\eta$ of—			
					0.33	0.50	0.67	0.82
Basln								
0.299	0.13	0.042	-0.043	0.0189	0.141	0.086	0.115	0.079
0.300	0.63	0.080	-0.040	0.0192	0.143	0.085	0.116	0.080
0.300	1.14	0.119	-0.039	0.0198	0.139	0.084	0.115	0.079
0.300	1.61	0.153	-0.038	0.0204	0.139	0.083	0.115	0.077
0.300	2.13	0.193	-0.036	0.0215	0.139	0.084	0.113	0.075
0.300	4.14	0.347	-0.032	0.0270	0.134	0.081	0.110	0.067
0.300	6.11	0.491	-0.028	0.0359	0.119	0.081	0.103	0.049
0.299	8.11	0.640	-0.022	0.0499	0.097	0.069	0.070	0.022
0.299	10.11	0.770	-0.011	0.0752	0.084	0.041	-0.027	-0.029
0.299	11.14	0.827	-0.004	0.0955	0.089	-0.003	-0.112	-0.097
0.298	12.14	0.861	0.001	0.1231	0.046	-0.068	-0.249	-0.196
0.300	13.12	0.877	0.008	0.1522	-0.003	-0.210	-0.324	-0.299
0.300	14.12	0.888	0.013	0.1830	-0.134	-0.299	-0.392	-0.382
0.299	15.14	0.899	0.012	0.2154	-0.244	-0.399	-0.429	-0.464
0.299	16.10	0.882	0.013	0.2368	-0.354	-0.493	-0.454	-0.557
0.299	17.11	0.879	0.019	0.2605	-0.460	-0.522	-0.481	-0.564
Temod								
0.302	0.14	0.075	-0.057	0.0181	-0.058	-0.051	-0.064	-0.048
0.302	0.63	0.117	-0.056	0.0180	-0.054	-0.050	-0.060	-0.044
0.302	1.12	0.155	-0.055	0.0191	-0.052	-0.050	-0.061	-0.044
0.302	1.63	0.197	-0.056	0.0201	-0.049	-0.048	-0.060	-0.044
0.302	2.13	0.234	-0.055	0.0210	-0.047	-0.048	-0.058	-0.044
0.302	4.13	0.386	-0.053	0.0271	-0.041	-0.032	-0.047	-0.039
0.302	6.12	0.543	-0.051	0.0369	-0.027	-0.026	-0.038	-0.037
0.302	8.12	0.696	-0.048	0.0525	-0.012	-0.023	-0.045	-0.067
0.301	10.15	0.833	-0.039	0.0841	-0.014	-0.033	-0.144	-0.130
0.301	11.11	0.878	-0.035	0.1069	-0.042	-0.065	-0.210	-0.184
0.301	12.14	0.915	-0.027	0.1356	-0.083	-0.161	-0.285	-0.267
0.301	13.13	0.931	-0.023	0.1658	-0.141	-0.274	-0.354	-0.370
0.300	14.14	0.931	-0.023	0.1968	-0.234	-0.403	-0.404	-0.462
0.300	15.12	0.932	-0.017	0.2249	-0.333	-0.466	-0.438	-0.500
0.300	16.14	0.930	-0.014	0.2503	-0.435	-0.510	-0.462	-0.523
0.299	17.13	0.919	-0.009	0.2712	-0.514	-0.538	-0.475	-0.519
Fulmod								
0.302	0.14	0.082	-0.058	0.0199	-0.071	-0.053	-0.062	-0.047
0.303	0.64	0.123	-0.058	0.0201	-0.067	-0.052	-0.064	-0.048
0.300	1.15	0.168	-0.057	0.0208	-0.065	-0.052	-0.064	-0.046
0.300	1.65	0.202	-0.056	0.0217	-0.063	-0.050	-0.059	-0.046
0.301	2.14	0.245	-0.056	0.0229	-0.057	-0.049	-0.058	-0.045
0.301	4.14	0.395	-0.053	0.0292	-0.047	-0.039	-0.051	-0.046
0.301	6.14	0.557	-0.050	0.0397	-0.032	-0.031	-0.044	-0.048
0.301	8.14	0.711	-0.049	0.0537	-0.018	-0.027	-0.037	-0.057
0.300	10.13	0.860	-0.044	0.0733	-0.014	-0.032	-0.042	-0.094
0.300	11.13	0.917	-0.039	0.0938	-0.025	-0.057	-0.070	-0.193
0.300	12.14	0.949	-0.034	0.1224	-0.049	-0.177	-0.182	-0.324
0.299	13.14	0.953	-0.025	0.1645	-0.083	-0.338	-0.317	-0.418
0.299	14.13	0.952	-0.025	0.1972	-0.169	-0.429	-0.402	-0.477
0.299	15.13	0.963	-0.022	0.2264	-0.262	-0.492	-0.428	-0.503
0.299	16.14	0.960	-0.025	0.2509	-0.344	-0.520	-0.443	-0.527
0.298	17.13	0.963	-0.024	0.2743	-0.487	-0.532	-0.483	-0.542

Table 4. Longitudinal Characteristics and Trailing-Edge Pressure Coefficients at  $M_\infty = 0.400$ 

$M_\infty$	$\alpha$ , deg	$C_L$	$C_m$	$C_D$	$C_{p,te}$ for $\eta$ of—			
					0.33	0.50	0.67	0.82
Basln								
0.401	0.09	0.042	-0.042	0.0184	0.137	0.091	0.123	0.082
0.401	0.58	0.077	-0.041	0.0187	0.137	0.090	0.121	0.081
0.401	1.09	0.120	-0.039	0.0192	0.137	0.090	0.121	0.079
0.401	1.60	0.157	-0.038	0.0201	0.136	0.089	0.120	0.078
0.402	2.07	0.192	-0.038	0.0210	0.136	0.089	0.120	0.077
0.402	4.10	0.350	-0.034	0.0270	0.130	0.086	0.116	0.068
0.402	6.11	0.509	-0.030	0.0369	0.120	0.082	0.106	0.053
0.402	8.09	0.659	-0.024	0.0522	0.097	0.066	0.071	0.023
0.401	10.09	0.784	-0.010	0.0807	0.082	0.009	-0.051	-0.037
0.402	11.11	0.829	-0.003	0.1022	0.067	-0.039	-0.165	-0.102
0.401	12.10	0.870	0.003	0.1291	0.031	-0.126	-0.210	-0.195
0.400	13.08	0.895	0.007	0.1587	-0.048	-0.231	-0.295	-0.269
0.401	14.07	0.907	0.008	0.1916	-0.213	-0.291	-0.392	-0.364
0.401	15.06	0.908	0.007	0.2190	-0.303	-0.377	-0.444	-0.409
0.400	16.08	0.902	0.003	0.2433	-0.425	-0.466	-0.454	-0.484
0.400	17.07	0.882	0.016	0.2620	-0.507	-0.521	-0.483	-0.566
Temod								
0.399	0.11	0.085	-0.059	0.0189	-0.070	-0.060	-0.073	-0.057
0.400	0.58	0.124	-0.058	0.0192	-0.068	-0.059	-0.071	-0.055
0.401	1.10	0.165	-0.058	0.0200	-0.065	-0.058	-0.071	-0.055
0.401	1.58	0.203	-0.057	0.0207	-0.067	-0.051	-0.064	-0.051
0.401	2.08	0.245	-0.057	0.0220	-0.065	-0.049	-0.064	-0.051
0.402	4.10	0.405	-0.055	0.0288	-0.051	-0.043	-0.056	-0.047
0.402	6.09	0.570	-0.054	0.0395	-0.036	-0.035	-0.046	-0.048
0.402	8.10	0.725	-0.049	0.0572	-0.029	-0.031	-0.061	-0.080
0.401	10.09	0.850	-0.039	0.0928	-0.047	-0.059	-0.172	-0.155
0.401	11.10	0.896	-0.034	0.1182	-0.084	-0.119	-0.250	-0.214
0.400	12.09	0.932	-0.028	0.1450	-0.126	-0.181	-0.327	-0.257
0.400	13.12	0.945	-0.028	0.1756	-0.196	-0.317	-0.386	-0.342
0.400	14.13	0.955	-0.026	0.2055	-0.279	-0.384	-0.424	-0.431
0.400	15.07	0.952	-0.026	0.2307	-0.376	-0.455	-0.448	-0.503
0.400	16.10	0.950	-0.023	0.2555	-0.466	-0.516	-0.471	-0.549
0.399	17.11	0.938	-0.013	0.2769	-0.550	-0.547	-0.487	-0.580
Fulmod								
0.401	0.10	0.089	-0.061	0.0201	-0.079	-0.057	-0.074	-0.054
0.402	0.60	0.132	-0.059	0.0205	-0.075	-0.055	-0.072	-0.052
0.399	1.08	0.168	-0.059	0.0213	-0.073	-0.053	-0.071	-0.051
0.400	1.58	0.212	-0.059	0.0222	-0.070	-0.053	-0.070	-0.051
0.401	2.08	0.250	-0.057	0.0230	-0.068	-0.054	-0.066	-0.052
0.400	4.09	0.410	-0.055	0.0301	-0.053	-0.048	-0.061	-0.052
0.400	6.09	0.572	-0.053	0.0411	-0.037	-0.042	-0.053	-0.052
0.400	8.11	0.734	-0.052	0.0566	-0.032	-0.030	-0.044	-0.063
0.401	10.10	0.877	-0.042	0.0838	-0.032	-0.048	-0.067	-0.155
0.400	11.09	0.912	-0.036	0.1114	-0.051	-0.130	-0.162	-0.281
0.399	12.10	0.940	-0.029	0.1426	-0.094	-0.241	-0.301	-0.363
0.399	13.08	0.952	-0.027	0.1735	-0.135	-0.380	-0.364	-0.451
0.399	14.10	0.966	-0.030	0.2060	-0.242	-0.399	-0.418	-0.468
0.398	16.08	0.971	-0.031	0.2552	-0.445	-0.525	-0.487	-0.602
0.398	17.09	0.977	-0.027	0.2775	-0.537	-0.541	-0.527	-0.608

Table 5. Longitudinal Characteristics and Trailing-Edge Pressure Coefficients at  $M_\infty = 0.725$ 

$M_\infty$	$\alpha$ , deg	$C_L$	$C_m$	$C_D$	$C_{p,te}$ for $\eta$ of—			
					0.33	0.50	0.67	0.82
Basln								
0.727	0.05	0.038	-0.047	0.0187	0.164	0.121	0.155	0.105
0.726	0.53	0.083	-0.045	0.0191	0.163	0.121	0.155	0.103
0.726	1.05	0.130	-0.044	0.0199	0.161	0.121	0.154	0.102
0.725	1.53	0.171	-0.045	0.0208	0.159	0.120	0.153	0.100
0.726	2.06	0.219	-0.044	0.0221	0.156	0.119	0.153	0.097
0.725	4.03	0.402	-0.043	0.0303	0.140	0.116	0.148	0.084
0.727	6.02	0.590	-0.042	0.0454	0.129	0.111	0.143	0.071
0.725	7.05	0.679	-0.037	0.0576	0.124	0.100	0.093	0.032
0.726	8.05	0.754	-0.030	0.0741	0.123	0.076	-0.044	-0.048
0.725	9.02	0.787	-0.023	0.0937	0.117	-0.046	-0.228	-0.171
0.725	10.03	0.814	-0.020	0.1152	0.074	-0.175	-0.301	-0.185
0.727	11.01	0.844	-0.015	0.1388	-0.031	-0.253	-0.334	-0.313
0.725	12.04	0.860	-0.017	0.1633	-0.252	-0.359	-0.387	-0.336
0.724	13.03	0.874	-0.020	0.1906	-0.359	-0.389	-0.435	-0.404
0.725	13.36	0.878	-0.024	0.1999	-0.429	-0.420	-0.415	-0.406
Temod								
0.726	0.06	0.091	-0.067	0.0198	-0.048	-0.029	-0.044	-0.028
0.727	0.54	0.136	-0.067	0.0205	-0.047	-0.028	-0.043	-0.029
0.728	1.06	0.187	-0.068	0.0215	-0.043	-0.026	-0.040	-0.029
0.728	1.53	0.231	-0.069	0.0227	-0.040	-0.024	-0.039	-0.029
0.725	2.07	0.279	-0.069	0.0245	-0.038	-0.024	-0.038	-0.029
0.724	4.04	0.472	-0.072	0.0343	-0.026	-0.018	-0.032	-0.029
0.723	6.03	0.670	-0.071	0.0517	-0.018	-0.012	-0.034	-0.042
0.725	8.06	0.824	-0.066	0.0849	-0.034	-0.049	-0.203	-0.142
0.722	9.06	0.861	-0.060	0.1057	-0.064	-0.126	-0.289	-0.283
0.726	10.05	0.896	-0.060	0.1304	-0.132	-0.236	-0.359	-0.334
0.727	11.02	0.924	-0.056	0.1543	-0.215	-0.304	-0.392	-0.382
0.725	12.00	0.928	-0.048	0.1758	-0.323	-0.377	-0.474	-0.412
Fulmod								
0.728	0.04	0.087	-0.068	0.0208	-0.045	-0.025	-0.046	-0.026
0.726	0.54	0.134	-0.068	0.0213	-0.044	-0.024	-0.042	-0.024
0.726	1.04	0.184	-0.068	0.0221	-0.042	-0.023	-0.041	-0.026
0.725	1.53	0.230	-0.068	0.0233	-0.040	-0.021	-0.039	-0.026
0.725	2.03	0.278	-0.069	0.0248	-0.038	-0.022	-0.038	-0.026
0.725	4.04	0.471	-0.071	0.0350	-0.025	-0.015	-0.032	-0.027
0.724	6.04	0.668	-0.070	0.0530	-0.017	-0.011	-0.037	-0.047
0.726	7.06	0.758	-0.068	0.0688	-0.017	-0.021	-0.066	-0.104
0.724	8.03	0.815	-0.064	0.0865	-0.038	-0.057	-0.184	-0.204
0.724	9.05	0.859	-0.057	0.1077	-0.066	-0.143	-0.289	-0.297
0.725	10.04	0.882	-0.056	0.1317	-0.153	-0.279	-0.341	-0.401
0.723	11.03	0.885	-0.055	0.1551	-0.281	-0.375	-0.427	-0.464
0.723	11.96	0.905	-0.059	0.1792	-0.376	-0.410	-0.435	-0.461

Table 6. Longitudinal Characteristics and Trailing-Edge Pressure Coefficients at  $M_\infty = 0.800$ 

$M_\infty$	$\alpha$ , deg	$C_L$	$C_m$	$C_D$	$C_{p,te}$ for $\eta$ of—			
					0.33	0.50	0.67	0.82
Basln								
0.801	0.03	0.037	-0.050	0.0194	0.172	0.140	0.172	0.119
0.801	0.53	0.087	-0.049	0.0199	0.172	0.138	0.170	0.117
0.801	1.02	0.137	-0.049	0.0208	0.169	0.137	0.169	0.116
0.799	1.55	0.187	-0.048	0.0221	0.166	0.137	0.169	0.114
0.799	2.01	0.234	-0.049	0.0238	0.162	0.136	0.169	0.112
0.798	3.05	0.339	-0.051	0.0291	0.155	0.135	0.170	0.110
0.799	4.05	0.441	-0.055	0.0377	0.150	0.134	0.155	0.063
0.798	5.05	0.534	-0.055	0.0482	0.152	0.130	0.063	0.032
0.799	6.03	0.604	-0.053	0.0604	0.153	0.101	-0.081	0.012
0.800	7.04	0.665	-0.049	0.0752	0.129	0.011	-0.190	-0.050
0.800	8.01	0.722	-0.045	0.0914	0.089	-0.117	-0.242	-0.105
0.799	9.03	0.762	-0.047	0.1104	-0.052	-0.241	-0.158	-0.258
0.799	10.04	0.807	-0.044	0.1324	-0.213	-0.288	-0.203	-0.301
0.800	11.01	0.833	-0.037	0.1531	-0.248	-0.336	-0.404	-0.383
0.800	12.04	0.862	-0.032	0.1755	-0.309	-0.386	-0.456	-0.429
Temod								
0.801	0.02	0.091	-0.071	0.0208	-0.020	0.001	-0.017	-0.007
0.802	0.55	0.147	-0.072	0.0217	-0.019	0.002	-0.016	-0.007
0.802	1.02	0.197	-0.074	0.0229	-0.017	0.002	-0.016	-0.008
0.802	1.52	0.248	-0.075	0.0248	-0.015	0.003	-0.016	-0.011
0.801	2.05	0.306	-0.077	0.0272	-0.012	0.002	-0.016	-0.017
0.799	3.03	0.408	-0.082	0.0337	-0.008	0.001	-0.022	-0.024
0.800	4.03	0.513	-0.089	0.0438	-0.006	-0.004	-0.006	-0.036
0.800	5.06	0.613	-0.095	0.0569	-0.010	-0.024	-0.080	-0.093
0.798	6.02	0.680	-0.089	0.0690	-0.025	-0.046	-0.232	-0.171
0.795	7.03	0.732	-0.083	0.0831	-0.050	-0.120	-0.309	-0.243
0.798	8.04	0.783	-0.080	0.1010	-0.110	-0.273	-0.337	-0.265
0.800	9.02	0.827	-0.080	0.1206	-0.229	-0.343	-0.351	-0.306
0.799	10.01	0.875	-0.085	0.1438	-0.320	-0.324	-0.380	-0.386
0.798	11.05	0.907	-0.078	0.1667	-0.334	-0.377	-0.442	-0.464
Fulmod								
0.798	0.03	0.090	-0.072	0.0222	-0.021	-0.003	-0.026	-0.008
0.798	0.54	0.145	-0.072	0.0224	-0.019	0.000	-0.022	-0.006
0.800	1.07	0.199	-0.073	0.0235	-0.017	0.002	-0.018	-0.004
0.800	1.52	0.246	-0.074	0.0251	-0.017	0.001	-0.017	-0.008
0.799	2.03	0.297	-0.076	0.0274	-0.015	0.001	-0.016	-0.012
0.801	3.06	0.409	-0.081	0.0342	-0.011	0.001	-0.016	-0.019
0.799	4.05	0.517	-0.088	0.0437	-0.005	0.002	-0.011	-0.026
0.799	5.06	0.616	-0.091	0.0566	-0.004	-0.017	-0.046	-0.083
0.798	6.03	0.685	-0.089	0.0700	-0.015	-0.045	-0.156	-0.179
0.799	7.03	0.743	-0.084	0.0866	-0.049	-0.143	-0.242	-0.310
0.799	8.03	0.785	-0.081	0.1037	-0.112	-0.272	-0.319	-0.342
0.800	9.05	0.837	-0.080	0.1248	-0.222	-0.323	-0.353	-0.375
0.803	10.06	0.883	-0.083	0.1490	-0.297	-0.322	-0.414	-0.429
0.800	10.75	0.903	-0.077	0.1637	-0.350	-0.364	-0.457	-0.476

Table 7. Longitudinal Characteristics and Trailing-Edge Pressure Coefficients at  $M_\infty = 0.850$ 

$M_\infty$	$\alpha$ , deg	$C_L$	$C_m$	$C_D$	$C_{p,te}$ for $\eta$ of—			
					0.33	0.50	0.67	0.82
Basln								
0.853	0.03	0.044	-0.056	0.0219	0.177	0.154	0.187	0.137
0.853	0.54	0.103	-0.057	0.0230	0.172	0.154	0.187	0.136
0.849	1.05	0.152	-0.058	0.0242	0.166	0.152	0.184	0.134
0.849	1.55	0.206	-0.060	0.0266	0.163	0.150	0.182	0.133
0.849	2.02	0.255	-0.064	0.0299	0.158	0.146	0.167	0.128
0.850	3.05	0.352	-0.068	0.0388	0.149	0.133	0.035	0.094
0.849	4.02	0.427	-0.068	0.0479	0.132	0.116	-0.084	0.034
0.850	5.02	0.499	-0.066	0.0592	0.103	0.069	-0.174	-0.026
0.851	6.03	0.562	-0.060	0.0715	0.066	-0.067	-0.255	-0.106
0.850	7.02	0.617	-0.056	0.0851	0.036	-0.220	-0.318	-0.166
0.849	8.01	0.674	-0.052	0.1011	-0.124	-0.284	-0.364	-0.216
0.850	9.01	0.723	-0.054	0.1194	-0.285	-0.373	-0.348	-0.397
0.851	10.04	0.780	-0.056	0.1406	-0.365	-0.420	-0.296	-0.433
Temod								
0.851	0.03	0.103	-0.080	0.0236	0.018	0.027	0.016	0.012
0.851	0.54	0.163	-0.084	0.0254	0.019	0.030	0.021	0.016
0.851	1.03	0.219	-0.089	0.0277	0.020	0.032	0.027	0.017
0.850	1.53	0.276	-0.094	0.0309	0.021	0.034	0.030	0.018
0.850	2.05	0.336	-0.101	0.0355	0.024	0.035	0.038	0.014
0.849	3.03	0.435	-0.111	0.0454	0.024	0.031	-0.044	-0.042
0.850	4.01	0.520	-0.114	0.0565	0.016	0.011	-0.186	-0.145
0.849	5.02	0.592	-0.113	0.0683	0.004	-0.042	-0.271	-0.216
0.852	6.04	0.649	-0.107	0.0819	-0.033	-0.199	-0.333	-0.332
0.849	7.01	0.694	-0.097	0.0943	-0.110	-0.320	-0.362	-0.382
0.849	8.03	0.742	-0.092	0.1104	-0.250	-0.406	-0.382	-0.411
0.850	9.02	0.786	-0.090	0.1283	-0.372	-0.451	-0.400	-0.434
0.850	10.04	0.836	-0.094	0.1499	-0.444	-0.436	-0.423	-0.481
Fulmod								
0.849	0.02	0.101	-0.082	0.0253	0.012	0.018	0.004	0.012
0.852	0.54	0.159	-0.086	0.0268	0.020	0.026	0.014	0.015
0.852	1.04	0.219	-0.090	0.0288	0.024	0.033	0.026	0.020
0.852	1.54	0.275	-0.096	0.0318	0.022	0.036	0.032	0.022
0.851	2.04	0.333	-0.101	0.0356	0.021	0.037	0.029	0.015
0.847	3.03	0.433	-0.108	0.0444	0.021	0.029	-0.025	-0.029
0.851	4.02	0.521	-0.113	0.0562	0.019	0.002	-0.151	-0.132
0.849	5.04	0.599	-0.111	0.0685	0.001	-0.051	-0.257	-0.229
0.848	6.02	0.661	-0.107	0.0820	-0.036	-0.173	-0.284	-0.324
0.851	7.04	0.710	-0.102	0.0981	-0.137	-0.319	-0.342	-0.396
0.849	8.07	0.754	-0.093	0.1140	-0.279	-0.349	-0.396	-0.458
0.847	9.06	0.798	-0.093	0.1323	-0.389	-0.426	-0.414	-0.453
0.848	9.87	0.845	-0.094	0.1509	-0.436	-0.433	-0.443	-0.472

Table 8. Longitudinal Characteristics and Trailing-Edge Pressure Coefficients at  $M_\infty = 0.900$ 

$M_\infty$	$\alpha$ , deg	$C_L$	$C_m$	$C_D$	$C_{p,te}$ for $\eta$ of—			
					0.33	0.50	0.67	0.82
Basln								
0.900	0.01	0.027	-0.061	0.0328	0.156	0.147	0.105	0.086
0.898	0.52	0.077	-0.063	0.0330	0.146	0.141	0.073	0.064
0.900	1.01	0.114	-0.061	0.0354	0.125	0.125	0.023	0.025
0.899	1.53	0.161	-0.063	0.0375	0.104	0.110	-0.021	0.001
0.901	2.03	0.199	-0.063	0.0414	0.066	0.073	-0.080	-0.020
0.903	3.05	0.279	-0.065	0.0500	-0.003	0.003	-0.156	-0.060
0.900	4.02	0.369	-0.070	0.0591	-0.050	-0.049	-0.214	-0.089
0.902	5.03	0.451	-0.075	0.0720	-0.102	-0.110	-0.278	-0.153
0.898	6.04	0.534	-0.076	0.0850	-0.140	-0.230	-0.336	-0.212
0.897	7.03	0.604	-0.076	0.0997	-0.179	-0.348	-0.389	-0.285
0.900	8.05	0.673	-0.080	0.1188	-0.294	-0.437	-0.447	-0.341
0.898	9.04	0.737	-0.081	0.1373	-0.402	-0.487	-0.469	-0.375
Temod								
0.901	0.02	0.088	-0.091	0.0355	0.095	0.088	0.060	0.024
0.900	0.51	0.145	-0.100	0.0367	0.075	0.075	0.020	-0.009
0.900	1.02	0.201	-0.107	0.0395	0.052	0.058	-0.024	-0.048
0.898	2.02	0.307	-0.118	0.0470	0.001	0.008	-0.128	-0.126
0.900	3.05	0.398	-0.126	0.0576	-0.068	-0.060	-0.224	-0.219
0.899	4.04	0.486	-0.134	0.0692	-0.121	-0.128	-0.283	-0.324
0.899	5.02	0.568	-0.138	0.0826	-0.178	-0.210	-0.347	-0.441
0.898	6.01	0.645	-0.139	0.0974	-0.223	-0.325	-0.382	-0.501
0.899	7.02	0.709	-0.137	0.1136	-0.259	-0.420	-0.431	-0.539
0.899	8.02	0.763	-0.132	0.1297	-0.368	-0.470	-0.462	-0.575
0.898	8.72	0.794	-0.127	0.1407	-0.453	-0.497	-0.472	-0.581
Fulmod								
0.901	0.02	0.080	-0.093	0.0376	0.091	0.080	0.048	0.014
0.899	0.55	0.149	-0.104	0.0381	0.067	0.065	0.001	-0.019
0.900	1.01	0.195	-0.108	0.0404	0.046	0.047	-0.041	-0.057
0.898	1.53	0.254	-0.113	0.0431	0.026	0.029	-0.078	-0.091
0.897	2.03	0.304	-0.117	0.0466	-0.002	0.004	-0.124	-0.129
0.898	3.06	0.400	-0.124	0.0565	-0.064	-0.060	-0.215	-0.223
0.903	4.03	0.485	-0.133	0.0693	-0.129	-0.143	-0.279	-0.316
0.901	5.04	0.574	-0.137	0.0827	-0.168	-0.209	-0.348	-0.456
0.898	6.05	0.648	-0.135	0.0974	-0.206	-0.332	-0.390	-0.490
0.900	7.04	0.710	-0.135	0.1145	-0.261	-0.413	-0.447	-0.540
0.903	8.03	0.777	-0.138	0.1344	-0.367	-0.469	-0.494	-0.587

Table 9. Wing Pressure Coefficients for Basln for  $M_\infty = 0.300$ 

[Blanks indicate defective data]

$x/c$	$C_p$ for $\alpha = 8.1^\circ$ ; $C_L = 0.640$ ; and $\eta$ of—				$C_p$ for $\alpha = 12.1^\circ$ ; $C_L = 0.861$ ; and $\eta$ of—				$C_p$ for $\alpha = 15.1^\circ$ ; $C_L = 0.899$ ; and $\eta$ of—			
	0.33	0.50	0.67	0.82	0.33	0.50	0.67	0.82	0.33	0.50	0.67	0.82
Upper surface												
0.00	-1.171	-1.675	-2.738	-1.702	-2.435	-3.691	-1.584	-2.120	-2.037	-2.020	-0.888	-1.127
0.05	-1.322	-1.366	-1.597	-1.526	-2.296	-2.777	-1.536	-1.650	-1.865	-1.400	-0.833	-0.920
0.10	-1.053	-1.141	-1.241		-1.655	-1.753	-1.320		-1.544	-1.193	-0.834	
0.14	-0.931	-1.028	-1.055	-1.034	-1.339	-1.382	-1.261	-1.177	-1.271	-1.084	-0.875	-0.650
0.20	-0.829	-0.867	-0.953	-0.892	-1.125	-1.074	-1.106	-1.077	-1.158	-0.954	-0.793	-0.641
0.25	-0.742	-0.804	-0.847	-0.797	-0.980	-0.932	-0.997	-0.990	-1.163	-0.907	-0.761	-0.649
0.30	-0.696	-0.719	-0.758	-0.702	-0.872	-0.812	-0.890	-0.882	-1.139	-0.873	-0.728	-0.622
0.35		-0.669	-0.696	-0.645		-0.738	-0.849	-0.787		-0.846	-0.736	-0.611
0.40	-0.589	-0.596	-0.611	-0.567	-0.698	-0.656	-0.781	-0.702	-1.029	-0.792	-0.693	-0.604
0.50	-0.429		-0.477	-0.438	-0.540		-0.682	-0.544	-0.869		-0.656	-0.572
0.60	-0.329	-0.332	-0.364		-0.410	-0.395	-0.587		-0.703	-0.619	-0.620	
0.74	-0.179	-0.197	-0.202	-0.217	-0.246	-0.279	-0.466		-0.337	-0.519	-0.569	-0.547
0.78	-0.138	-0.150	-0.172	-0.181	-0.205	-0.228	-0.441		-0.316	-0.466	-0.526	-0.570
0.84	-0.084	-0.095	-0.106	-0.137	-0.149	-0.182	-0.382		-0.289	-0.408	-0.506	-0.533
0.87	-0.056	-0.068	-0.069	-0.102	-0.122	-0.153	-0.349		-0.271	-0.381	-0.480	-0.502
0.90	-0.032	-0.041	-0.042	-0.070	-0.101	-0.132	-0.332		-0.251	-0.364	-0.462	-0.493
0.96	0.046	0.043	0.024	-0.017	-0.029	-0.069	-0.290		-0.225	-0.307	-0.409	-0.469
1.00	0.097	0.069	0.070	0.022	0.046	-0.068	-0.249		-0.196	-0.244	-0.399	-0.429
Lower surface												
0.00	-1.171	-1.675	-2.738	-1.702	-2.435	-3.691	-1.584	-2.120	-2.037	-2.020	-0.888	-1.127
0.03		0.633	0.679	0.637		0.772	0.725	0.674		0.771	0.722	0.643
0.05	0.520	0.531	0.580	0.480	0.687	0.685	0.655	0.591	0.734	0.688	0.663	0.583
0.10	0.370	0.400	0.444	0.420	0.534	0.545	0.533	0.504	0.579	0.551	0.551	0.485
0.20	0.230	0.275	0.306	0.299	0.374	0.410	0.385	0.380	0.419	0.431	0.401	0.376
0.25	0.188	0.217	0.241	0.258	0.320	0.333	0.311	0.330	0.365	0.338	0.321	0.317
0.40	0.036	0.082		0.126	0.134	0.181		0.178	0.157	0.179		0.161
0.50	0.006	0.048	0.092	0.083	0.083	0.117	0.117	0.116	0.094	0.093	0.103	0.082
0.60	0.041	0.061	0.081	0.073	0.099	0.110	0.081	0.083	0.095	0.074	0.047	0.035
0.74	0.043	0.056	0.057	0.060	0.077	0.068	0.023	0.037	0.049	-0.010	-0.033	-0.033
0.78	0.039	0.054	0.057	0.041	0.058	0.057	-0.001	0.001	0.016	-0.038	-0.075	-0.083
0.82	0.041	0.062	0.059	0.056	0.048	0.050	-0.020	0.006	-0.015	-0.055	-0.104	-0.085
0.88	0.053	0.064	0.071	0.045	0.046	0.039	-0.030	-0.034	-0.039	-0.101	-0.122	-0.152
0.94	0.076	0.070	0.061	0.044	0.053	0.012	-0.105	-0.076	-0.078	-0.187	-0.233	-0.235
1.00	0.097	0.069	0.070	0.022	0.046	-0.068	-0.249	-0.196	-0.244	-0.399	-0.429	-0.464

Table 10. Wing Pressure Coefficients for Temod for  $M_\infty = 0.300$ 

[Blanks indicate defective data]

$x/c$	$C_p$ for $\alpha = 8.1^\circ$ ; $C_L = 0.696$ ; and $\eta$ of—				$C_p$ for $\alpha = 11.1^\circ$ ; $C_L = 0.878$ ; and $\eta$ of—				$C_p$ for $\alpha = 12.1^\circ$ ; $C_L = 0.915$ ; and $\eta$ of—				$C_p$ for $\alpha = 15.1^\circ$ ; $C_L = 0.932$ ; and $\eta$ of—			
	0.33	0.50	0.67	0.82	0.33	0.50	0.67	0.82	0.33	0.50	0.67	0.82	0.33	0.50	0.67	0.82
Upper surface																
0.00	-1.300	-1.943	-2.252	-1.548	-3.828	-4.149	-1.366	-1.515	-2.251	-3.217	-1.159	-1.760	-1.742	-1.771	-0.680	-0.733
0.05	-1.356		-1.803	-1.837	-1.906		-1.429	-1.590	-2.279		-1.173	-1.667	-1.629		-0.645	-0.820
0.10	-1.076		-1.315	-1.244	-1.423		-1.450	-1.585	-1.776		-1.203	-1.354	-1.513		-0.644	-0.636
0.14	-0.955	-1.057	-1.171	-1.092	-1.214	-1.321	-1.390	-1.541	-1.439	-1.533	-1.184	-1.256	-1.414	-0.966	-0.654	-0.595
0.20	-0.838	-0.903	-0.980	-0.936	-1.033	-1.095	-1.207	-1.378	-1.163	-1.195	-1.080	-1.130	-1.286	-0.895	-0.620	-0.595
0.25	-0.757	-0.827	-0.882	-0.828	-0.924	-0.984	-1.091	-1.212	-1.031	-1.022	-0.990	-1.024	-1.168	-0.863	-0.611	-0.613
0.30	-0.708	-0.745	-0.784	-0.737	-0.837	-0.873	-0.966	-1.033	-0.900	-0.897	-0.888	-0.901	-1.047	-0.848	-0.592	-0.584
0.35		-0.694	-0.723	-0.674		-0.802	-0.900	-0.876		-0.813	-0.870	-0.801		-0.846	-0.628	-0.587
0.40	-0.609	-0.617	-0.639	-0.607	-0.698	-0.702	-0.809	-0.750	-0.721	-0.720	-0.813	-0.713	-0.909	-0.798	-0.600	-0.588
0.50	-0.457		-0.491	-0.460	-0.542		-0.684	-0.539	-0.579		-0.732	-0.547	-0.823		-0.595	-0.565
0.60	-0.351	-0.356	-0.382		-0.417	-0.401	-0.572		-0.454	-0.456	-0.643		-0.731	-0.676	-0.595	
0.74	-0.194		-0.218	-0.220	-0.244		-0.424	-0.274	-0.284		-0.521	-0.353	-0.581		-0.578	-0.577
0.78	-0.160	-0.213	-0.188	-0.186	-0.205	-0.240	-0.399	-0.249	-0.246	-0.311	-0.498	-0.340	-0.542	-0.594	-0.589	-0.582
0.84	-0.113	-0.150	-0.128	-0.151	-0.153	-0.180	-0.337	-0.217	-0.190	-0.262	-0.435	-0.322	-0.486	-0.565	-0.559	-0.584
0.87	-0.094	-0.120		-0.109	-0.126	-0.148		-0.190	-0.167	-0.234		-0.292	-0.455	-0.546		-0.569
0.90	-0.082	-0.099	-0.080		-0.116	-0.131	-0.281		-0.155	-0.219	-0.375		-0.445	-0.546	-0.518	
0.96	-0.043	-0.028	-0.042	-0.065	-0.077	-0.062	-0.238	-0.160	-0.118	-0.151	-0.333	-0.267	-0.399	-0.466	-0.500	-0.545
1.00	-0.012	-0.023	-0.045	-0.067	-0.042	-0.065	-0.210	-0.184	-0.083	-0.161	-0.285	-0.267	-0.333	-0.466	-0.438	-0.500
Lower surface																
0.00	-1.300	-1.943	-2.252	-1.548	-3.828	-4.149	-1.366	-1.515	-2.251	-3.217	-1.159	-1.760	-1.742	-1.771	-0.680	-0.733
0.03	0.653	0.669	0.704	0.336	0.777	0.788	0.732	0.368	0.776	0.792	0.734	0.356	0.810	0.794	0.725	0.331
0.05	0.551	0.558	0.616	0.490	0.701	0.699	0.662	0.603	0.714	0.706	0.668	0.609	0.753	0.707	0.669	0.595
0.10	0.399	0.435	0.482	0.455	0.539	0.556	0.541	0.515	0.560	0.567	0.552	0.513	0.600	0.568	0.563	0.499
0.20	0.259	0.311	0.344	0.335	0.378	0.424	0.398	0.400	0.401	0.439	0.408	0.408	0.442	0.462	0.418	0.401
0.25	0.221	0.245	0.277	0.292	0.334	0.340	0.326	0.344	0.357	0.348	0.334	0.351	0.392	0.353	0.334	0.334
0.40	0.070	0.122		0.165	0.151	0.200		0.208	0.165	0.210		0.212	0.179	0.210		0.190
0.50	0.035	0.094	0.136	0.120	0.104	0.150	0.162	0.148	0.113	0.152	0.161	0.147	0.113	0.127	0.138	0.107
0.60	0.047	0.054	0.113	0.087	0.103	0.099	0.124	0.098	0.110	0.098	0.113	0.090	0.094	0.058	0.075	0.032
0.74	0.048	0.062	0.065	0.055	0.088	0.083	0.050	0.048	0.087	0.067	0.031	0.032	0.047	-0.011	-0.027	-0.048
0.78	0.069		0.090	0.034	0.096		0.058	0.012	0.090		0.035	-0.008	0.034	-0.044	-0.108	
0.82	0.149	0.138	0.140	0.117	0.165	0.141	0.099	0.091	0.155	0.119	0.073	0.070	0.089	0.019	-0.011	-0.028
0.88	0.262	0.236	0.245	0.202	0.273	0.240	0.201	0.168	0.263	0.210	0.175	0.145	0.187	0.107	0.104	0.042
0.94	0.342	0.307		0.202	0.354	0.301		0.191	0.344	0.266		0.168	0.266	0.145		0.117
1.00	-0.012	-0.023	-0.045	-0.067	-0.042	-0.065	-0.210	-0.184	-0.083	-0.161	-0.285	-0.267	-0.333	-0.466	-0.438	-0.500

Table 11. Wing Pressure Coefficients for Fulmod for  $M_\infty = 0.300$ 

[Blanks indicate defective data]

$x/c$	$C_p$ for $\alpha = 8.1^\circ$ ; $C_L = 0.711$ ; and $\eta$ of—				$C_p$ for $\alpha = 10.1^\circ$ ; $C_L = 0.860$ ; and $\eta$ of—				$C_p$ for $\alpha = 11.1^\circ$ ; $C_L = 0.917$ ; and $\eta$ of—				$C_p$ for $\alpha = 15.1^\circ$ ; $C_L = 0.963$ ; and $\eta$ of—			
	0.33	0.50	0.67	0.82	0.33	0.50	0.67	0.82	0.33	0.50	0.67	0.82	0.33	0.50	0.67	0.82
Upper surface																
0.00	-0.945	-1.379	-1.234		-2.181	-2.868	-2.827		-2.803	-3.662	-1.215		-0.988	-1.246	-0.307	
0.05	-1.445		-1.572	-1.651	-1.822		-2.005	-2.114	-2.008		-2.199	-1.521	-1.408		-1.152	-0.573
0.10			-1.285	-1.209			-1.559	-1.487			-1.673	-1.535			-0.883	-0.606
0.14	-0.882	-1.026	-1.066	-0.993	-1.056	-1.218	-1.278	-1.203	-1.144	-1.298	-1.369	-1.481	-1.466	-0.896	-0.762	-0.609
0.20	-0.819	-0.890	-0.962	-0.915	-0.946	-1.048	-1.119	-1.075	-1.007	-1.114	-1.185	-1.263	-1.402	-0.875	-0.683	-0.630
0.25	-0.748	-0.825	-0.862	-0.820	-0.859	-0.950	-0.994	-0.953	-0.912	-1.002	-1.050	-1.103	-1.322	-0.852	-0.677	-0.649
0.30	-0.707	-0.749	-0.782	-0.731	-0.797	-0.855	-0.889	-0.839	-0.836	-0.900	-0.934	-0.948	-1.187	-0.849	-0.665	-0.621
0.35		-0.703	-0.729	-0.670		-0.788	-0.822	-0.760		-0.828	-0.867	-0.828		-0.852	-0.706	-0.610
0.40	-0.609	-0.624	-0.642	-0.606	-0.669	-0.691	-0.720	-0.679	-0.696	-0.729	-0.759	-0.736	-0.949	-0.820	-0.677	-0.602
0.50	-0.461		-0.501	-0.464	-0.513		-0.556	-0.522	-0.540		-0.594	-0.566	-0.808		-0.654	-0.578
0.60	-0.355	-0.356	-0.388		-0.392	-0.390	-0.428		-0.412	-0.415	-0.468		-0.663	-0.725	-0.635	
0.74	-0.199		-0.221	-0.230	-0.222		-0.244	-0.272	-0.232		-0.283	-0.326	-0.498		-0.579	-0.590
0.78	-0.164	-0.211	-0.192	-0.190	-0.185	-0.219	-0.218	-0.233	-0.194	-0.240	-0.260	-0.291	-0.457	-0.644	-0.589	
0.84	-0.115	-0.139	-0.129	-0.156	-0.131	-0.154	-0.150	-0.194	-0.138	-0.179	-0.188	-0.261	-0.403	-0.610	-0.546	-0.593
0.87	-0.098	-0.121		-0.117	-0.108	-0.126		-0.154	-0.115	-0.149		-0.230	-0.377	-0.581		-0.579
0.90	-0.084	-0.094	-0.082		-0.094	-0.101	-0.094		-0.102	-0.126	-0.128		-0.368	-0.573	-0.501	
0.96	-0.047	-0.032		-0.066	-0.052	-0.037		-0.099	-0.065	-0.059		-0.190	-0.326	-0.495		-0.548
1.00	-0.018	-0.027	-0.037	-0.057	-0.014	-0.032	-0.042	-0.094	-0.025	-0.057	-0.070	-0.193	-0.262	-0.492	-0.428	-0.503
Lower surface																
0.00	-0.945	-1.379	-1.234		-2.181	-2.868	-2.827		-2.803	-3.662	-1.215		-0.988	-1.246	-0.307	
0.03	0.607	0.597	0.640	0.274	0.710	0.713	0.719	0.332	0.750	0.748	0.742	0.304	0.813	0.756	0.723	0.278
0.05	0.468	0.540	0.570		0.577	0.649	0.660		0.629	0.686	0.698		0.705	0.691	0.680	
0.10		0.425				0.516				0.548				0.552		
0.20	0.253	0.306	0.335	0.338	0.339	0.391	0.414	0.414	0.379	0.428	0.450	0.409	0.446	0.451	0.439	0.391
0.25	0.215	0.237	0.268	0.289	0.295	0.311	0.341	0.357	0.335	0.341	0.374	0.349	0.398	0.341	0.354	0.324
0.40	0.063	0.113		0.160	0.123	0.179		0.215	0.155	0.205		0.210	0.186	0.199		0.175
0.50	0.028	0.086	0.135	0.116	0.080	0.137	0.184	0.161	0.108	0.152	0.204	0.154	0.124	0.118	0.163	0.095
0.60	0.046	0.042	0.111	0.085	0.093	0.090	0.150	0.115	0.115	0.100	0.163	0.100	0.112	0.046	0.095	0.022
0.74	0.044	0.055	0.050	0.055	0.079	0.084	0.069	0.076	0.099	0.086	0.069	0.053	0.065	-0.023	-0.009	-0.062
0.78	0.067		0.090	0.031	0.094		0.108	0.046	0.109		0.108	0.014	0.059		-0.022	-0.119
0.82	0.142	0.130	0.137	0.116	0.164	0.146	0.151	0.127	0.171	0.141	0.146	0.095	0.110	0.005	0.005	-0.038
0.88	0.255	0.235	0.250	0.201	0.272	0.248	0.264	0.202	0.280	0.243	0.262	0.169	0.211	0.099	0.126	0.030
0.94	0.339	0.301		0.245	0.354	0.305		0.242	0.364	0.298		0.201	0.290	0.130		0.053
1.00	-0.018	-0.027	-0.037	-0.057	-0.014	-0.032	-0.042	-0.094	-0.025	-0.057	-0.070	-0.193	-0.262	-0.492	-0.428	-0.503

Table 12. Wing Pressure Coefficients for Basln for  $M_\infty = 0.400$ 

[Blanks indicate defective data]

$x/c$	$C_p$ for $\alpha = 8.1^\circ$ ; $C_L = 0.659$ ; and $\eta$ of—				$C_p$ for $\alpha = 12.1^\circ$ ; $C_L = 0.870$ ; and $\eta$ of—				$C_p$ for $\alpha = 15.1^\circ$ ; $C_L = 0.908$ ; and $\eta$ of—			
	0.33	0.50	0.67	0.82	0.33	0.50	0.67	0.82	0.33	0.50	0.67	0.82
Upper surface												
0.00	-0.912	-1.389	-1.862	-1.158	-1.956	-2.588	-2.356	-1.815	-1.860	-1.799	-0.860	-1.265
0.05	-1.343	-1.403	-1.642	-1.738	-2.208	-2.523	-1.669	-1.904	-1.595	-1.258	-0.799	-1.113
0.10	-1.076	-1.182	-1.276		-1.746	-1.948	-1.249		-1.427	-1.056	-0.769	
0.14	-0.953	-1.067	-1.089	-1.077	-1.461	-1.541	-1.132	-1.190	-1.232	-0.984	-0.806	-0.883
0.20	-0.852	-0.901	-0.976	-0.927	-1.191	-1.155	-1.062	-1.067	-1.137	-0.917	-0.747	-0.856
0.25	-0.761	-0.832	-0.871	-0.824	-1.028	-0.969	-0.969	-0.968	-1.100	-0.884	-0.732	-0.828
0.30	-0.716	-0.746	-0.779	-0.726	-0.910	-0.829	-0.868	-0.865	-1.043	-0.865	-0.704	-0.776
0.35		-0.695	-0.711	-0.663		-0.742	-0.794	-0.772		-0.845	-0.704	-0.705
0.40	-0.606	-0.614	-0.628	-0.585	-0.720	-0.658	-0.716	-0.686	-0.940	-0.799	-0.677	-0.680
0.50	-0.447		-0.487	-0.452	-0.561		-0.584	-0.533	-0.862		-0.640	-0.607
0.60	-0.344	-0.345	-0.366		-0.428	-0.425	-0.480		-0.745	-0.635	-0.611	
0.74	-0.186	-0.197	-0.203	-0.218	-0.265	-0.305	-0.366	-0.318	-0.573	-0.552	-0.566	-0.524
0.78	-0.142	-0.154	-0.170	-0.183	-0.222	-0.265	-0.342	-0.295	-0.525	-0.506	-0.565	-0.514
0.84	-0.088	-0.095	-0.103	-0.130	-0.166	-0.220	-0.304	-0.270	-0.463	-0.482	-0.534	-0.495
0.87	-0.060	-0.066	-0.071	-0.103	-0.139	-0.195	-0.284	-0.253	-0.435	-0.459	-0.516	-0.477
0.90	-0.029	-0.038	-0.043	-0.072	-0.107	-0.176	-0.270	-0.244	-0.414	-0.442	-0.504	-0.462
0.96	0.048	0.044	0.020	-0.016	-0.036	-0.131	-0.237	-0.215	-0.359	-0.393	-0.481	-0.437
1.00	0.097	0.066	0.071	0.023	0.031	-0.126	-0.210	-0.195	-0.303	-0.377	-0.444	-0.409
Lower surface												
0.00	-0.912	-1.389	-1.862	-1.158	-1.956	-2.588	-2.356	-1.815	-1.860	-1.799	-0.860	-1.265
0.03		0.635	0.673	0.630		0.758	0.737	0.688		0.767	0.731	0.675
0.05	0.522	0.543	0.577	0.436	0.680	0.677	0.666	0.385	0.728	0.687	0.667	0.600
0.10	0.374	0.403	0.442	0.417	0.533	0.547	0.536	0.472	0.582	0.559	0.548	0.507
0.20	0.226	0.274	0.307	0.296	0.363	0.390	0.391	0.363	0.412	0.422	0.399	0.382
0.25	0.182	0.224	0.244	0.255	0.309	0.334	0.320	0.318	0.355	0.346	0.321	0.325
0.40	0.037	0.082		0.123	0.137	0.166		0.161	0.157	0.178		0.165
0.50	-0.001	0.040	0.083	0.080	0.081	0.102	0.114	0.100	0.086	0.090	0.090	0.089
0.60	0.029	0.050	0.068	0.067	0.085	0.084	0.075	0.070	0.075	0.063	0.029	0.042
0.74	0.041	0.056	0.053	0.056	0.063	0.054	0.023	0.020	0.027	-0.004	-0.043	-0.026
0.78	0.038	0.054	0.057	0.045	0.053	0.042	0.010	-0.002	-0.001	-0.032	-0.078	-0.064
0.82	0.042	0.066	0.056	0.052	0.050	0.041	-0.005	-0.008	-0.026	-0.046	-0.110	-0.073
0.88	0.056	0.067	0.070	0.041	0.044	0.009	-0.033	-0.050	-0.061	-0.095	-0.144	-0.138
0.94	0.077	0.074	0.060	0.033	0.042	-0.018	-0.092	-0.097	-0.110	-0.175	-0.250	-0.216
1.00	0.097	0.066	0.071	0.023	0.031	-0.126	-0.210	-0.195	-0.303	-0.377	-0.444	-0.409

Table 13. Wing Pressure Coefficients for Temod for  $M_\infty = 0.400$ 

[Blanks indicate defective data]

$x/c$	$C_p$ for $\alpha = 8.1^\circ$ ; $C_L = 0.725$ ; and $\eta$ of—				$C_p$ for $\alpha = 10.1^\circ$ ; $C_L = 0.850$ ; and $\eta$ of—				$C_p$ for $\alpha = 11.1^\circ$ ; $C_L = 0.896$ ; and $\eta$ of—				$C_p$ for $\alpha = 15.1^\circ$ ; $C_L = 0.952$ ; and $\eta$ of—			
	0.33	0.50	0.67	0.82	0.33	0.50	0.67	0.82	0.33	0.50	0.67	0.82	0.33	0.50	0.67	0.82
Upper surface																
0.00	-1.086	-1.622	-1.644	-1.180	-2.121	-2.642	-1.360	-1.982	-1.828	-2.572	-1.221	-1.653	-1.544	-1.685	-0.662	-1.600
0.05	-1.399		-2.007	-1.887	-1.781		-1.618	-2.496	-2.205		-1.333	-1.844	-1.496		-0.634	-1.355
0.10	-1.117		-1.407	-1.410	-1.348		-1.598	-1.757	-1.642		-1.358	-1.539	-1.446		-0.636	-0.910
0.14	-0.996	-1.105	-1.206	-1.174	-1.163	-1.300	-1.486	-1.344	-1.330	-1.426	-1.326	-1.428	-1.364	-0.956	-0.644	-0.864
0.20	-0.873	-0.942	-1.008	-0.979	-1.002	-1.083	-1.253	-1.042	-1.107	-1.121	-1.175	-1.245	-1.235	-0.891	-0.619	-0.826
0.25	-0.783	-0.875	-0.910	-0.852	-0.894	-0.984	-1.109	-0.891	-0.974	-0.991	-1.068	-1.082	-1.162	-0.865	-0.622	-0.778
0.30	-0.740	-0.777	-0.813	-0.760	-0.828	-0.866	-0.955	-0.784	-0.880	-0.867	-0.954	-0.932	-1.073	-0.838	-0.603	-0.706
0.35		-0.726	-0.742	-0.692		-0.796	-0.854	-0.712		-0.792	-0.885	-0.809		-0.829	-0.627	-0.653
0.40	-0.636	-0.647	-0.659	-0.621	-0.694	-0.701	-0.750	-0.639	-0.721	-0.699	-0.806	-0.712	-0.904	-0.787	-0.606	-0.629
0.50	-0.481		-0.512	-0.482	-0.539		-0.593	-0.496	-0.567		-0.690	-0.546	-0.809		-0.601	-0.570
0.60	-0.371	-0.373	-0.392		-0.411	-0.396	-0.478		-0.437	-0.425	-0.591		-0.714	-0.665	-0.602	
0.74	-0.210		-0.231	-0.232	-0.242		-0.344	-0.258	-0.271		-0.457	-0.299	-0.586		-0.581	-0.540
0.78	-0.175	-0.226	-0.195	-0.192	-0.206	-0.239	-0.319	-0.225	-0.233	-0.292	-0.430	-0.267	-0.555	-0.592	-0.594	-0.539
0.84	-0.124	-0.163	-0.140	-0.158	-0.150	-0.183	-0.266	-0.199	-0.176	-0.234	-0.374	-0.243	-0.504	-0.573	-0.564	-0.545
0.87	-0.105	-0.130	-0.121	-0.128	-0.148		-0.166	-0.153	-0.202		-0.215	-0.477	-0.542			-0.525
0.90	-0.084	-0.110	-0.093		-0.107	-0.129	-0.220		-0.131	-0.181	-0.323		-0.462	-0.539	-0.529	
0.96	-0.050	-0.041	-0.054	-0.079	-0.073	-0.065	-0.178	-0.137	-0.100	-0.113	-0.282	-0.193	-0.431	-0.467	-0.507	-0.514
1.00	-0.029	-0.031	-0.061	-0.080	-0.047	-0.059	-0.172	-0.155	-0.084	-0.119	-0.250	-0.214	-0.376	-0.455	-0.448	-0.503
Lower surface																
0.00	-1.086	-1.622	-1.644	-1.180	-2.121	-2.642	-1.360	-1.982	-1.828	-2.572	-1.221	-1.653	-1.544	-1.685	-0.662	-1.600
0.03	0.646	0.661	0.685	0.365	0.736	0.746	0.715	0.406	0.754	0.764	0.726	0.399	0.805	0.790	0.722	0.381
0.05	0.550	0.551	0.596	0.371	0.647	0.648	0.638	0.508	0.676	0.673	0.651	0.552	0.744	0.701	0.667	0.610
0.10	0.399	0.431	0.462	0.439	0.491	0.516	0.510	0.497	0.523	0.539	0.524	0.507	0.597	0.567	0.555	0.513
0.20	0.252	0.300	0.330	0.318	0.329	0.372	0.371	0.367	0.358	0.398	0.384	0.379	0.431	0.450	0.409	0.399
0.25	0.207	0.247	0.263	0.273	0.279	0.307	0.302	0.315	0.307	0.328	0.313	0.324	0.378	0.349	0.327	0.334
0.40	0.065	0.109		0.148	0.120	0.161		0.179	0.140	0.179		0.187	0.176	0.199		0.189
0.50	0.027	0.082	0.120	0.104	0.070	0.121	0.139	0.126	0.085	0.131	0.140	0.127	0.102	0.119	0.125	0.112
0.60	0.028	0.031	0.094	0.070	0.063	0.061	0.103	0.078	0.074	0.068	0.097	0.077	0.071	0.041	0.057	0.038
0.74	0.030	0.053	0.053	0.042	0.053	0.066	0.044	0.036	0.057	0.060	0.028	0.024	0.019	-0.019	-0.040	-0.041
0.78	0.060		0.082	0.029	0.075		0.063	0.016	0.075		0.042	0.001	0.017		-0.049	-0.084
0.82	0.149	0.140	0.136	0.109	0.159	0.140	0.109	0.091	0.156	0.128	0.084	0.073	0.082	0.017	-0.018	-0.013
0.88	0.266	0.236	0.239	0.197	0.273	0.235	0.208	0.175	0.268	0.222	0.182	0.156	0.187	0.114	0.099	0.062
0.94	0.337	0.310		0.201	0.344	0.302		0.187	0.340	0.285		0.177	0.254	0.153		0.097
1.00	-0.029	-0.031	-0.061	-0.080	-0.047	-0.059	-0.172	-0.155	-0.084	-0.119	-0.250	-0.214	-0.376	-0.455	-0.448	-0.503

Table 14. Wing Pressure Coefficients for Fulmod for  $M_\infty = 0.400$ 

[Blanks indicate defective data]

$x/c$	$C_p$ for $\alpha = 8.1^\circ$ ; $C_L = 0.734$ ; and $\eta$ of—				$C_p$ for $\alpha = 10.1^\circ$ ; $C_L = 0.877$ ; and $\eta$ of—				$C_p$ for $\alpha = 11.1^\circ$ ; $C_L = 0.912$ ; and $\eta$ of—			
	0.33	0.50	0.67	0.82	0.33	0.50	0.67	0.82	0.33	0.50	0.67	0.82
Upper surface												
0.00	-1.485	-0.759	-1.103	-1.011		-1.687	-2.126	-1.033	-1.745	-2.102	-0.610	
0.05		-1.616	-1.703	-1.845		-2.153	-1.676	-2.128		-2.293	-1.131	
0.10		-1.332	-1.247			-1.605	-1.619			-1.620	-1.196	
0.14	-0.909	-1.061	-1.090	-1.028	-1.084	-1.245	-1.324	-1.510	-1.216	-1.384	-1.342	
0.20	-0.846	-0.925	-0.999	-0.951	-0.970	-1.069	-1.148	-1.241	-1.043	-1.106	-1.176	
0.25	-0.769	-0.861	-0.897	-0.840	-0.875	-0.973	-1.027	-1.043	-0.933	-0.985	-1.063	
0.30	-0.731	-0.778	-0.817	-0.754	-0.815	-0.871	-0.913	-0.891	-0.856	-0.883	-0.938	
0.35		-0.726	-0.747	-0.694		-0.804	-0.830	-0.782		-0.820	-0.852	
0.40	-0.631	-0.645	-0.666	-0.626	-0.689	-0.708	-0.732	-0.693	-0.713	-0.728	-0.746	
0.50	-0.481		-0.520	-0.481	-0.533		-0.565	-0.535	-0.553		-0.591	
0.60	-0.371	-0.373	-0.395		-0.410	-0.401	-0.431		-0.426	-0.452	-0.476	
0.74	-0.212		-0.227	-0.240	-0.236		-0.254	-0.290	-0.250		-0.334	
0.78	-0.174	-0.215	-0.191	-0.201	-0.196	-0.229	-0.223	-0.255	-0.209	-0.304	-0.311	
0.84	-0.124	-0.145	-0.136	-0.161	-0.144	-0.164	-0.163	-0.222	-0.155	-0.242	-0.257	
0.87	-0.108	-0.127		-0.124	-0.121	-0.139		-0.190	-0.132	-0.217		
0.90	-0.087	-0.102	-0.088		-0.100	-0.117	-0.113		-0.111	-0.195	-0.211	
0.96	-0.050	-0.045		-0.074	-0.061	-0.058		-0.145	-0.076	-0.131		
1.00	-0.032	-0.030	-0.044	-0.063	-0.032	-0.048	-0.067	-0.155	-0.051	-0.130	-0.162	
Lower surface												
0.00	0.594	-0.759	-1.103	-1.011	0.704	0.704	0.715	0.337	0.737	0.737	0.726	0.318
0.05	0.453	0.588	0.635	0.311	0.567	0.645	0.655		0.609	0.676	0.670	
0.10		0.540	0.566			0.521				0.546		
0.20	0.247	0.294	0.331	0.327	0.331	0.378	0.406	0.377	0.361	0.400	0.416	0.369
0.25	0.204	0.247	0.266	0.280	0.283	0.315	0.334	0.323	0.312	0.329	0.341	0.313
0.40	0.063	0.106		0.149	0.123	0.168		0.185	0.144	0.179		0.176
0.50	0.023	0.079	0.121	0.108	0.075	0.123	0.167	0.134	0.091	0.125	0.167	0.118
0.60	0.027	0.022	0.099	0.076	0.072	0.061	0.132	0.089	0.085	0.058	0.124	0.066
0.74	0.028	0.050	0.044	0.043	0.062	0.069	0.059	0.043	0.069	0.054	0.045	0.010
0.78	0.059		0.086	0.033		0.085		0.096	0.022	0.089		0.074
0.82	0.147	0.136	0.141	0.108	0.164	0.143	0.145	0.095	0.164	0.120	0.117	0.053
0.88	0.264	0.233	0.241	0.198	0.278	0.243	0.248	0.178	0.277	0.220	0.220	0.133
0.94	0.337	0.308		0.247	0.351	0.307		0.218	0.352	0.279		0.167
1.00	-0.032	-0.030	-0.044	-0.063	-0.032	-0.048	-0.067	-0.155	-0.051	-0.130	-0.162	-0.281

Table 15. Wing Pressure Coefficients for Basln for  $M_\infty = 0.725$ 

[Blanks indicate defective data]

$x/c$	$C_p$ for $\alpha = 1.5^\circ$ ; $C_L = 0.171$ ; and $\eta$ of—				$C_p$ for $\alpha = 7.1^\circ$ ; $C_L = 0.679$ ; and $\eta$ of—				$C_p$ for $\alpha = 10.0^\circ$ ; $C_L = 0.814$ ; and $\eta$ of—			
	0.33	0.50	0.67	0.82	0.33	0.50	0.67	0.82	0.33	0.50	0.67	0.82
Upper surface												
0.00	0.756	0.752	0.787	0.766	0.448	0.337	0.044	0.347	0.046	-0.068	-0.114	0.069
0.05	-0.252	-0.286	-0.312	-0.282	-1.370	-1.451	-1.526	-1.640	-1.789	-1.771	-0.822	-1.757
0.10	-0.393	-0.442	-0.472		-1.375	-1.418	-1.550		-1.747	-1.545	-0.813	
0.14	-0.463	-0.519	-0.492	-0.453	-0.867	-1.459	-1.525	-1.628	-1.744	-1.302	-0.789	-1.103
0.20	-0.507	-0.512	-0.586	-0.645	-1.059	-1.307	-1.563	-1.213	-1.720	-1.085	-0.755	-1.176
0.25	-0.486	-0.545	-0.571	-0.592	-1.201	-1.238	-1.544	-1.273	-1.274	-0.989	-0.753	-1.114
0.30	-0.519	-0.528	-0.555	-0.494	-0.931	-1.218	-1.106	-0.934	-0.964	-0.843	-0.758	-0.821
0.35		-0.524	-0.526	-0.482		-0.764	-0.824	-0.760		-0.760	-0.763	-0.707
0.40	-0.499	-0.481	-0.484	-0.423	-0.717	-0.623	-0.657	-0.650	-0.630	-0.714	-0.757	-0.645
0.50	-0.357		-0.375	-0.320	-0.510		-0.445	-0.455	-0.500		-0.721	-0.547
0.60	-0.283	-0.267	-0.280		-0.365	-0.320	-0.345		-0.388	-0.467	-0.633	
0.74	-0.147	-0.132	-0.139	-0.142	-0.183	-0.162	-0.189	-0.164	-0.243	-0.333	-0.538	-0.401
0.78	-0.105	-0.097	-0.105	-0.113	-0.132	-0.119	-0.151	-0.127	-0.198	-0.300	-0.511	-0.373
0.84	-0.065	-0.048	-0.054	-0.069	-0.072	-0.061	-0.083	-0.079	-0.150	-0.255	-0.464	-0.326
0.87	-0.041	-0.030	-0.023	-0.042	-0.042	-0.033	-0.051	-0.054	-0.121	-0.237	-0.440	-0.305
0.90	-0.006	-0.006	0.005	-0.015	-0.008	-0.005	-0.022	-0.033	-0.087	-0.220	-0.414	-0.290
0.96	0.090	0.079	0.077	0.052	0.074	0.076	0.041	0.011	0.005	-0.187	-0.358	-0.234
1.00	0.159	0.120	0.153	0.100	0.124	0.100	0.093	0.032	0.074	-0.175	-0.301	-0.185
Lower surface												
0.00	0.756	0.752	0.787	0.766	0.448	0.337	0.044	0.347	0.046	-0.068	-0.114	0.069
0.03		-0.140	-0.097	-0.139		0.521	0.565	0.523		0.650	0.659	0.606
0.05	-0.085	-0.057	-0.088	-0.156	0.433	0.453	0.474	0.427	0.581	0.577	0.571	0.488
0.10	-0.083	-0.071	-0.043	-0.026	0.314	0.331	0.362	0.350	0.444	0.447	0.447	0.421
0.20	-0.126	-0.096	-0.047	-0.042	0.178	0.216	0.253	0.242	0.288	0.304	0.323	0.293
0.25	-0.148	-0.106	-0.084	-0.050	0.133	0.172	0.189	0.202	0.235	0.260	0.254	0.253
0.40	-0.251	-0.212		-0.128	-0.022	0.020		0.068	0.059	0.078		0.093
0.50	-0.248	-0.200	-0.150	-0.126	-0.058	-0.017	0.029	0.027	0.004	0.022	0.042	0.034
0.60	-0.170	-0.145	-0.111	-0.095	-0.025	-0.004	0.021	0.019	0.011	0.004	0.007	0.003
0.74	-0.083	-0.053	-0.035	-0.039	0.012	0.032	0.035	0.024	0.016	0.003	-0.020	-0.030
0.78	-0.059	-0.028	-0.015	-0.022	0.020	0.041	0.045	0.023	0.017	0.000	-0.037	-0.042
0.82	-0.029	0.002	0.006	-0.002	0.033	0.059	0.049	0.030	0.022	0.004	-0.051	-0.049
0.88	0.015	0.027	0.040	0.019	0.056	0.066	0.065	0.024	0.027	-0.034	-0.087	-0.079
0.94	0.071	0.075	0.078	0.045	0.088	0.086	0.066	0.018	0.040	-0.053	-0.152	-0.123
1.00	0.159	0.120	0.153	0.100	0.124	0.100	0.093	0.032	0.074	-0.175	-0.301	-0.185

Table 16. Wing Pressure Coefficients for Temod for  $M_\infty = 0.725$ 

[Blanks indicate defective data]

$x/c$	$C_p$ for $\alpha = 1.1^\circ$ ; $C_L = 0.187$ ; and $\eta$ of—				$C_p$ for $\alpha = 6.0^\circ$ ; $C_L = 0.670$ ; and $\eta$ of—				$C_p$ for $\alpha = 8.1^\circ$ ; $C_L = 0.824$ ; and $\eta$ of—			
	0.33	0.50	0.67	0.82	0.33	0.50	0.67	0.82	0.33	0.50	0.67	0.82
Upper surface												
0.00	0.728	0.724	0.775	0.729	0.572	0.464	0.140	0.440	0.286	0.158	-0.121	0.195
0.05	-0.212		-0.227	-0.221	-1.221		-1.275	-1.482	-1.590		-1.629	-1.765
0.10	-0.365		-0.441	-0.335	-1.060		-1.362	-1.443	-1.515		-1.674	-1.713
0.14	-0.452	-0.477	-0.545	-0.424	-0.877	-1.204	-1.438	-1.510	-1.541	-1.548	-1.486	-1.731
0.20	-0.482	-0.492	-0.561	-0.625	-1.031	-1.199	-1.455	-1.126	-1.101	-1.551	-1.007	-1.411
0.25	-0.470	-0.533	-0.556	-0.563	-1.163	-1.219	-1.419	-1.365	-1.128	-1.558	-0.964	-1.266
0.30	-0.508	-0.522	-0.547	-0.487	-0.821	-1.113	-1.344	-0.981	-1.141	-1.414	-0.925	-0.981
0.35		-0.524	-0.525	-0.478		-0.806	-0.783	-0.712		-0.936	-0.870	-0.822
0.40	-0.507	-0.485	-0.486	-0.451	-0.731	-0.661	-0.632	-0.605	-0.812	-0.748	-0.799	-0.745
0.50	-0.380		-0.378	-0.316	-0.543		-0.476	-0.432	-0.556		-0.651	-0.535
0.60	-0.298	-0.275	-0.280		-0.392	-0.356	-0.359		-0.405	-0.365	-0.532	
0.74	-0.155		-0.136	-0.125	-0.208		-0.183	-0.194	-0.227		-0.407	-0.244
0.78	-0.119	-0.182	-0.104	-0.094	-0.166	-0.207	-0.146	-0.155	-0.187	-0.248	-0.378	-0.216
0.84	-0.077	-0.102	-0.060	-0.063	-0.112	-0.125	-0.091	-0.115	-0.130	-0.163	-0.328	-0.186
0.87	-0.069	-0.098		-0.037	-0.091	-0.110		-0.082	-0.109	-0.144		-0.158
0.90	-0.045	-0.069	-0.027		-0.067	-0.081	-0.049		-0.084	-0.117	-0.279	
0.96	-0.024	-0.013	-0.011	-0.019	-0.031	-0.018	-0.020	-0.043	-0.045	-0.045	-0.230	-0.127
1.00	-0.043	-0.026	-0.040	-0.029	-0.018	-0.012	-0.034	-0.042	-0.034	-0.049	-0.203	-0.142
Lower surface												
0.00	0.728	0.724	0.775	0.729	0.572	0.464	0.140	0.440	0.286	0.158	-0.121	0.195
0.03	-0.199	-0.160	-0.151	-0.111	0.457	0.472	0.521	0.299	0.592	0.591	0.624	0.372
0.05	-0.113	-0.172	-0.106	-0.124	0.386	0.379	0.433	0.278	0.507	0.503	0.534	0.401
0.10	-0.102	-0.098	-0.065	-0.037	0.273	0.296	0.327	0.327	0.379	0.396	0.412	0.403
0.20	-0.136	-0.108	-0.058	-0.049	0.148	0.190	0.229	0.229	0.236	0.270	0.297	0.284
0.25	-0.154	-0.121	-0.095	-0.058	0.107	0.147	0.167	0.190	0.187	0.224	0.231	0.245
0.40	-0.250	-0.212		-0.123	-0.036	0.009		0.069	0.031	0.070		0.106
0.50	-0.248	-0.181	-0.127	-0.121	-0.070	-0.007	0.042	0.033	-0.013	0.043	0.073	0.061
0.60	-0.197	-0.196	-0.102	-0.106	-0.059	-0.055	0.028	0.008	-0.018	-0.023	0.042	0.021
0.74	-0.116	-0.080	-0.047	-0.075	-0.026	0.009	0.025	-0.001	-0.004	0.026	0.012	-0.011
0.78	-0.037		0.008	-0.045	0.033		0.071	0.009	0.049		0.044	-0.008
0.82	0.092	0.082	0.096	0.066	0.150	0.139	0.145	0.106	0.163	0.146	0.111	0.082
0.88	0.232	0.206	0.219	0.188	0.287	0.259	0.265	0.219	0.298	0.257	0.218	0.193
0.94	0.308	0.290		0.243	0.368	0.342		0.256	0.376	0.346		0.237
1.00	-0.043	-0.026	-0.040	-0.029	-0.018	-0.012	-0.034	-0.042	-0.034	-0.049	-0.203	-0.142

Table 17. Wing Pressure Coefficients for Fulmod for  $M_\infty = 0.725$ 

[Blanks indicate defective data]

$x/c$	$C_p$ for $\alpha = 1.0^\circ$ ; $C_L = 0.184$ ; and $\eta$ of—				$C_p$ for $\alpha = 6.0^\circ$ ; $C_L = 0.668$ ; and $\eta$ of—				$C_p$ for $\alpha = 8.0^\circ$ ; $C_L = 0.815$ ; and $\eta$ of—			
	0.33	0.50	0.67	0.82	0.33	0.50	0.67	0.82	0.33	0.50	0.67	0.82
Upper surface												
0.00	-0.297	0.750	0.729	0.691	-1.427	0.578	0.528	0.585	-1.731	0.383	0.306	0.384
0.05			-0.351	-0.275			-1.441	-1.510			-1.671	-1.679
0.10			-0.490	-0.377			-1.525	-1.556			-1.730	-1.556
0.14	-0.359	-0.468	-0.453	-0.398	-0.709	-1.417	-1.530	-1.447	-1.667	-1.652	-1.334	-1.303
0.20	-0.463	-0.485	-0.541	-0.602	-0.970	-1.072	-1.484	-1.192	-1.112	-1.598	-1.098	-1.192
0.25	-0.461	-0.532	-0.543	-0.552	-0.949	-1.061	-1.474	-1.328	-1.051	-1.570	-1.018	-1.034
0.30	-0.503	-0.522	-0.540	-0.484	-0.807	-0.985	-1.084	-0.899	-0.986	-1.107	-0.942	-0.908
0.35		-0.522	-0.520	-0.475		-0.807	-0.729	-0.746		-0.890	-0.863	-0.812
0.40	-0.506	-0.484	-0.481	-0.451	-0.730	-0.677	-0.596	-0.631	-0.762	-0.705	-0.776	-0.726
0.50	-0.381		-0.378	-0.317	-0.540		-0.456	-0.441	-0.555		-0.627	-0.550
0.60	-0.297	-0.276	-0.282		-0.390	-0.358	-0.347		-0.401	-0.355	-0.513	
0.74	-0.156		-0.137	-0.128	-0.207		-0.180	-0.198	-0.224		-0.382	-0.314
0.78	-0.121	-0.159	-0.106	-0.096	-0.168	-0.190	-0.143	-0.161	-0.185	-0.236	-0.351	-0.282
0.84	-0.078	-0.090	-0.062	-0.066	-0.114	-0.116	-0.091	-0.121	-0.129	-0.159	-0.296	-0.252
0.87	-0.070	-0.091		-0.039	-0.094	-0.104		-0.086	-0.108	-0.147		-0.218
0.90	-0.047	-0.059	-0.027		-0.069	-0.074	-0.050		-0.083	-0.114	-0.249	
0.96	-0.024	-0.011		-0.022	-0.033	-0.022		-0.049	-0.051	-0.054		-0.184
1.00	-0.042	-0.023	-0.041	-0.026	-0.017	-0.011	-0.037	-0.047	-0.038	-0.057	-0.184	-0.204
Lower surface												
0.00	-0.328	0.750	0.729	0.691	0.382	0.578	0.528	0.585	0.521	0.383	0.306	0.384
0.03	-0.246	-0.437	-0.243	-0.113	0.267	0.330	0.411	0.217	0.478	0.534	0.293	
0.05		-0.286	-0.119		0.344	0.380			0.393	0.474	0.486	
0.10		-0.042				0.311				0.401		
0.20	-0.136	-0.102	-0.057	-0.045	0.144	0.184	0.222	0.229	0.227	0.263	0.291	0.285
0.25	-0.157	-0.112	-0.090	-0.057	0.101	0.145	0.164	0.188	0.179	0.218	0.228	0.239
0.40	-0.253	-0.214		-0.127	-0.040	0.000		0.063	0.024	0.061		0.099
0.50	-0.252	-0.181	-0.128	-0.121	-0.072	-0.011	0.038	0.031	-0.018	0.034	0.071	0.054
0.60	-0.199	-0.203	-0.102	-0.103	-0.063	-0.068	0.025	0.006	-0.022	-0.035	0.041	0.013
0.74	-0.117	-0.082	-0.047	-0.077	-0.031	0.003	0.017	-0.007	-0.006	0.016	0.009	-0.024
0.78	-0.039		0.007	-0.047	0.029		0.068	0.004	0.047		0.044	-0.023
0.82	0.089	0.082	0.092	0.060	0.147	0.137	0.142	0.102	0.161	0.139	0.111	0.070
0.88	0.225	0.205	0.211	0.181	0.284	0.255	0.259	0.217	0.295	0.253	0.221	0.181
0.94	0.299	0.289		0.233	0.362	0.341		0.267	0.373	0.338		0.229
1.00	-0.042	-0.023	-0.041	-0.026	-0.017	-0.011	-0.037	-0.047	-0.038	-0.057	-0.184	-0.204

Table 18. Wing Pressure Coefficients for Basln for  $M_\infty = 0.800$ 

[Blanks indicate defective data]

$x/c$	$C_p$ for $\alpha = 1.5^\circ$ ; $C_L = 0.187$ ; and $\eta$ of—				$C_p$ for $\alpha = 3.1^\circ$ ; $C_L = 0.339$ ; and $\eta$ of—				$C_p$ for $\alpha = 7.0^\circ$ ; $C_L = 0.665$ ; and $\eta$ of—				$C_p$ for $\alpha = 11.0^\circ$ ; $C_L = 0.833$ ; and $\eta$ of—				
	0.33	0.50	0.67	0.82	0.33	0.50	0.67	0.82	0.33	0.50	0.67	0.82	0.33	0.50	0.67	0.82	
Upper surface																	
0.00	0.766	0.754	0.792	0.765	0.842	0.824	0.777	0.818	0.640	0.573	0.329	0.574	0.220	0.133	-0.012	0.219	
0.05	-0.213	-0.247	-0.268	-0.270	-0.424	-0.440	-0.504	-0.547	-1.052	-1.074	-1.100	-1.181	-1.479	-1.414	-0.927	-1.547	
0.10	-0.359	-0.431	-0.473		-0.501	-0.629	-0.685		-1.128	-1.118	-1.190		-1.473	-1.027	-0.797		
0.14	-0.441	-0.576	-0.547	-0.397	-0.523	-0.733	-0.793	-0.517	-1.186	-1.199	-1.202	-1.294	-1.414	-0.853	-0.762	-1.483	
0.20	-0.664	-0.543	-0.695	-0.665	-0.743	-0.799	-0.904	-0.724	-0.911	-1.196	-1.003	-0.986	-1.088	-0.719	-0.720	-1.131	
0.25	-0.468	-0.632	-0.727	-0.998	-0.841	-0.837	-0.934	-1.063	-1.024	-1.213	-0.789	-1.166	-0.980	-0.714	-0.698	-0.927	
0.30	-0.527	-0.661	-0.740	-0.859	-0.721	-0.872	-0.973	-1.134	-1.054	-1.228	-0.671	-1.105	-0.930	-0.695	-0.685	-0.796	
0.35		-0.720	-0.767	-0.570		-0.810	-1.004	-1.003		-1.263	-0.634	-0.888		-0.695	-0.675	-0.700	
0.40	-0.740	-0.667	-0.531	-0.434	-0.810	-0.853	-1.025	-0.720	-1.019	-0.932	-0.615	-0.790	-0.839	-0.677	-0.664	-0.672	
0.50	-0.440		-0.444	-0.309	-0.562		-0.413	-0.355	-0.882		-0.573	-0.493	-0.760		-0.631	-0.640	
0.60	-0.302	-0.276	-0.276		-0.322	-0.281	-0.274		-0.444	-0.534	-0.505		-0.655	-0.585	-0.586		
0.74	-0.146	-0.123	-0.125	-0.131	-0.153	-0.125	-0.119	-0.130	-0.203	-0.309	-0.404	-0.287	-0.512	-0.511	-0.539	-0.533	
0.78	-0.101	-0.088	-0.089	-0.104	-0.107	-0.088	-0.083	-0.100	-0.151	-0.256	-0.374	-0.261	-0.471	-0.490	-0.526	-0.506	
0.84	-0.057	-0.035	-0.035	-0.056	-0.056	-0.034	-0.030	-0.053	-0.090	-0.170	-0.327	-0.219	-0.416	-0.465	-0.508	-0.469	
0.87	-0.031	-0.018	-0.006	-0.028	-0.028	-0.015	-0.001	-0.027	-0.060	-0.135	-0.305	-0.200	-0.387	-0.447	-0.497	-0.446	
0.90	0.007	0.008	0.022	0.001	0.009	0.012	0.026	0.000	-0.025	-0.099	-0.281	-0.179	-0.357	-0.429	-0.484	-0.435	
0.96	0.105	0.094	0.095	0.068	0.102	0.097	0.097	0.064	0.063	-0.019	-0.233	-0.117	-0.288	-0.381	-0.447	-0.401	
1.00	0.166	0.137	0.169	0.114	0.155	0.135	0.170	0.110	0.129	0.011	-0.190	-0.050	-0.248	-0.336	-0.404	-0.383	
Lower surface																	
0.00	0.766	0.754	0.792	0.765	0.842	0.824	0.777	0.818	0.640	0.573	0.329	0.574	0.220	0.133	-0.012	0.219	
0.03		-0.170	-0.137	-0.174		0.080	0.133	0.099		0.473	0.511	0.464		0.662	0.666	0.615	
0.05	-0.093	-0.080	-0.111	-0.147	0.082	0.088	0.088	-0.011	0.408	0.419	0.422	0.310	0.605	0.590	0.579	0.512	
0.10	-0.086	-0.084	-0.064	-0.046	0.038	0.047	0.074	0.092	0.298	0.306	0.319	0.308	0.471	0.466	0.455	0.431	
0.20	-0.132	-0.114	-0.065	-0.056	-0.039	-0.016	0.035	0.035	0.165	0.187	0.219	0.200	0.311	0.318	0.330	0.303	
0.25	-0.161	-0.123	-0.104	-0.063	-0.075	-0.034	-0.013	0.019	0.115	0.150	0.155	0.166	0.251	0.274	0.260	0.263	
0.40	-0.285	-0.247		-0.152	-0.210	-0.171		-0.089	-0.049	-0.018		0.015	0.063	0.077		0.087	
0.50	-0.285	-0.232	-0.176	-0.146	-0.224	-0.175	-0.118	-0.099	-0.091	-0.058	-0.028	-0.030	-0.005	0.007	0.024	0.020	
0.60	-0.194	-0.169	-0.127	-0.110	-0.151	-0.128	-0.087	-0.076	-0.059	-0.051	-0.041	-0.044	-0.010	-0.022	-0.019	-0.017	
0.74	-0.092	-0.057	-0.038	-0.043	-0.067	-0.034	-0.016	-0.024	-0.021	-0.008	-0.030	-0.047	-0.027	-0.035	-0.048	-0.064	
0.78	-0.064	-0.028	-0.014	-0.023	-0.043	-0.009	0.005	-0.008	-0.008	0.002	-0.035	-0.049	-0.032	-0.044	-0.072	-0.080	
0.82	-0.030	0.007	0.012	0.001	-0.014	0.022	0.027	0.011	0.010	0.019	-0.037	-0.045	-0.035	-0.047	-0.088	-0.094	
0.88	0.018	0.035	0.047	0.027	0.028	0.043	0.057	0.030	0.034	0.012	-0.054	-0.055	-0.057	-0.106	-0.135	-0.141	
0.94	0.081	0.089	0.090	0.056	0.083	0.093	0.095	0.055	0.074	0.029	-0.091	-0.068	-0.093	-0.148	-0.209	-0.219	
1.00	0.166	0.137	0.169	0.114	0.155	0.135	0.170	0.110	0.129	0.011	-0.190	-0.050	-0.248	-0.336	-0.404	-0.383	

Table 19. Wing Pressure Coefficients for Temod for  $M_\infty = 0.800$ 

[Blanks indicate defective data]

$x/c$	$C_p$ for $\alpha = 1.0^\circ$ ; $C_L = 0.197$ ; and $\eta$ of—				$C_p$ for $\alpha = 2.1^\circ$ ; $C_L = 0.306$ ; and $\eta$ of—				$C_p$ for $\alpha = 6.0^\circ$ ; $C_L = 0.680$ ; and $\eta$ of—				$C_p$ for $\alpha = 9.0^\circ$ ; $C_L = 0.827$ ; and $\eta$ of—			
	0.33	0.50	0.67	0.82	0.33	0.50	0.67	0.82	0.33	0.50	0.67	0.82	0.33	0.50	0.67	0.82
Upper surface																
0.00	0.720	0.719	0.766	0.717	0.817	0.805	0.802	0.815	0.718	0.660	0.391	0.637	0.435	0.352	0.109	0.398
0.05	-0.153		-0.161	-0.191	-0.294		-0.315	-0.387	-0.966		-0.864	-1.063	-1.310		-1.277	-1.397
0.10	-0.313		-0.418	-0.308	-0.412		-0.577	-0.470	-1.046		-1.083	-1.107	-1.300		-1.166	-1.378
0.14	-0.422	-0.466	-0.557	-0.366	-0.490	-0.515	-0.701	-0.454	-1.012	-1.068	-1.170	-1.220	-1.342	-1.301	-0.859	-1.418
0.20	-0.584	-0.503	-0.634	-0.644	-0.692	-0.682	-0.774	-0.686	-0.834	-1.096	-1.226	-0.922	-1.285	-1.225	-0.723	-1.252
0.25	-0.462	-0.604	-0.675	-0.952	-0.663	-0.690	-0.804	-1.005	-0.975	-1.169	-1.150	-1.139	-1.087	-0.884	-0.694	-1.192
0.30	-0.508	-0.642	-0.711	-0.785	-0.523	-0.712	-0.839	-1.002	-0.945	-1.181	-0.794	-1.191	-1.039	-0.810	-0.666	-1.025
0.35		-0.683	-0.728	-0.589		-0.770	-0.860	-0.883		-1.155	-0.645	-0.975		-0.791	-0.643	-0.842
0.40	-0.716	-0.664	-0.594	-0.487	-0.795	-0.815	-0.896	-0.694	-1.022	-1.123	-0.626	-0.885	-0.773	-0.769	-0.618	-0.777
0.50	-0.475		-0.455	-0.311	-0.558		-0.441	-0.343	-0.913		-0.594	-0.559	-0.718		-0.570	-0.639
0.60	-0.318	-0.292	-0.279		-0.338	-0.300	-0.284		-0.490	-0.516	-0.540		-0.650	-0.670	-0.528	
0.74	-0.155		-0.121	-0.119	-0.164		-0.122	-0.130	-0.216		-0.445	-0.301	-0.528		-0.477	-0.407
0.78	-0.116	-0.166	-0.086	-0.086	-0.125	-0.167	-0.088	-0.095	-0.160	-0.227	-0.420	-0.264	-0.487	-0.552	-0.467	-0.372
0.84	-0.069	-0.075	-0.043	-0.052	-0.075	-0.079	-0.044	-0.059	-0.091	-0.138	-0.375	-0.225	-0.413	-0.504	-0.448	-0.339
0.87	-0.059	-0.076		-0.025	-0.063	-0.078		-0.030	-0.070	-0.130		-0.186	-0.375	-0.473		-0.304
0.90	-0.034	-0.051	-0.009		-0.038	-0.053	-0.010		-0.046	-0.104	-0.328		-0.337	-0.459	-0.426	
0.96	-0.009	0.004	0.010	-0.003	-0.010	0.003	0.010	-0.005	-0.020	-0.034	-0.279	-0.149	-0.273	-0.380	-0.400	-0.272
1.00	-0.017	0.002	-0.016	-0.008	-0.012	0.002	-0.016	-0.017	-0.025	-0.046	-0.232	-0.171	-0.229	-0.343	-0.351	-0.306
Lower surface																
0.00	0.720	0.719	0.766	0.717	0.817	0.805	0.802	0.815	0.718	0.660	0.391	0.637	0.435	0.352	0.109	0.398
0.03	-0.249	-0.202	-0.230	-0.146	-0.053	-0.018	-0.001	-0.035	0.426	0.432	0.470	0.255	0.607	0.593	0.610	0.363
0.05	-0.146	-0.202	-0.154	-0.190	-0.011	-0.068	-0.008	-0.093	0.363	0.335	0.389	0.283	0.525	0.502	0.524	0.467
0.10	-0.122	-0.121	-0.099	-0.071	-0.025	-0.021	0.007	0.027	0.260	0.270	0.294	0.286	0.398	0.401	0.405	0.388
0.20	-0.154	-0.131	-0.087	-0.072	-0.083	-0.059	-0.011	-0.004	0.138	0.165	0.201	0.188	0.251	0.272	0.289	0.268
0.25	-0.177	-0.144	-0.122	-0.079	-0.111	-0.080	-0.055	-0.019	0.094	0.124	0.139	0.153	0.198	0.223	0.220	0.226
0.40	-0.295	-0.252		-0.150	-0.237	-0.198		-0.106	-0.059	-0.026		0.022	0.024	0.052		0.072
0.50	-0.294	-0.213	-0.151	-0.143	-0.247	-0.172	-0.110	-0.109	-0.097	-0.040	0.001	-0.016	-0.036	0.013	0.034	0.016
0.60	-0.226	-0.218	-0.118	-0.117	-0.194	-0.189	-0.088	-0.093	-0.086	-0.093	-0.018	-0.039	-0.054	-0.069	-0.010	-0.030
0.74	-0.124	-0.083	-0.046	-0.078	-0.108	-0.066	-0.031	-0.065	-0.048	-0.018	-0.023	-0.057	-0.060	-0.037	-0.046	-0.082
0.78	-0.033		0.018	-0.040	-0.020		0.030	-0.031	0.023		0.016	-0.042	-0.002		-0.022	-0.079
0.82	0.104	0.097	0.109	0.077	0.117	0.109	0.119	0.085	0.153	0.132	0.093	0.064	0.125	0.088	0.054	0.024
0.88	0.243	0.221	0.232	0.202	0.257	0.234	0.244	0.210	0.295	0.255	0.212	0.189	0.266	0.201	0.175	0.149
0.94	0.316	0.302		0.243	0.332	0.318		0.249	0.374	0.343		0.243	0.342	0.289		0.214
1.00	-0.017	0.002	-0.016	-0.008	-0.012	0.002	-0.016	-0.017	-0.025	-0.046	-0.232	-0.171	-0.229	-0.343	-0.351	-0.306

Table 20. Wing Pressure Coefficients for Fulmod for  $M_\infty = 0.800$ 

[Blanks indicate defective data]

$x/c$	$C_p$ for $\alpha = 1.1^\circ$ ; $C_L = 0.199$ ; and $\eta$ of—				$C_p$ for $\alpha = 2.0^\circ$ ; $C_L = 0.297$ ; and $\eta$ of—				$C_p$ for $\alpha = 6.0^\circ$ ; $C_L = 0.685$ ; and $\eta$ of—				$C_p$ for $\alpha = 9.1^\circ$ ; $C_L = 0.837$ ; and $\eta$ of—			
	0.33	0.50	0.67	0.82	0.33	0.50	0.67	0.82	0.33	0.50	0.67	0.82	0.33	0.50	0.67	0.82
Upper surface																
0.00	0.756	0.728	0.703		0.806	0.788	0.777		0.712	0.684	0.729		0.507	0.461	0.530	
0.05	-0.274		-0.302	-0.265	-0.421		-0.432	-0.444	-1.107		-1.040	-1.062	-1.426		-1.268	-1.365
0.10			-0.510	-0.365			-0.664	-0.463			-1.203	-1.203			-1.221	-1.352
0.14	-0.338	-0.470	-0.438	-0.347	-0.391	-0.562	-0.602	-0.407	-1.218	-1.212	-1.261	-1.213	-1.444	-1.357	-0.952	-1.198
0.20	-0.527	-0.524	-0.612	-0.643	-0.668	-0.612	-0.694	-0.685	-0.817	-1.167	-1.225	-0.987	-1.332	-1.053	-0.821	-1.144
0.25	-0.470	-0.614	-0.665	-0.945	-0.544	-0.685	-0.766	-0.999	-0.934	-1.189	-1.229	-1.184	-1.064	-0.924	-0.770	-1.055
0.30	-0.512	-0.646	-0.709	-0.749	-0.537	-0.732	-0.809	-0.966	-0.872	-1.200	-1.151	-1.209	-0.966	-0.851	-0.727	-0.952
0.35		-0.692	-0.721	-0.567		-0.783	-0.840	-0.852		-1.144	-0.814	-0.944		-0.819	-0.691	-0.864
0.40	-0.710	-0.638	-0.593	-0.494	-0.801	-0.833	-0.882	-0.634	-1.002	-1.090	-0.717	-0.858	-0.807	-0.785	-0.660	-0.784
0.50	-0.471		-0.460	-0.317	-0.540		-0.450	-0.343	-0.895		-0.642	-0.571	-0.741		-0.604	-0.551
0.60	-0.318	-0.293	-0.283		-0.335	-0.302	-0.287		-0.485	-0.464	-0.543		-0.658	-0.651	-0.554	
0.74	-0.159		-0.125	-0.126	-0.168		-0.126	-0.138	-0.218		-0.396	-0.297	-0.523		-0.499	-0.421
0.78	-0.119	-0.155	-0.089	-0.092	-0.127	-0.157	-0.091	-0.102	-0.163	-0.225	-0.357	-0.261	-0.478	-0.521	-0.483	-0.400
0.84	-0.075	-0.076	-0.045	-0.057	-0.081	-0.080	-0.045	-0.063	-0.093	-0.147	-0.297	-0.223	-0.401	-0.476	-0.457	-0.385
0.87	-0.060	-0.072		-0.028	-0.064	-0.074		-0.033	-0.070	-0.131		-0.180	-0.363	-0.445		-0.356
0.90	-0.040	-0.044	-0.012		-0.043	-0.047	-0.013		-0.045	-0.102	-0.239		-0.324	-0.429	-0.430	
0.96	-0.007	0.002		-0.004	-0.009	-0.001		-0.007	-0.014	-0.045		-0.150	-0.259	-0.363		-0.344
1.00	-0.017	0.002	-0.018	-0.004	-0.015	0.001	-0.016	-0.012	-0.015	-0.045	-0.156	-0.179	-0.222	-0.323	-0.353	-0.375
Lower surface																
0.00	0.756	0.728	0.703		0.806	0.788	0.777		0.712	0.684	0.729		0.507	0.461	0.530	
0.03	-0.437	-0.520	-0.339	-0.153	-0.192	-0.287	-0.168	-0.053	0.342	0.263	0.343	0.174	0.548	0.477	0.517	0.287
0.05	-0.262	-0.264	-0.163		-0.151	-0.224	-0.016		0.234	0.289	0.332		0.415	0.477	0.476	
0.10	-0.051					0.030				0.287				0.414		
0.20	-0.148	-0.120	-0.075	-0.056	-0.090	-0.058	-0.011	0.003	0.131	0.162	0.196	0.194	0.248	0.269	0.284	0.273
0.25	-0.171	-0.131	-0.111	-0.069	-0.117	-0.073	-0.054	-0.017	0.088	0.125	0.137	0.153	0.195	0.224	0.217	0.225
0.40	-0.294	-0.250		-0.147	-0.245	-0.202		-0.109	-0.064	-0.031		0.020	0.022	0.046		0.070
0.50	-0.288	-0.211	-0.150	-0.138	-0.248	-0.174	-0.115	-0.109	-0.100	-0.043	0.004	-0.017	-0.036	0.009	0.032	0.014
0.60	-0.225	-0.226	-0.115	-0.116	-0.198	-0.199	-0.091	-0.095	-0.087	-0.103	-0.011	-0.039	-0.054	-0.080	-0.010	-0.031
0.74	-0.125	-0.083	-0.046	-0.079	-0.113	-0.069	-0.034	-0.069	-0.046	-0.020	-0.011	-0.059	-0.058	-0.040	-0.042	-0.087
0.78	-0.032		0.016	-0.043	-0.022		0.026	-0.036	0.026		0.034	-0.045	0.001		-0.021	-0.086
0.82	0.102	0.096	0.108	0.074	0.114	0.106	0.118	0.079	0.155	0.129	0.112	0.063	0.126	0.085	0.055	0.017
0.88	0.235	0.214	0.221	0.190	0.250	0.226	0.233	0.199	0.296	0.251	0.230	0.187	0.267	0.197	0.174	0.139
0.94	0.305	0.302		0.249	0.323	0.318		0.262	0.374	0.340		0.245	0.342	0.287		0.192
1.00	-0.017	0.002	-0.018	-0.004	-0.015	0.001	-0.016	-0.012	-0.015	-0.045	-0.156	-0.179	-0.222	-0.323	-0.353	-0.375

Table 21. Wing Pressure Coefficients for Basln for  $M_\infty = 0.850$ 

[Blanks indicate defective data]

$x/c$	$C_p$ for $\alpha = 0.5^\circ$ ; $C_L = 0.103$ ; and $\eta$ of—				$C_p$ for $\alpha = 4.0^\circ$ ; $C_L = 0.427$ ; and $\eta$ of—				$C_p$ for $\alpha = 8.0^\circ$ ; $C_L = 0.674$ ; and $\eta$ of—				
	0.33	0.50	0.67	0.82	0.33	0.50	0.67	0.82	0.33	0.50	0.67	0.82	
Upper surface													
0.00	0.639	0.636	0.699	0.586	0.865	0.834	0.771	0.824	0.660	0.606	0.393	0.624	
0.05	-0.042	-0.069	-0.057	-0.057	-0.454	-0.463	-0.489	-0.539	-0.983	-0.971	-0.978	-1.031	
0.10	-0.211	-0.283	-0.287		-0.600	-0.615	-0.638		-1.045	-1.027	-1.066		
0.14	-0.305	-0.440	-0.376	-0.260	-0.494	-0.737	-0.746	-0.800	-1.091	-1.087	-1.024	-1.153	
0.20	-0.532	-0.432	-0.537	-0.523	-0.634	-0.794	-0.873	-0.632	-0.923	-1.079	-0.675	-0.927	
0.25	-0.503	-0.496	-0.584	-0.836	-0.791	-0.826	-0.921	-0.951	-0.932	-1.109	-0.572	-1.051	
0.30	-0.404	-0.546	-0.620	-0.757	-0.763	-0.847	-0.955	-1.072	-1.035	-1.132	-0.537	-1.110	
0.35		-0.608	-0.684	-0.698		-0.901	-0.982	-0.925		-1.055	-0.519	-0.858	
0.40	-0.652	-0.677	-0.726	-0.643	-0.844	-0.953	-1.011	-0.859	-1.004	-0.709	-0.503	-0.762	
0.50	-0.526		-0.708	-0.566	-0.758		-0.494	-0.656	-0.683		-0.483	-0.527	
0.60	-0.492	-0.334	-0.345		-0.816	-0.523	-0.419		-0.600	-0.587	-0.463		
0.74	-0.122	-0.091	-0.075	-0.085	-0.269	-0.253	-0.325	-0.250	-0.504	-0.495	-0.454	-0.403	
0.78	-0.081	-0.054	-0.034	-0.060	-0.207	-0.172	-0.280	-0.207	-0.467	-0.464	-0.450	-0.390	
0.84	-0.031	-0.002	0.009	-0.018	-0.100	-0.061	-0.227	-0.145	-0.396	-0.419	-0.445	-0.363	
0.87	-0.007	0.012	0.030	0.006	-0.054	-0.023	-0.206	-0.118	-0.356	-0.397	-0.440	-0.348	
0.90	0.030	0.035	0.056	0.027	-0.007	0.010	-0.177	-0.098	-0.315	-0.374	-0.432	-0.335	
0.96	0.123	0.110	0.122	0.093	0.087	0.076	-0.123	-0.021	-0.192	-0.324	-0.404	-0.283	
1.00	0.172	0.154	0.187	0.136	0.132	0.116	-0.084	0.034	-0.124	-0.284	-0.364	-0.216	
Lower surface													
0.00	0.639	0.636	0.699	0.586	0.865	0.834	0.771	0.824	0.660	0.606	0.393	0.624	
0.03		-0.478	-0.597	-0.643		0.152	0.200	0.151		0.497	0.522	0.462	
0.05	-0.257	-0.228	-0.273	-0.474	0.155	0.156	0.142	0.048	0.446	0.439	0.434	0.318	
0.10	-0.182	-0.203	-0.215	-0.192	0.099	0.103	0.109	0.113	0.335	0.328	0.332	0.312	
0.20	-0.205	-0.215	-0.180	-0.165	0.004	0.010	0.056	0.039	0.191	0.204	0.226	0.196	
0.25	-0.233	-0.212	-0.206	-0.160	-0.039	-0.002	0.006	0.026	0.139	0.164	0.159	0.160	
0.40	-0.395	-0.382		-0.235	-0.200	-0.180		-0.110	-0.047	-0.028		-0.008	
0.50	-0.465	-0.329	-0.262	-0.206	-0.234	-0.190	-0.148	-0.132	-0.108	-0.085	-0.061	-0.068	
0.60	-0.246	-0.217	-0.170	-0.148	-0.163	-0.152	-0.121	-0.118	-0.089	-0.092	-0.084	-0.092	
0.74	-0.112	-0.069	-0.045	-0.058	-0.084	-0.051	-0.056	-0.084	-0.070	-0.063	-0.079	-0.115	
0.78	-0.075	-0.032	-0.018	-0.030	-0.055	-0.024	-0.051	-0.069	-0.063	-0.060	-0.099	-0.124	
0.82	-0.032	0.008	0.016	-0.003	-0.020	0.008	-0.035	-0.058	-0.055	-0.051	-0.106	-0.130	
0.88	0.023	0.037	0.050	0.034	0.017	0.014	-0.046	-0.044	-0.052	-0.086	-0.136	-0.153	
0.94	0.087	0.105	0.107	0.072	0.065	0.075	-0.048	-0.030	-0.054	-0.110	-0.193	-0.189	
1.00	0.172	0.154	0.187	0.136	0.132	0.116	-0.084	0.034	-0.124	-0.284	-0.364	-0.216	

Table 22. Wing Pressure Coefficients for Temod for  $M_\infty = 0.850$ 

[Blanks indicate defective data]

$x/c$	$C_p$ for $\alpha = 0.0^\circ$ ; $C_L = 0.103$ ; and $\eta$ of—				$C_p$ for $\alpha = 3.0^\circ$ ; $C_L = 0.435$ ; and $\eta$ of—				$C_p$ for $\alpha = 7.0^\circ$ ; $C_L = 0.694$ ; and $\eta$ of—			
	0.33	0.50	0.67	0.82	0.33	0.50	0.67	0.82	0.33	0.50	0.67	0.82
Upper surface												
0.00	0.577	0.593	0.633	0.527	0.857	0.833	0.804	0.829	0.741	0.689	0.461	0.691
0.05	0.002		0.025	0.006	-0.348		-0.307	-0.403	-0.838		-0.770	-0.914
0.10	-0.178		-0.243	-0.153	-0.486		-0.562	-0.542	-0.960		-0.971	-0.980
0.14	-0.296	-0.359	-0.389	-0.234	-0.429	-0.620	-0.695	-0.626	-1.016	-1.012	-1.037	-1.086
0.20	-0.505	-0.385	-0.482	-0.510	-0.614	-0.715	-0.776	-0.607	-0.796	-0.999	-1.045	-0.825
0.25	-0.355	-0.490	-0.543	-0.803	-0.769	-0.739	-0.830	-0.900	-0.885	-1.047	-0.687	-0.998
0.30	-0.388	-0.542	-0.600	-0.679	-0.726	-0.802	-0.877	-0.996	-0.999	-1.076	-0.535	-1.071
0.35		-0.598	-0.648	-0.644		-0.863	-0.911	-0.902		-1.114	-0.520	-0.838
0.40	-0.654	-0.661	-0.695	-0.646	-0.808	-0.914	-0.959	-0.876	-0.918	-0.922	-0.508	-0.800
0.50	-0.497		-0.692	-0.571	-0.690		-0.979	-0.814	-0.838		-0.488	-0.601
0.60	-0.551	-0.334	-0.352		-0.838	-0.810	-0.445		-0.804	-0.600	-0.463	
0.74	-0.127		-0.069	-0.079	-0.295		-0.333	-0.320	-0.446		-0.442	-0.408
0.78	-0.090	-0.118	-0.037	-0.049	-0.232	-0.218	-0.301	-0.256	-0.406	-0.520	-0.434	-0.401
0.84	-0.041	-0.036	0.000	-0.016	-0.124	-0.108	-0.243	-0.184	-0.337	-0.474	-0.425	-0.387
0.87	-0.032	-0.042		0.011	-0.078	-0.072		-0.128	-0.295	-0.450		-0.351
0.90	-0.008	-0.019		0.028		-0.039	-0.037	-0.174		-0.251	-0.436	-0.418
0.96	0.021	0.033	0.044	0.026	0.017	0.027	-0.087	-0.044	-0.169	-0.357	-0.403	-0.339
1.00	0.018	0.027	0.016	0.012	0.024	0.031	-0.044	-0.042	-0.110	-0.320	-0.362	-0.382
Lower surface												
0.00	0.577	0.593	0.633	0.527	0.857	0.833	0.804	0.829	0.741	0.689	0.461	0.691
0.03	-0.663	-0.561	-0.814	-0.513	0.061	0.059	0.081	-0.001	0.466	0.448	0.477	0.255
0.05	-0.289	-0.382	-0.396	-0.207	0.072	0.015	0.056	-0.006	0.401	0.364	0.397	0.328
0.10	-0.209	-0.252	-0.249	-0.206	0.042	0.037	0.049	0.071	0.295	0.293	0.299	0.287
0.20	-0.229	-0.230	-0.204	-0.174	-0.039	-0.024	0.018	0.019	0.163	0.178	0.203	0.181
0.25	-0.249	-0.241	-0.228	-0.174	-0.072	-0.046	-0.029	0.001	0.114	0.136	0.138	0.144
0.40	-0.411	-0.370		-0.225	-0.228	-0.192		-0.106	-0.061	-0.039		-0.008
0.50	-0.489	-0.298	-0.204	-0.198	-0.251	-0.172	-0.109	-0.118	-0.117	-0.067	-0.034	-0.060
0.60	-0.271	-0.263	-0.150	-0.144	-0.194	-0.198	-0.091	-0.100	-0.118	-0.141	-0.068	-0.089
0.74	-0.129	-0.090	-0.049	-0.083	-0.101	-0.060	-0.035	-0.081	-0.092	-0.078	-0.079	-0.131
0.78	-0.025		0.023	-0.037	-0.002		0.029	-0.044	-0.011		-0.042	-0.113
0.82	0.107	0.098	0.114	0.083	0.139	0.127	0.122	0.076	0.129	0.081	0.048	0.005
0.88	0.231	0.212	0.227	0.201	0.279	0.247	0.238	0.204	0.276	0.204	0.174	0.144
0.94	0.297	0.288		0.244	0.350	0.336		0.254	0.353	0.294		0.179
1.00	0.018	0.027	0.016	0.012	0.024	0.031	-0.044	-0.042	-0.110	-0.320	-0.362	-0.382

Table 23. Wing Pressure Coefficients for Fulmod for  $M_\infty = 0.850$ 

[Blanks indicate defective data]

$x/c$	$C_p$ for $\alpha = 0.0^\circ$ ; $C_L = 0.101$ ; and $\eta$ of—				$C_p$ for $\alpha = 3.0^\circ$ ; $C_L = 0.433$ ; and $\eta$ of—				$C_p$ for $\alpha = 6.0^\circ$ ; $C_L = 0.661$ ; and $\eta$ of—			
	0.33	0.50	0.67	0.82	0.33	0.50	0.67	0.82	0.33	0.50	0.67	0.82
Upper surface												
0.00	-0.117	0.696	0.652	0.617	-0.511	0.830	0.813	0.802	-0.910	0.785	0.759	0.794
0.05			-0.117	-0.067			-0.414	-0.443			-0.800	-0.798
0.10			-0.336	-0.215			-0.681	-0.830			-0.990	-0.988
0.14	-0.220	-0.346	-0.321	-0.245	-0.338	-0.560	-0.754	-0.573	-1.058	-1.025	-1.068	-1.022
0.20	-0.487	-0.391	-0.472	-0.507	-0.590	-0.660	-0.768	-0.603	-0.718	-0.997	-1.062	-0.835
0.25	-0.349	-0.493	-0.541	-0.810	-0.701	-0.743	-0.775	-0.892	-0.861	-1.038	-1.057	-1.026
0.30	-0.402	-0.542	-0.602	-0.679	-0.719	-0.803	-0.858	-0.961	-0.923	-1.067	-0.966	-1.128
0.35		-0.605	-0.648	-0.634		-0.860	-0.894	-0.894		-1.092	-0.774	-0.927
0.40	-0.662	-0.662	-0.703	-0.643	-0.818	-0.910	-0.954	-0.874	-0.876	-1.073	-0.654	-0.847
0.50	-0.502		-0.701	-0.539	-0.690		-0.977	-0.755	-0.786		-0.562	-0.633
0.60	-0.513	-0.312	-0.341		-0.836	-0.749	-0.458		-0.923	-0.578	-0.509	
0.74	-0.134		-0.074	-0.087	-0.290		-0.329	-0.303	-0.416		-0.458	-0.379
0.78	-0.096	-0.118	-0.041	-0.057	-0.228	-0.225	-0.286	-0.237	-0.363	-0.461	-0.444	-0.359
0.84	-0.048	-0.044	-0.006	-0.025	-0.122	-0.114	-0.218	-0.163	-0.268	-0.380	-0.416	-0.335
0.87	-0.038	-0.044		0.002	-0.077	-0.072		-0.109	-0.213	-0.337		-0.295
0.90	-0.014	-0.016	0.021		-0.038	-0.036	-0.141		-0.167	-0.306	-0.378	
0.96	0.014	0.025		0.020	0.016	0.021		-0.031	-0.080	-0.209		-0.275
1.00	0.012	0.018	0.004	0.012	0.021	0.029	-0.025	-0.029	-0.036	-0.173	-0.284	-0.324
Lower surface												
0.00	-0.954	-0.914	-0.711	-0.441	-0.049	-0.175	-0.062	-0.031	0.307	0.197	0.285	0.130
0.05	-0.492	-0.736	-0.593		-0.062	-0.113	0.055		0.204	0.230	0.286	
0.10		-0.203				0.092				0.264		
0.20	-0.216	-0.210	-0.193	-0.176	-0.036	-0.017	0.026	0.028	0.118	0.135	0.169	0.156
0.25	-0.247	-0.219	-0.202	-0.163	-0.076	-0.033	-0.019	0.008	0.071	0.101	0.107	0.117
0.40	-0.403	-0.357		-0.200	-0.222	-0.193		-0.105	-0.094	-0.074		-0.030
0.50	-0.446	-0.284	-0.198	-0.174	-0.246	-0.170	-0.105	-0.114	-0.142	-0.089	-0.045	-0.074
0.60	-0.274	-0.269	-0.141	-0.135	-0.195	-0.203	-0.087	-0.098	-0.130	-0.157	-0.065	-0.097
0.74	-0.130	-0.089	-0.044	-0.066	-0.102	-0.060	-0.030	-0.081	-0.084	-0.069	-0.057	-0.127
0.78	-0.030		0.019	-0.029	-0.003		0.033	-0.042	0.000		-0.018	-0.104
0.82	0.104	0.095	0.106	0.073	0.139	0.127	0.127	0.076	0.140	0.098	0.072	0.017
0.88	0.230	0.210	0.220	0.175	0.273	0.244	0.240	0.203	0.286	0.222	0.195	0.153
0.94	0.301	0.299		0.222	0.343	0.339		0.260	0.362	0.314		0.211
1.00	0.012	0.018	0.004	0.012	0.021	0.029	-0.025	-0.029	-0.036	-0.173	-0.284	-0.324

Table 24. Wing Pressure Coefficients for Basln for  $M_\infty = 0.900$ 

[Blanks indicate defective data]

$x/c$	$C_p$ for $\alpha = 0.5^\circ$ ; $C_L = 0.077$ ; and $\eta$ of—				$C_p$ for $\alpha = 4.0^\circ$ ; $C_L = 0.369$ ; and $\eta$ of—				$C_p$ for $\alpha = 9.0^\circ$ ; $C_L = 0.737$ ; and $\eta$ of—			
	0.33	0.50	0.67	0.82	0.33	0.50	0.67	0.82	0.33	0.50	0.67	0.82
Upper surface												
0.00	0.653	0.638	0.685	0.565	0.884	0.851	0.818	0.830	0.673	0.620	0.435	0.656
0.05	0.017	-0.003	0.014	0.010	-0.335	-0.317	-0.324	-0.348	-0.913	-0.887	-0.875	-0.916
0.10	-0.144	-0.225	-0.220		-0.498	-0.486	-0.494		-0.942	-0.927	-0.946	
0.14	-0.229	-0.353	-0.333	-0.185	-0.549	-0.604	-0.603	-0.635	-0.995	-0.977	-0.959	-1.010
0.20	-0.438	-0.417	-0.456	-0.432	-0.521	-0.679	-0.726	-0.504	-0.999	-0.990	-0.989	-0.885
0.25	-0.477	-0.496	-0.521	-0.734	-0.682	-0.726	-0.773	-0.813	-0.864	-1.013	-0.829	-0.939
0.30	-0.470	-0.553	-0.577	-0.691	-0.626	-0.725	-0.814	-0.836	-0.920	-1.055	-0.650	-1.064
0.35		-0.569	-0.629	-0.634		-0.766	-0.845	-0.818		-1.083	-0.581	-1.050
0.40	-0.608	-0.551	-0.689	-0.581	-0.710	-0.822	-0.869	-0.782	-0.953	-1.004	-0.569	-0.901
0.50	-0.496		-0.678	-0.716	-0.657		-0.857	-0.881	-0.859		-0.554	-0.695
0.60	-0.632	-0.722	-0.706		-0.771	-0.787	-0.378		-0.652	-0.645	-0.540	
0.74	-0.359	-0.244	-0.195	-0.189	-0.517	-0.373	-0.320	-0.349	-0.604	-0.608	-0.535	-0.522
0.78	-0.170	-0.145	-0.158	-0.142	-0.330	-0.321	-0.306	-0.324	-0.587	-0.599	-0.526	-0.495
0.84	-0.056	-0.055	-0.095	-0.082	-0.239	-0.265	-0.289	-0.290	-0.554	-0.575	-0.530	-0.484
0.87	-0.015	-0.014	-0.069	-0.053	-0.214	-0.237	-0.284	-0.267	-0.531	-0.565	-0.528	-0.468
0.90	0.022	0.023	-0.037	-0.027	-0.192	-0.206	-0.271	-0.244	-0.514	-0.550	-0.522	-0.456
0.96	0.102	0.101	0.028	0.033	-0.130	-0.127	-0.252	-0.165	-0.464	-0.522	-0.499	-0.415
1.00	0.146	0.141	0.073	0.064	-0.050	-0.049	-0.214	-0.089	-0.402	-0.487	-0.469	-0.375
Lower surface												
0.00	0.653	0.638	0.685	0.565	0.884	0.851	0.818	0.830	0.673	0.620	0.435	0.656
0.03	-0.581	-0.762	-0.859		0.148	0.113	0.067	-0.003	0.495	0.481	0.465	0.485
0.05	-0.262	-0.293	-0.566	-0.543	0.094	0.074	0.058	0.056	0.385	0.374	0.359	0.363
0.10	-0.161	-0.215	-0.217	-0.247	0.002	-0.007	0.008	-0.013	0.237	0.235	0.252	0.335
0.20	-0.188	-0.225	-0.226	-0.211	-0.042	-0.027	-0.050	-0.037	0.180	0.200	0.185	0.216
0.25	-0.211	-0.229	-0.230	-0.222	-0.042	-0.027	-0.050	-0.037				
0.40	-0.388	-0.406		-0.393	-0.242	-0.253		-0.201	-0.020	-0.016		-0.001
0.50	-0.524	-0.565	-0.484	-0.446	-0.376	-0.347	-0.261	-0.256	-0.099	-0.084	-0.061	-0.070
0.60	-0.504	-0.548	-0.552	-0.263	-0.322	-0.313	-0.268	-0.227	-0.096	-0.110	-0.089	-0.096
0.74	-0.190	-0.073	-0.034	-0.054	-0.158	-0.123	-0.128	-0.169	-0.101	-0.086	-0.079	-0.122
0.78	-0.073	-0.022	-0.008	-0.036	-0.130	-0.096	-0.134	-0.171	-0.097	-0.081	-0.098	-0.137
0.82	-0.020	0.015	0.012	-0.011	-0.102	-0.070	-0.126	-0.180	-0.093	-0.076	-0.104	-0.161
0.88	0.038	0.051	0.038	0.016	-0.069	-0.072	-0.135	-0.193	-0.107	-0.122	-0.139	-0.233
0.94	0.094	0.100	0.059	0.039	-0.044	-0.041	-0.158	-0.149	-0.145	-0.142	-0.184	-0.325
1.00	0.146	0.141	0.073	0.064	-0.050	-0.049	-0.214	-0.089	-0.402	-0.487	-0.469	-0.375

Table 25. Wing Pressure Coefficients for Temod for  $M_\infty = 0.900$ 

[Blanks indicate defective data]

$x/c$	$C_p$ for $\alpha = 0.0^\circ$ ; $C_L = 0.088$ ; and $\eta$ of—				$C_p$ for $\alpha = 3.0^\circ$ ; $C_L = 0.398$ ; and $\eta$ of—				$C_p$ for $\alpha = 7.0^\circ$ ; $C_L = 0.709$ ; and $\eta$ of—			
	0.33	0.50	0.67	0.82	0.33	0.50	0.67	0.82	0.33	0.50	0.67	0.82
Upper surface												
0.00	0.612	0.605	0.634	0.522	0.866	0.834	0.817	0.804	0.816	0.776	0.598	0.775
0.05	0.058		0.094	0.069	-0.249		-0.177	-0.238	-0.692		-0.545	-0.712
0.10	-0.111		-0.177	-0.089	-0.403		-0.429	-0.396	-0.815		-0.791	-0.785
0.14	-0.212	-0.311	-0.329	-0.153	-0.315	-0.506	-0.561	-0.444	-0.866	-0.853	-0.877	-0.893
0.20	-0.417	-0.366	-0.415	-0.410	-0.485	-0.584	-0.648	-0.489	-0.677	-0.850	-0.916	-0.677
0.25	-0.416	-0.462	-0.472	-0.695	-0.650	-0.624	-0.701	-0.768	-0.759	-0.902	-0.927	-0.858
0.30	-0.419	-0.500	-0.538	-0.623	-0.614	-0.685	-0.752	-0.800	-0.874	-0.918	-0.963	-0.963
0.35		-0.484	-0.590	-0.586		-0.748	-0.786	-0.757		-0.958	-0.927	-0.988
0.40	-0.579	-0.552	-0.642	-0.576	-0.700	-0.798	-0.835	-0.747	-0.825	-0.994	-0.697	-0.907
0.50	-0.445		-0.616	-0.752	-0.608		-0.820	-0.913	-0.746		-0.543	-0.810
0.60	-0.606	-0.666	-0.693		-0.759	-0.752	-0.788		-0.866	-0.708	-0.535	
0.74	-0.589		-0.341	-0.301	-0.712		-0.363	-0.360	-0.822		-0.523	-0.570
0.78	-0.385	-0.244	-0.215	-0.226	-0.650	-0.610	-0.337	-0.336	-0.602	-0.585	-0.512	-0.528
0.84	-0.119	-0.103	-0.127	-0.142	-0.339	-0.304	-0.315	-0.323	-0.455	-0.562	-0.507	-0.511
0.87	-0.062	-0.064		-0.091	-0.252	-0.262		-0.298	-0.413	-0.548		-0.463
0.90	-0.021	-0.024	-0.062		-0.205	-0.229	-0.297		-0.379	-0.537	-0.498	
0.96	0.054	0.052	0.014	0.001	-0.133	-0.134	-0.271	-0.241	-0.326	-0.480	-0.479	-0.419
1.00	0.095	0.088	0.060	0.024	-0.068	-0.060	-0.224	-0.219	-0.259	-0.420	-0.431	-0.539
Lower surface												
0.00	0.612	0.605	0.634	0.522	0.866	0.834	0.817	0.804	0.816	0.776	0.598	0.775
0.03	-0.725	-0.758	-0.861	-0.518	0.034	0.023	-0.015	-0.051	0.450	0.416	0.438	0.220
0.05	-0.652	-0.460	-0.713	-0.586	0.055	-0.021	-0.019	-0.027	0.391	0.342	0.361	0.250
0.10	-0.146	-0.243	-0.233	-0.479	0.035	0.004	-0.006	-0.011	0.292	0.280	0.273	0.256
0.20	-0.200	-0.236	-0.227	-0.230	-0.041	-0.049	-0.035	-0.052	0.160	0.160	0.182	0.152
0.25	-0.224	-0.240	-0.246	-0.242	-0.079	-0.081	-0.088	-0.073	0.109	0.123	0.118	0.121
0.40	-0.392	-0.410		-0.400	-0.271	-0.270		-0.206	-0.086	-0.076		-0.046
0.50	-0.544	-0.507	-0.570	-0.476	-0.424	-0.335	-0.298	-0.255	-0.167	-0.113	-0.073	-0.110
0.60	-0.511	-0.562	-0.528	-0.186	-0.347	-0.314	-0.156	-0.178	-0.173	-0.212	-0.108	-0.130
0.74	-0.102	-0.057	-0.006	-0.049	-0.138	-0.106	-0.096	-0.176	-0.155	-0.120	-0.101	-0.185
0.78	-0.002		0.054	-0.011	-0.029		-0.031	-0.130	-0.050		-0.049	-0.160
0.82	0.056	0.090	0.110	0.086	0.111	0.094	0.068	0.010	0.106	0.073	0.054	-0.023
0.88	0.117	0.169	0.187	0.179	0.242	0.216	0.194	0.150	0.258	0.201	0.183	0.130
0.94	0.184	0.230		0.233	0.313	0.293		0.206	0.332	0.296		0.213
1.00	0.095	0.088	0.060	0.024	-0.068	-0.060	-0.224	-0.219	-0.259	-0.420	-0.431	-0.539

Table 26. Wing Pressure Coefficients for Fulmod for  $M_\infty = 0.900$ 

[Blanks indicate defective data]

$x/c$	$C_p$ for $\alpha = 0.0^\circ$ ; $C_L = 0.080$ ; and $\eta$ of—				$C_p$ for $\alpha = 3.1^\circ$ ; $C_L = 0.400$ ; and $\eta$ of—				$C_p$ for $\alpha = 7.0^\circ$ ; $C_L = 0.710$ ; and $\eta$ of—			
	0.33	0.50	0.67	0.82	0.33	0.50	0.67	0.82	0.33	0.50	0.67	0.82
Upper surface												
0.00	-0.058	0.720	0.664	0.620	-0.499	0.839	0.804	0.769	-0.861	0.801	0.783	0.813
0.05	-0.260	-0.057	-0.001	-0.161	-0.480	-0.286	-0.284	-0.657	-0.931	-0.701	-0.956	-0.694
0.10	-0.140	-0.326	-0.251	-0.188	-0.267	-0.480	-0.617	-0.444	-0.964	-0.877	-0.956	-0.866
0.14	-0.403	-0.357	-0.393	-0.405	-0.459	-0.524	-0.640	-0.484	-0.677	-0.911	-0.927	-0.740
0.20	-0.400	-0.463	-0.487	-0.697	-0.576	-0.622	-0.660	-0.762	-0.755	-0.924	-0.940	-0.894
0.25	-0.411	-0.482	-0.532	-0.631	-0.595	-0.684	-0.719	-0.817	-0.854	-0.954	-0.994	-1.014
0.30	-0.485	-0.588	-0.592	-0.745	-0.768	-0.745	-0.769	-0.768	-0.991	-0.963	-0.963	-0.963
0.35	-0.580	-0.567	-0.634	-0.565	-0.701	-0.797	-0.827	-0.753	-0.836	-1.014	-0.794	-0.899
0.40	-0.451	-0.627	-0.742	-0.611	-0.864	-0.864	-0.905	-0.765	-0.603	-0.603	-0.753	-0.753
0.50	-0.606	-0.673	-0.705	-0.768	-0.776	-0.799	-0.871	-0.871	-0.635	-0.568	-0.547	-0.544
0.60	-0.599	-0.312	-0.309	-0.744	-0.343	-0.343	-0.362	-0.782	-0.573	-0.573	-0.534	-0.507
0.74	-0.390	-0.241	-0.214	-0.234	-0.578	-0.446	-0.326	-0.333	-0.314	-0.458	-0.555	-0.528
0.78	-0.126	-0.113	-0.142	-0.150	-0.296	-0.299	-0.305	-0.305	-0.414	-0.414	-0.448	-0.491
0.87	-0.067	-0.069	-0.098	-0.239	-0.265	-0.289	-0.289	-0.377	-0.537	-0.537	-0.513	-0.422
0.90	-0.026	-0.031	-0.080	-0.204	-0.230	-0.284	-0.284	-0.325	-0.468	-0.468	-0.447	-0.540
0.96	0.052	0.040	-0.011	-0.134	-0.131	-0.232	-0.232	-0.261	-0.413	-0.413	-0.447	-0.540
1.00	0.091	0.080	0.048	0.014	-0.064	-0.060	-0.215	-0.223	-0.261	-0.413	-0.447	-0.540
Lower surface												
0.00	-0.896	-0.879	-1.070	-0.583	-0.092	-0.243	-0.201	-0.076	0.367	0.244	0.302	0.147
0.05	-0.812	-0.851	-0.974	-0.080	-0.181	-0.039	-0.072	-0.262	0.276	0.300	0.304	0.159
0.10	-0.280	-0.170	-0.209	-0.179	-0.186	-0.042	-0.038	-0.028	-0.032	0.155	0.157	0.176
0.20	-0.208	-0.219	-0.219	-0.197	-0.080	-0.067	-0.082	-0.064	0.103	0.126	0.113	0.120
0.25	-0.386	-0.406	-0.361	-0.275	-0.266	-0.197	-0.243	-0.243	-0.170	-0.120	-0.079	-0.113
0.50	-0.532	-0.506	-0.539	-0.438	-0.416	-0.331	-0.334	-0.157	-0.178	-0.180	-0.219	-0.115
0.60	-0.517	-0.620	-0.493	-0.163	-0.326	-0.334	-0.139	-0.088	-0.176	-0.162	-0.126	-0.097
0.74	-0.109	-0.055	-0.008	-0.050	-0.139	-0.108	-0.108	-0.030	-0.126	-0.162	-0.126	-0.193
0.78	-0.012	0.051	-0.017	-0.028	-0.139	-0.108	-0.108	-0.030	-0.126	-0.162	-0.126	-0.163
0.82	0.046	0.100	0.106	0.080	0.111	0.093	0.067	0.011	0.105	0.070	0.052	-0.025
0.88	0.108	0.188	0.175	0.170	0.241	0.216	0.189	0.146	0.255	0.199	0.180	0.127
0.94	0.168	0.255	-0.209	0.310	0.298	-0.060	-0.215	-0.223	-0.261	-0.413	-0.447	-0.540
1.00	0.091	0.080	0.048	0.014	-0.064	-0.060	-0.215	-0.223	-0.261	-0.413	-0.447	-0.540

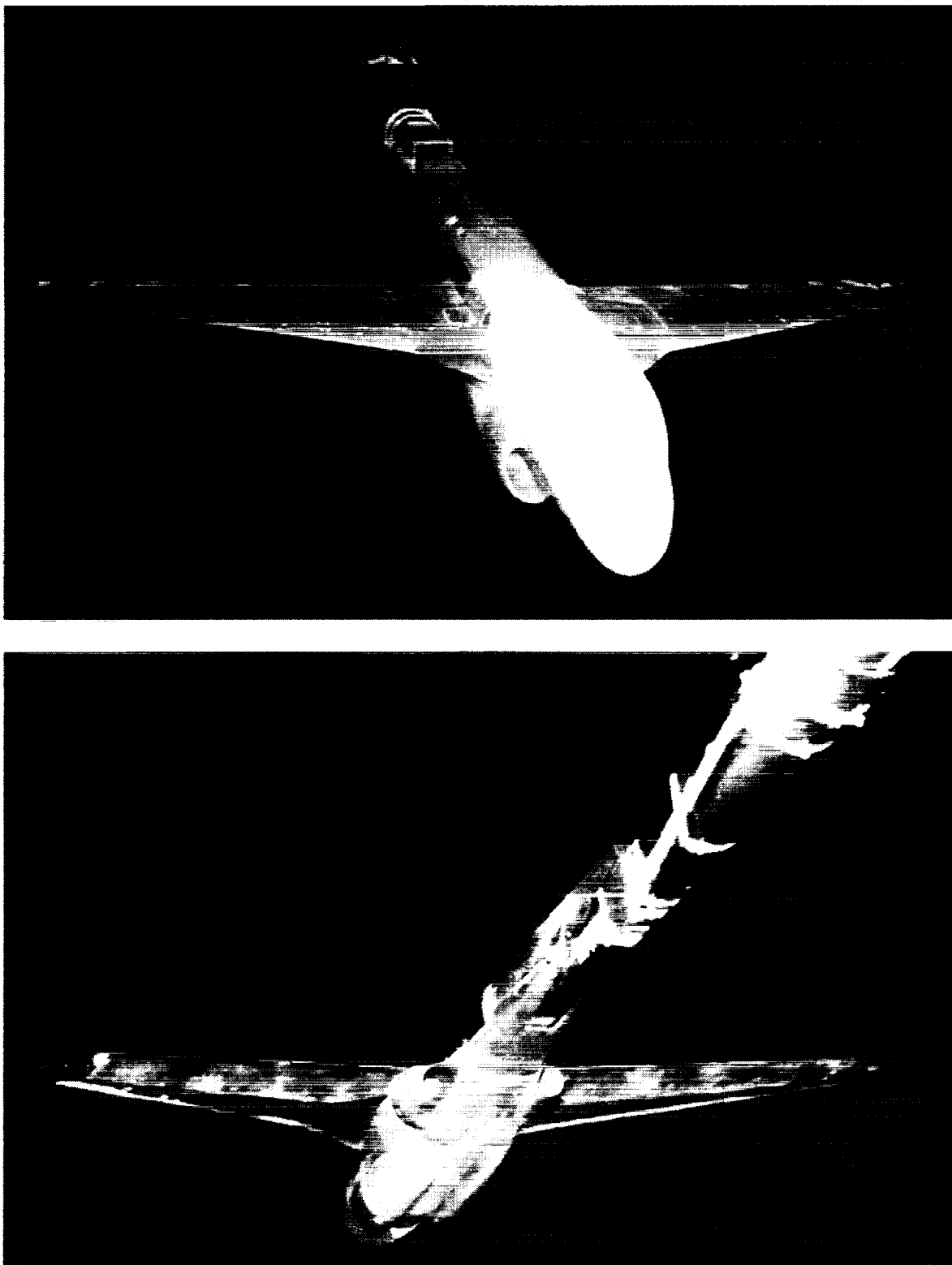
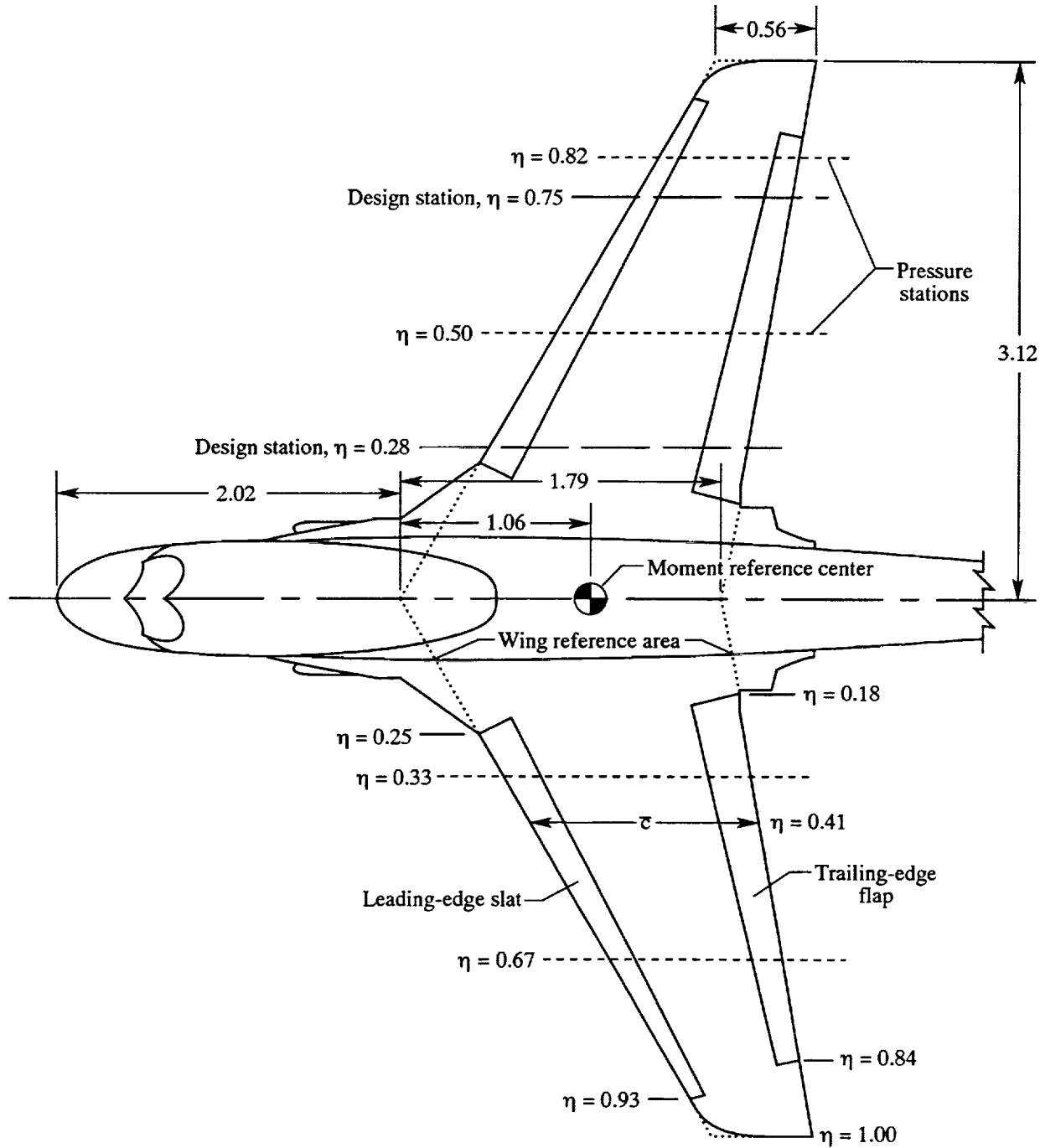
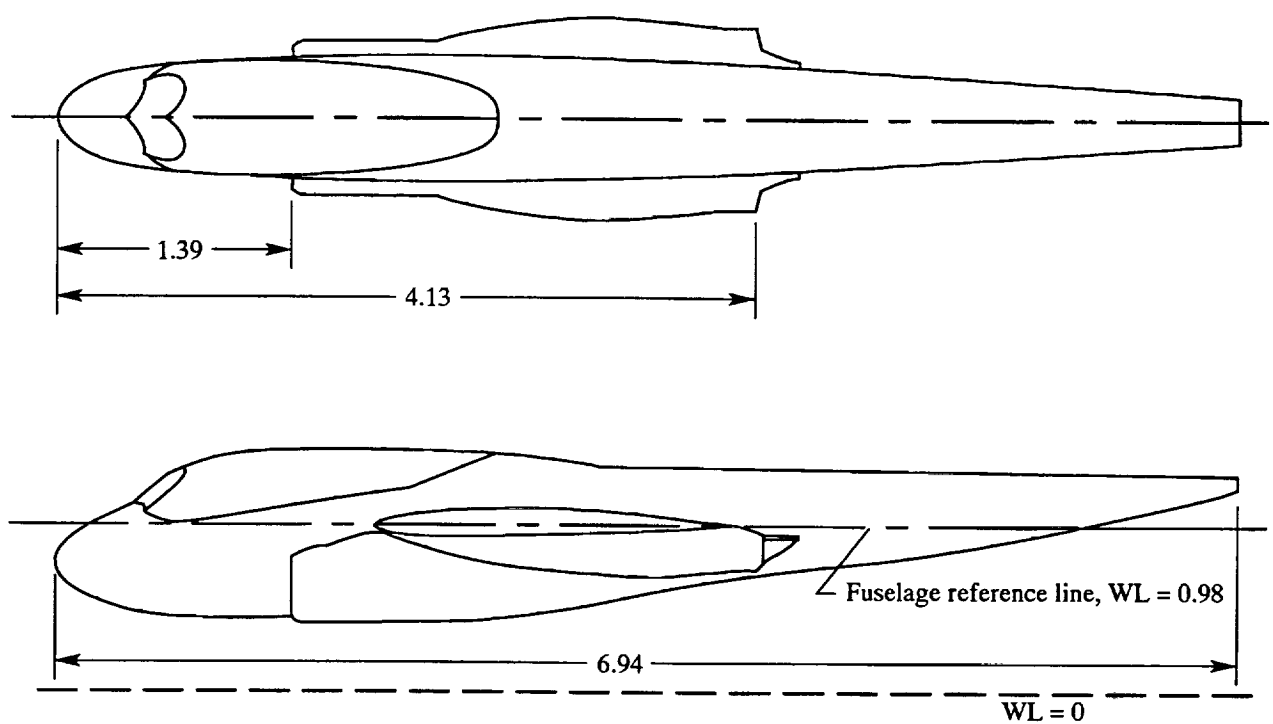


Figure 1. Photographs of 1/8.5-scale wing-fuselage model.



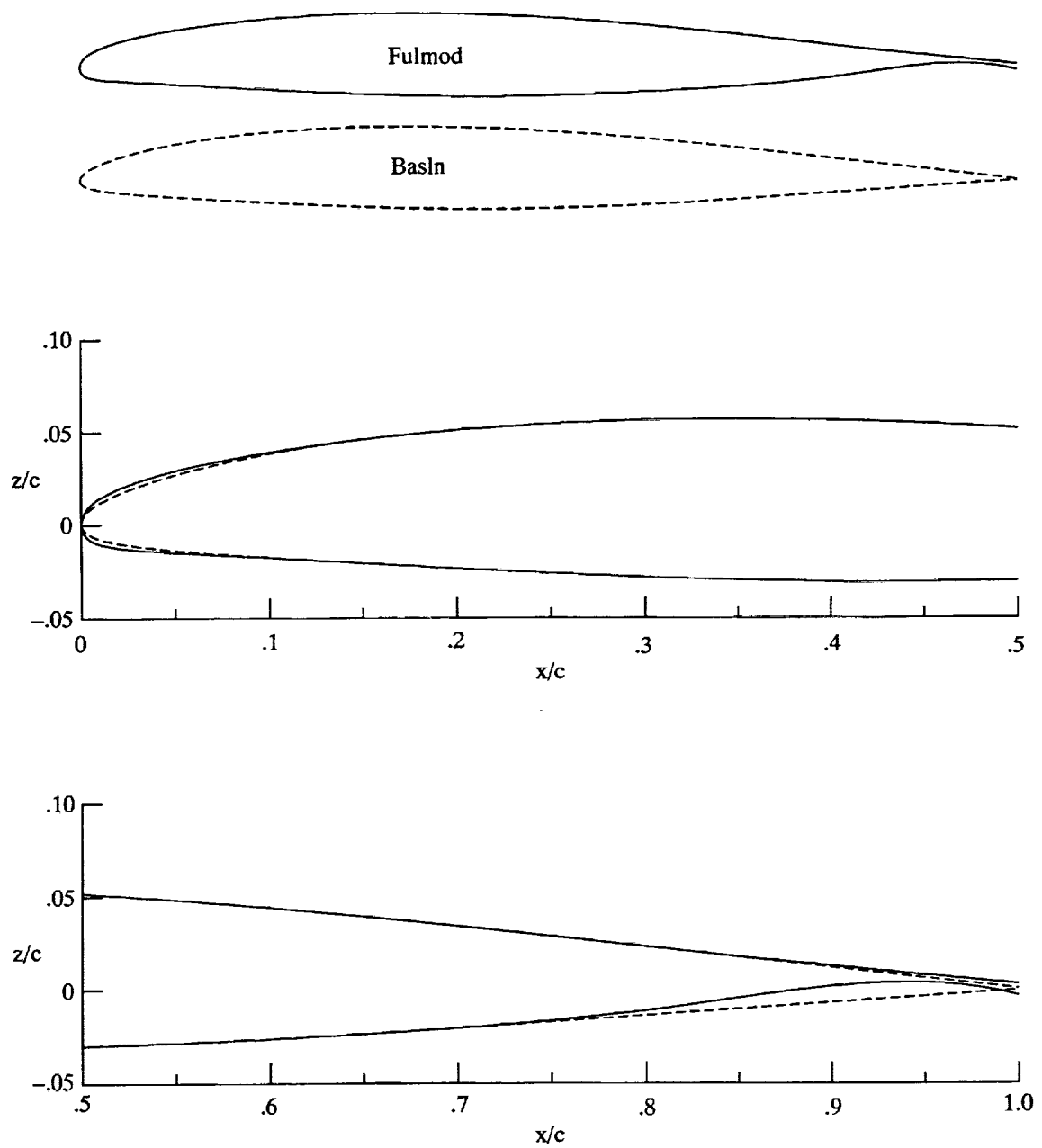
(a) Planform of wing and fuselage.

Figure 2. Sketch of 1/8.5-scale wing-fuselage model. Linear dimensions are in feet.  $AR = 5.31$ ;  $\Lambda_{c/4} = 25^\circ$ ;  $\Lambda_{le} = 30^\circ$ ;  $\Lambda_{te} = 10^\circ$ ;  $\lambda = 0.31$ ;  $\bar{c} = 1.28$  ft;  $S = 7.32$  ft $^2$ ; and  $\Gamma = -1^\circ$ .



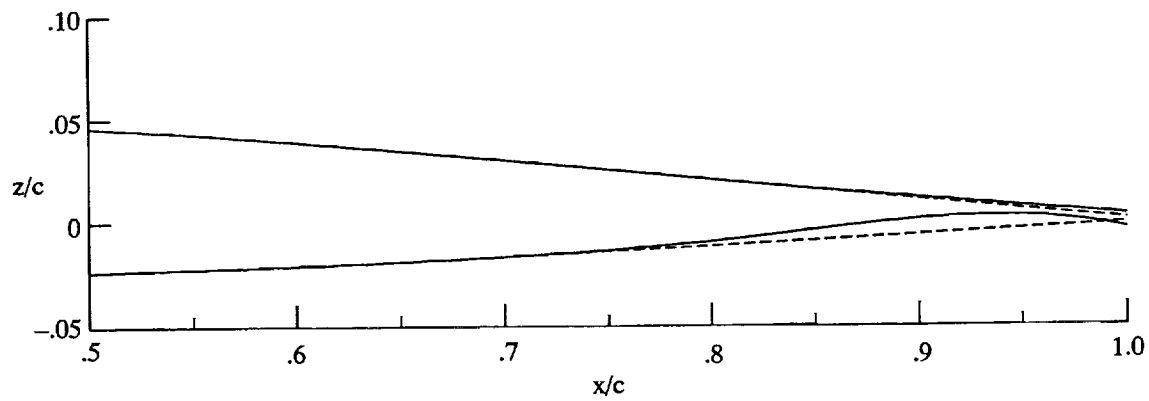
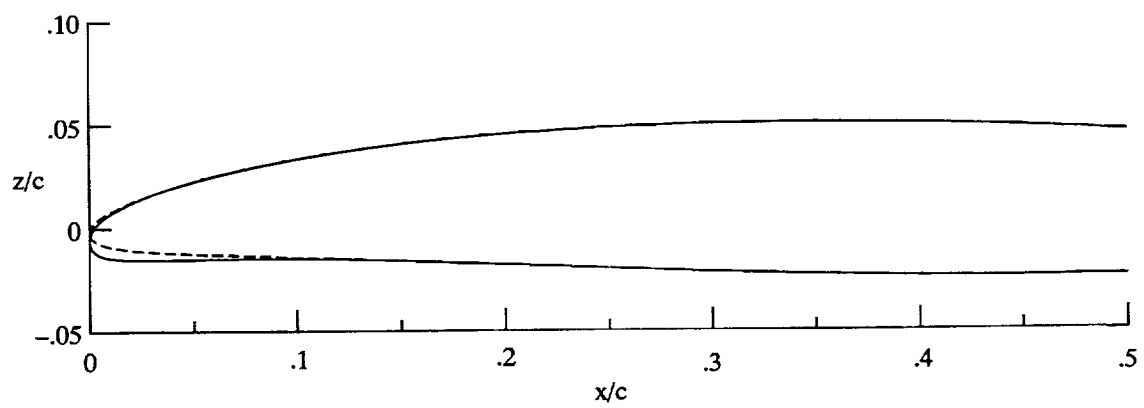
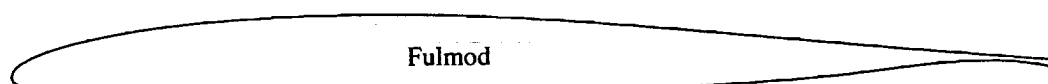
(b) Planform and side view of fuselage.

Figure 2. Continued.



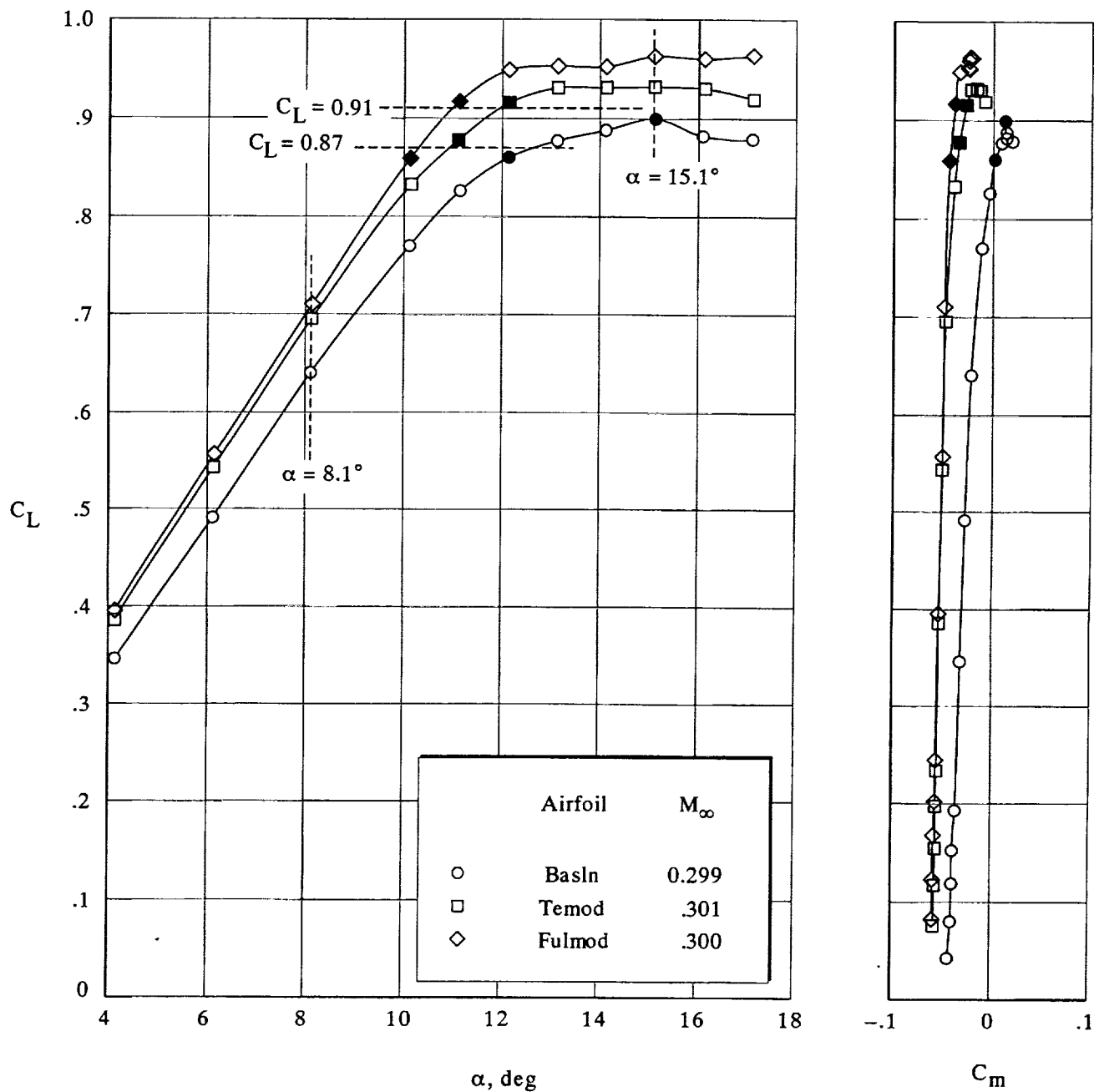
(c) Streamwise airfoils at inboard design station.  $\eta = 0.28$ ;  $t/c = 0.087$ .

Figure 2. Continued.



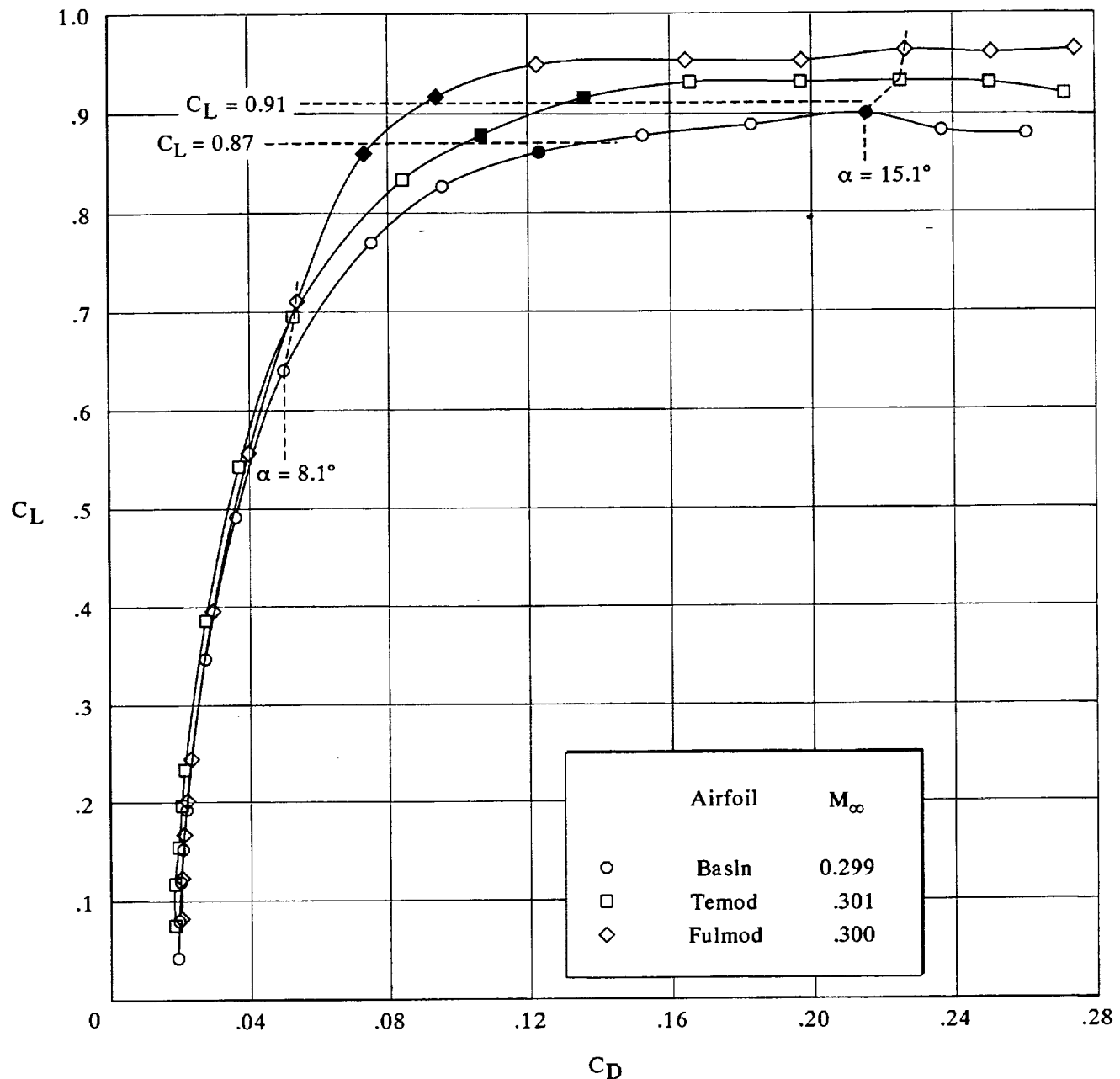
(d) Streamwise airfoils at outboard design station.  $\eta = 0.75$ ;  $t/c = 0.074$ .

Figure 2. Concluded.



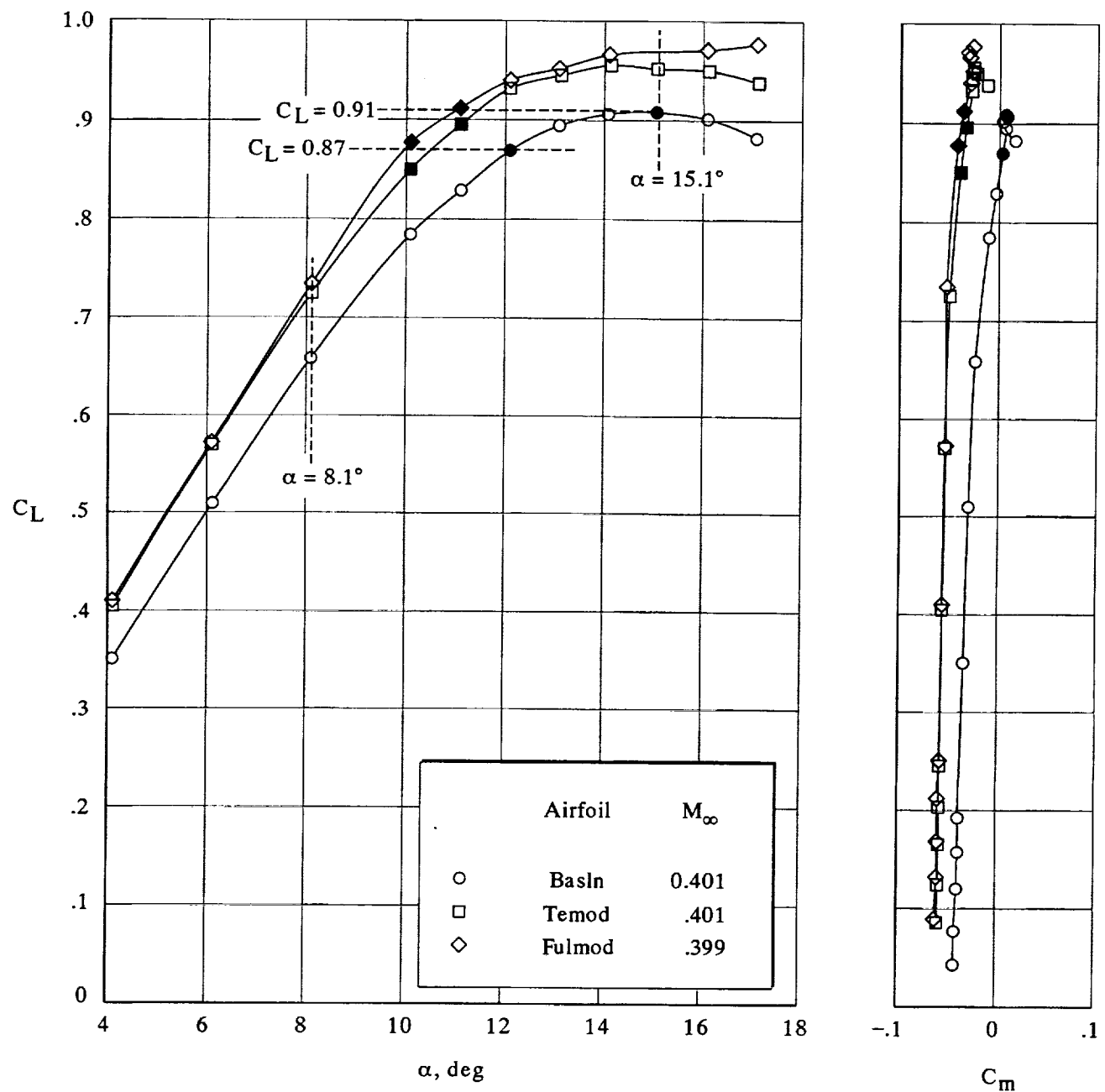
(a) Lift and pitching-moment coefficients.

Figure 3. Airfoil modification effects on longitudinal characteristics measured on EA-6B wing fuselage at  $M_\infty = 0.300$ . Solid symbols correspond to pressure distribution comparisons at similar lift coefficients.



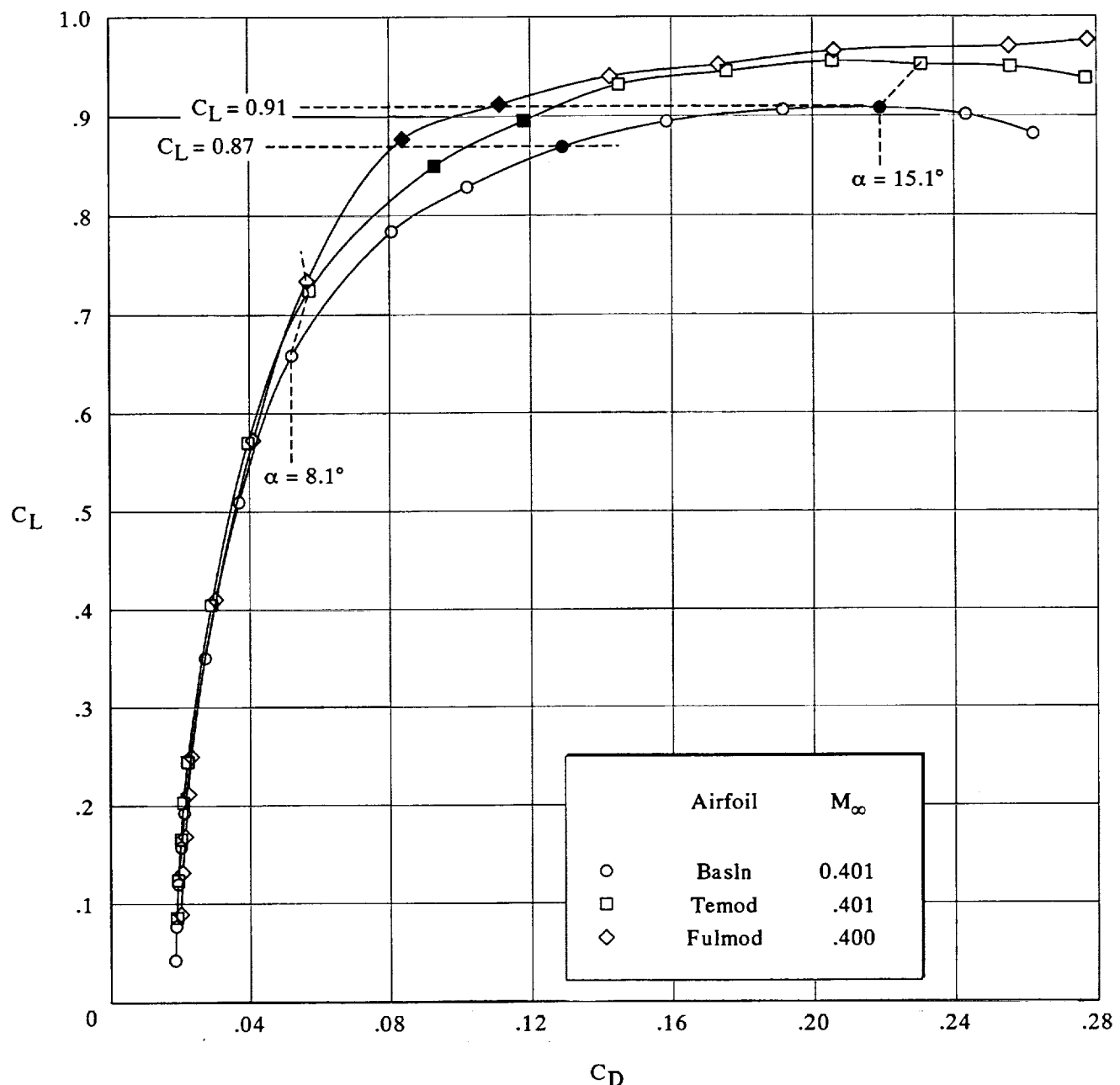
(b) Drag coefficient.

Figure 3. Concluded.



(a) Lift and pitching-moment coefficients.

Figure 4. Airfoil modification effects on longitudinal characteristics measured on EA-6B wing fuselage at  $M_\infty = 0.400$ . Solid symbols correspond to pressure distribution comparisons at similar lift coefficients.



(b) Drag coefficient.

Figure 4. Concluded.

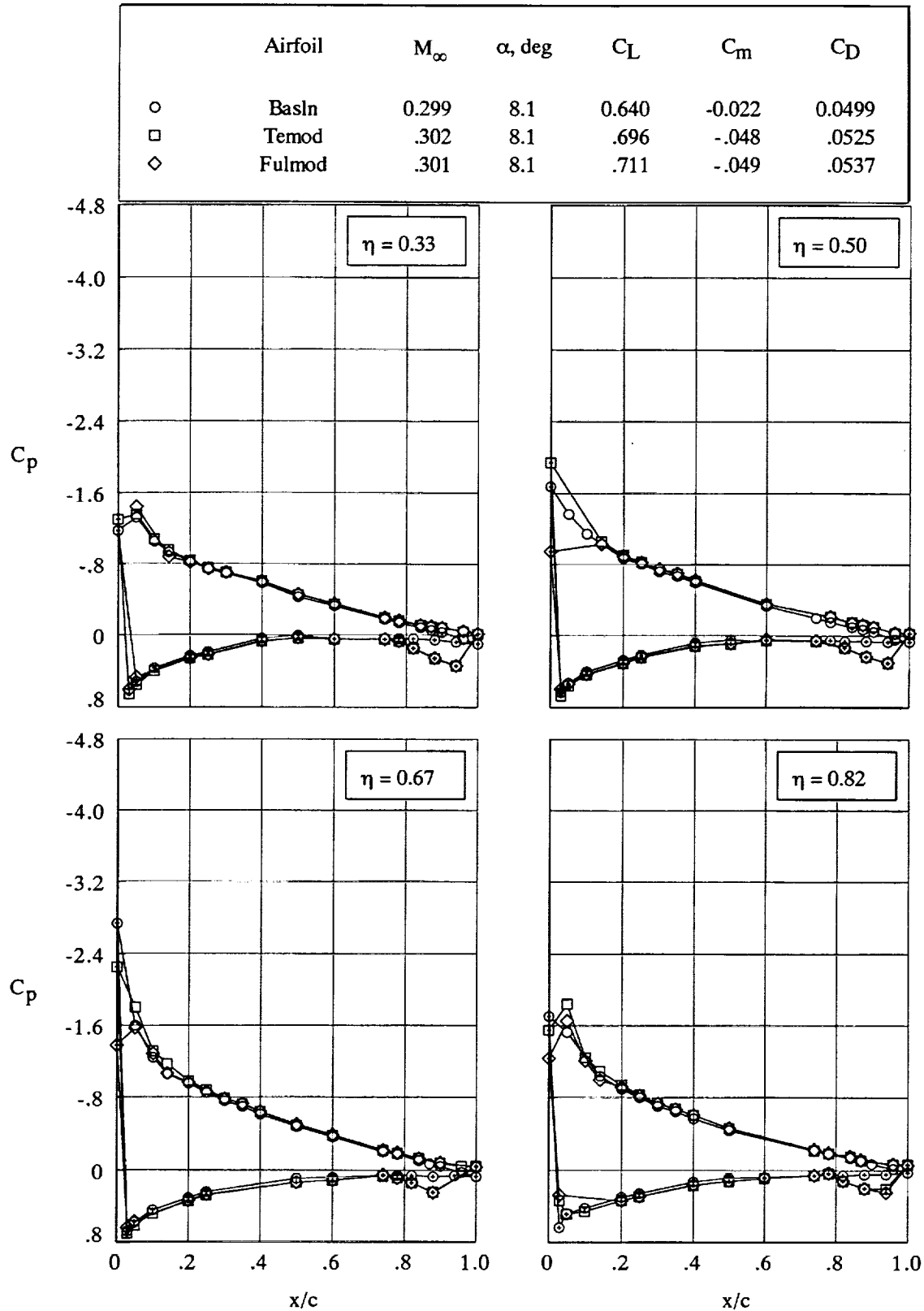


Figure 5. Chordwise pressure distributions measured on EA-6B wing fuselage at  $M_\infty = 0.300$  and  $\alpha = 8.1^\circ$ . Open symbols denote upper surface; + within symbol denotes lower surface.

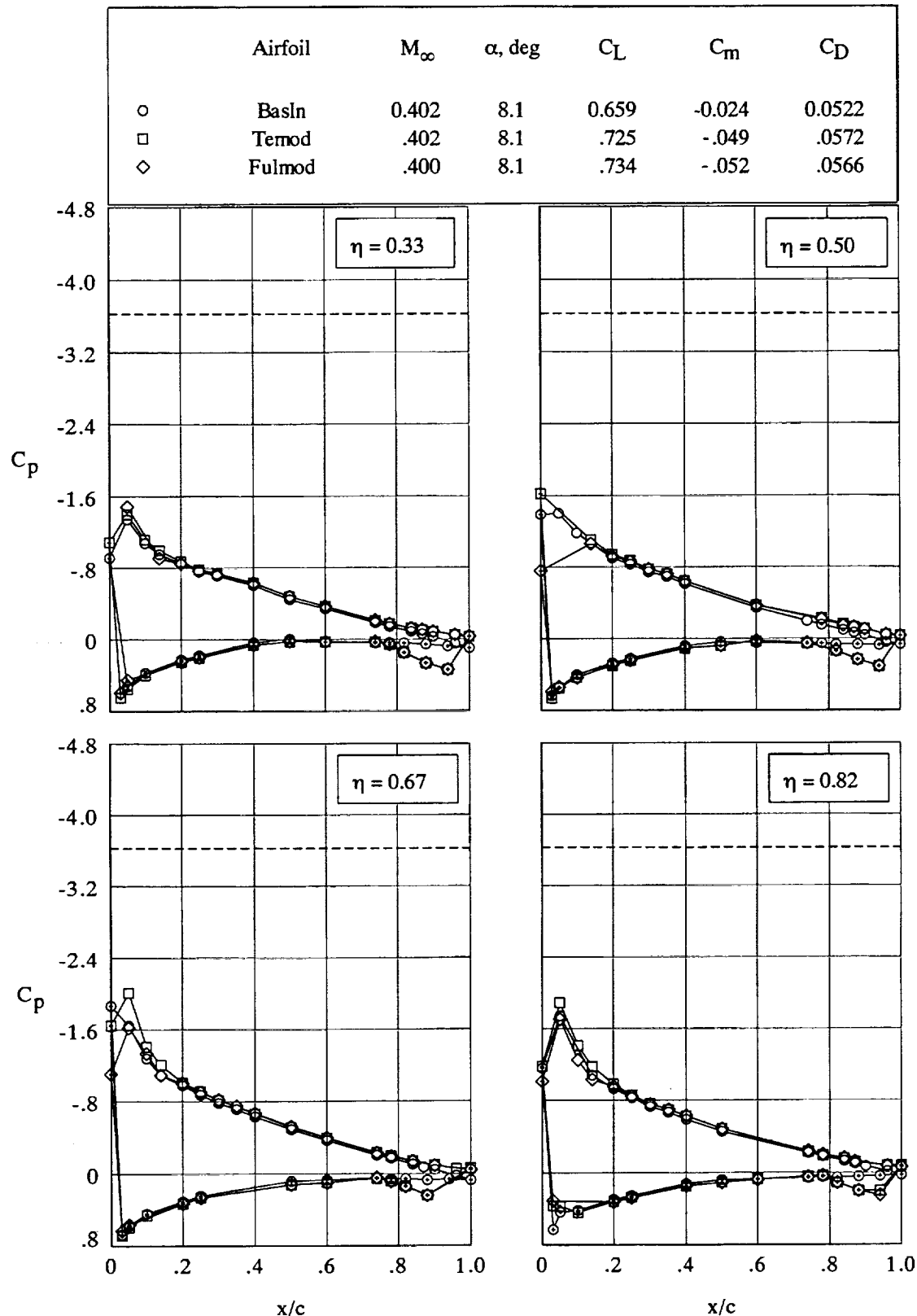


Figure 6. Chordwise pressure distributions measured on EA-6B wing fuselage at  $M_{\infty} = 0.400$  and  $\alpha = 8.1^\circ$ . Open symbols denote upper surface; + within symbol denotes lower surface. Dashed line indicates sonic  $C_p$ .

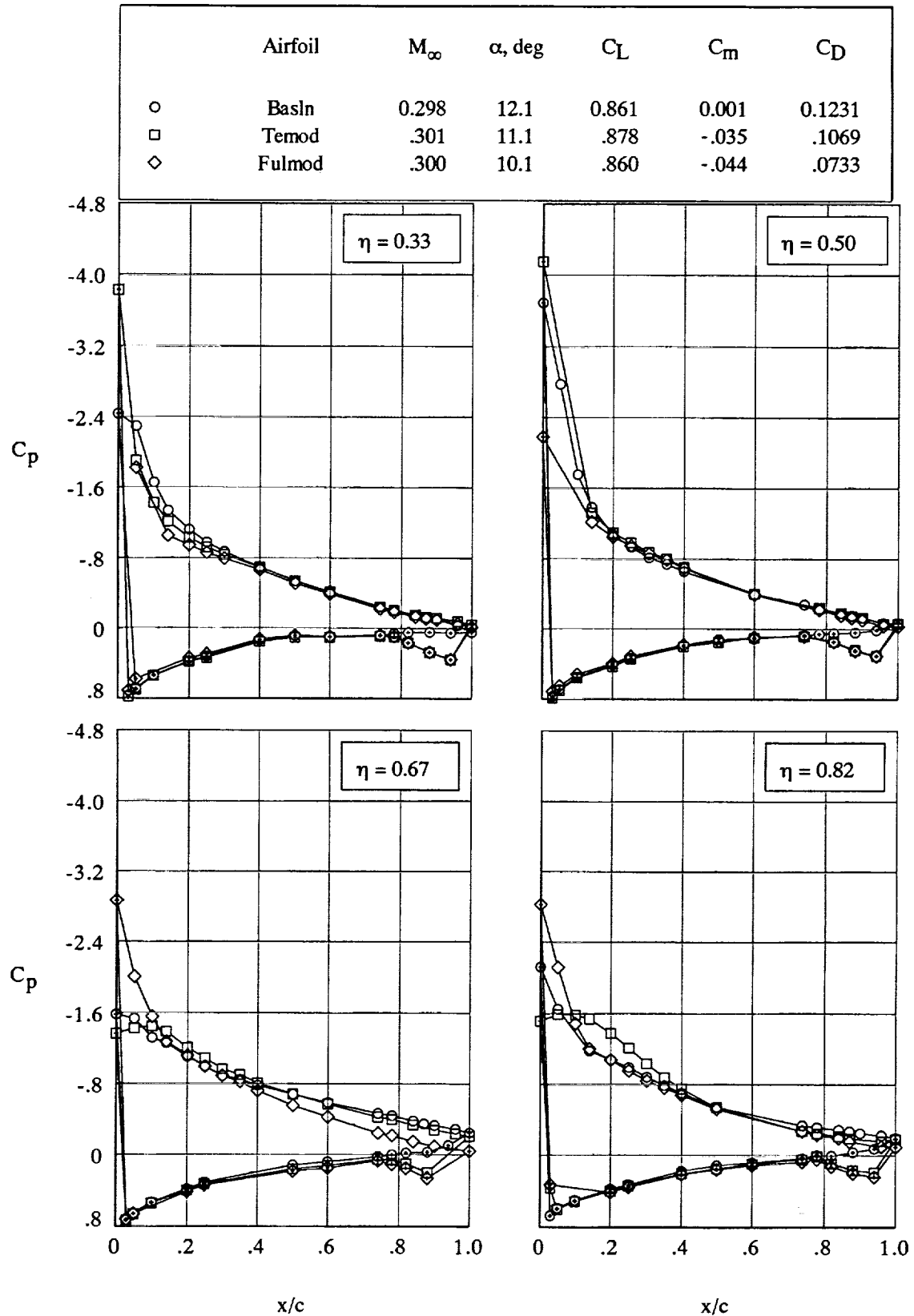


Figure 7. Chordwise pressure distributions measured on EA-6B wing fuselage at  $M_\infty = 0.300$  and  $C_L \approx 0.87$ . Open symbols denote upper surface; + within symbol denotes lower surface.

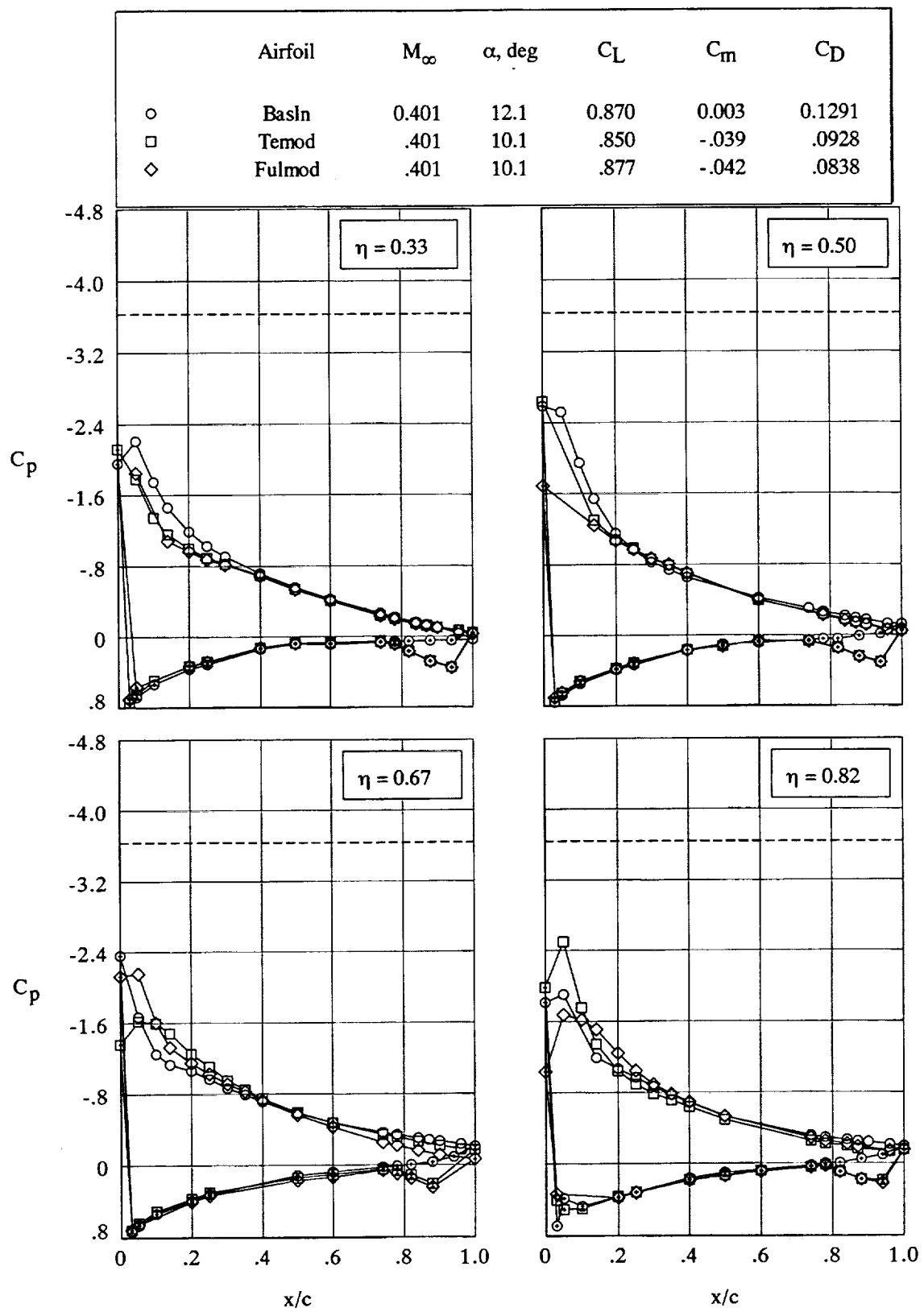


Figure 8. Chordwise pressure distributions measured on EA-6B wing fuselage at  $M_\infty = 0.400$  and  $C_L \approx 0.87$ . Open symbols denote upper surface; + within symbol denotes lower surface. Dashed line indicates sonic  $C_p$ .

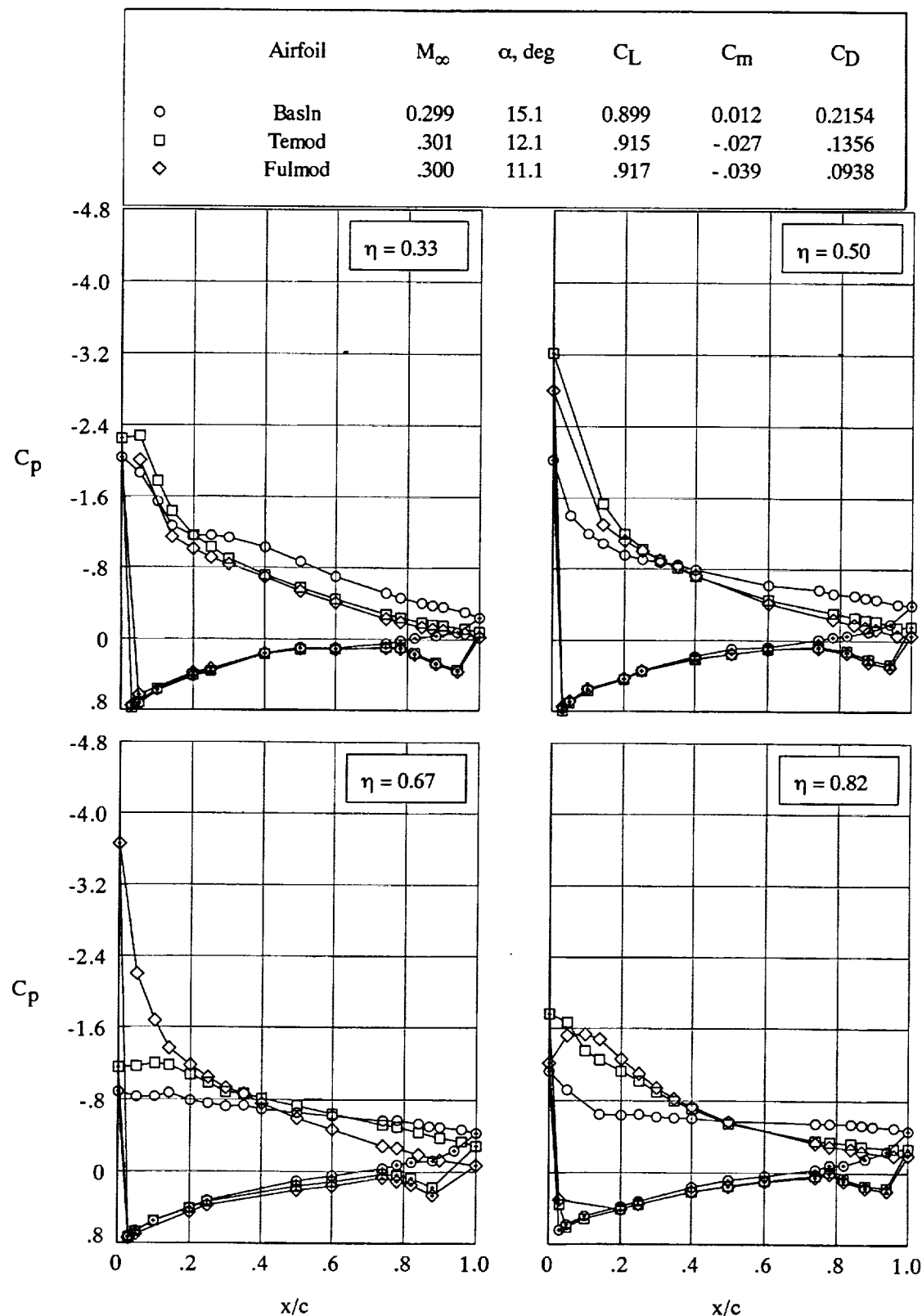


Figure 9. Chordwise pressure distributions measured on EA-6B wing fuselage at  $M_\infty = 0.300$  and  $C_L \approx 0.91$ . Open symbols denote upper surface; + within symbol denotes lower surface.

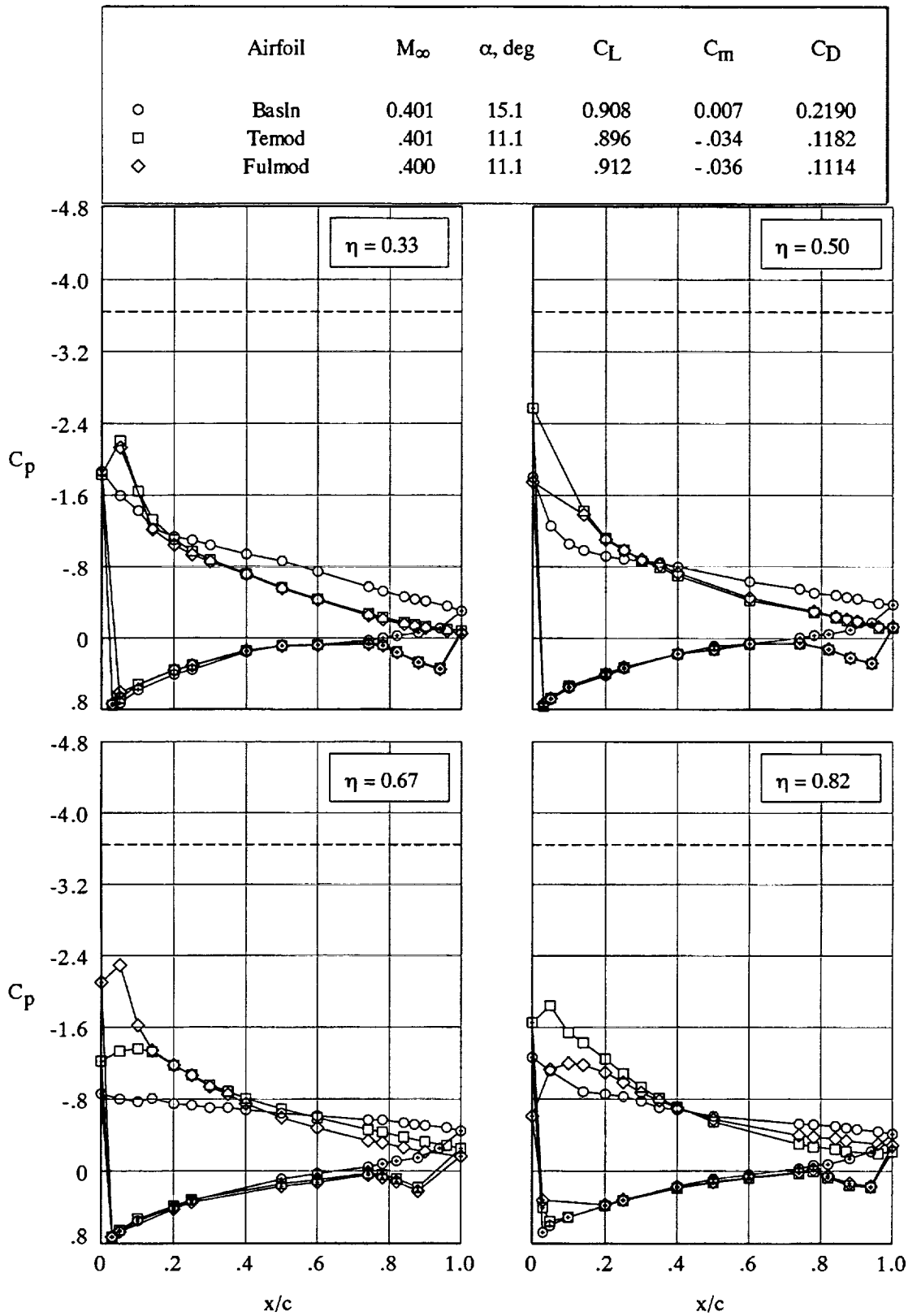


Figure 10. Chordwise pressure distributions measured on EA-6B wing fuselage at  $M_\infty = 0.400$  and  $C_L \approx 0.91$ . Open symbols denote upper surface; + within symbol denotes lower surface. Dashed line indicates sonic  $C_p$ .

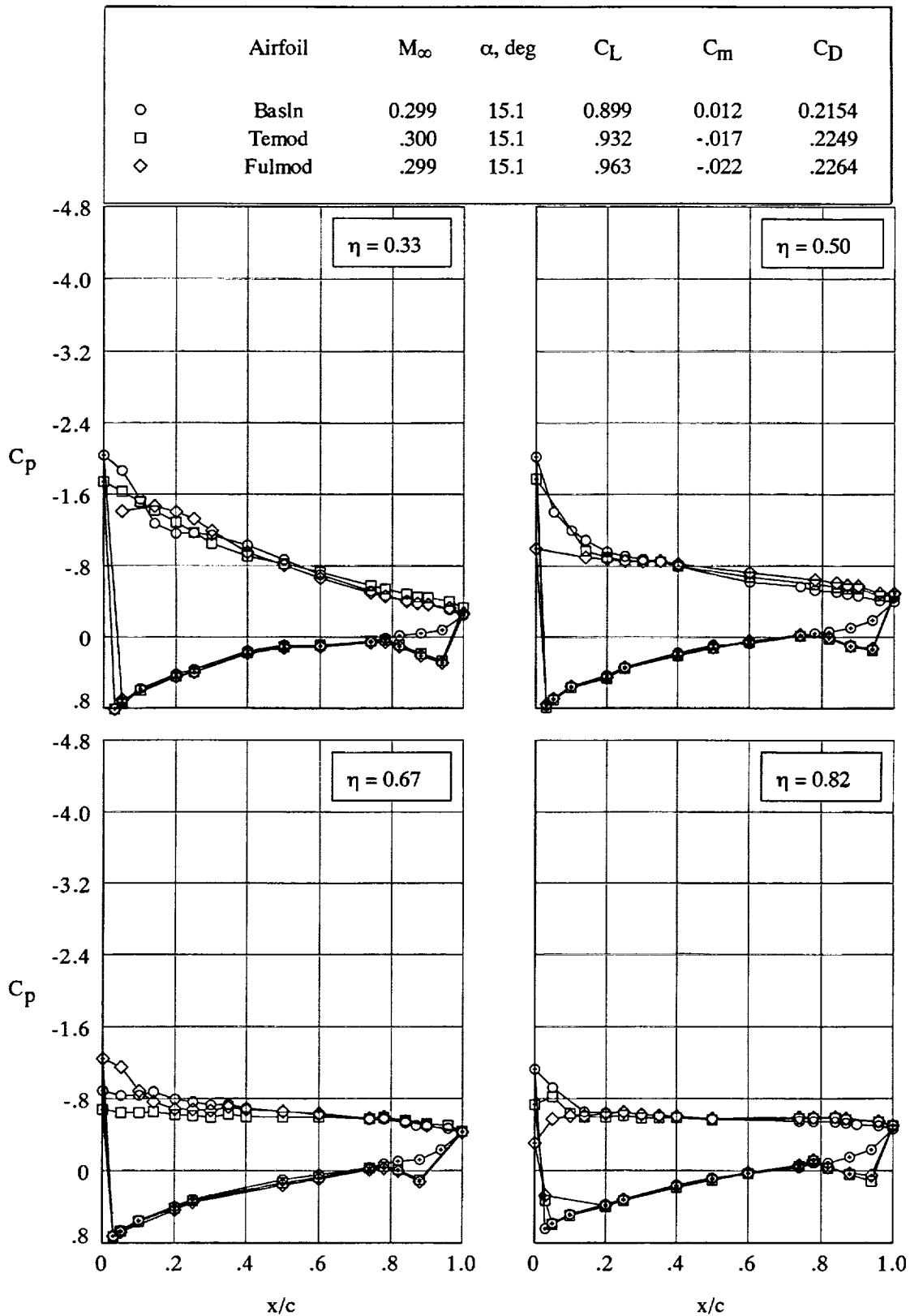


Figure 11. Chordwise pressure distributions measured on EA-6B wing fuselage at  $M_\infty = 0.300$  and  $\alpha = 15.1^\circ$ . Open symbols denote upper surface; + within symbol denotes lower surface.

Airfoil	$M_\infty$	$\alpha, \text{ deg}$	$C_L$	$C_m$	$C_D$
○ Basln	0.401	15.1	0.908	0.007	0.2190
□ Temod	.400	15.1	.952	-.026	.2307

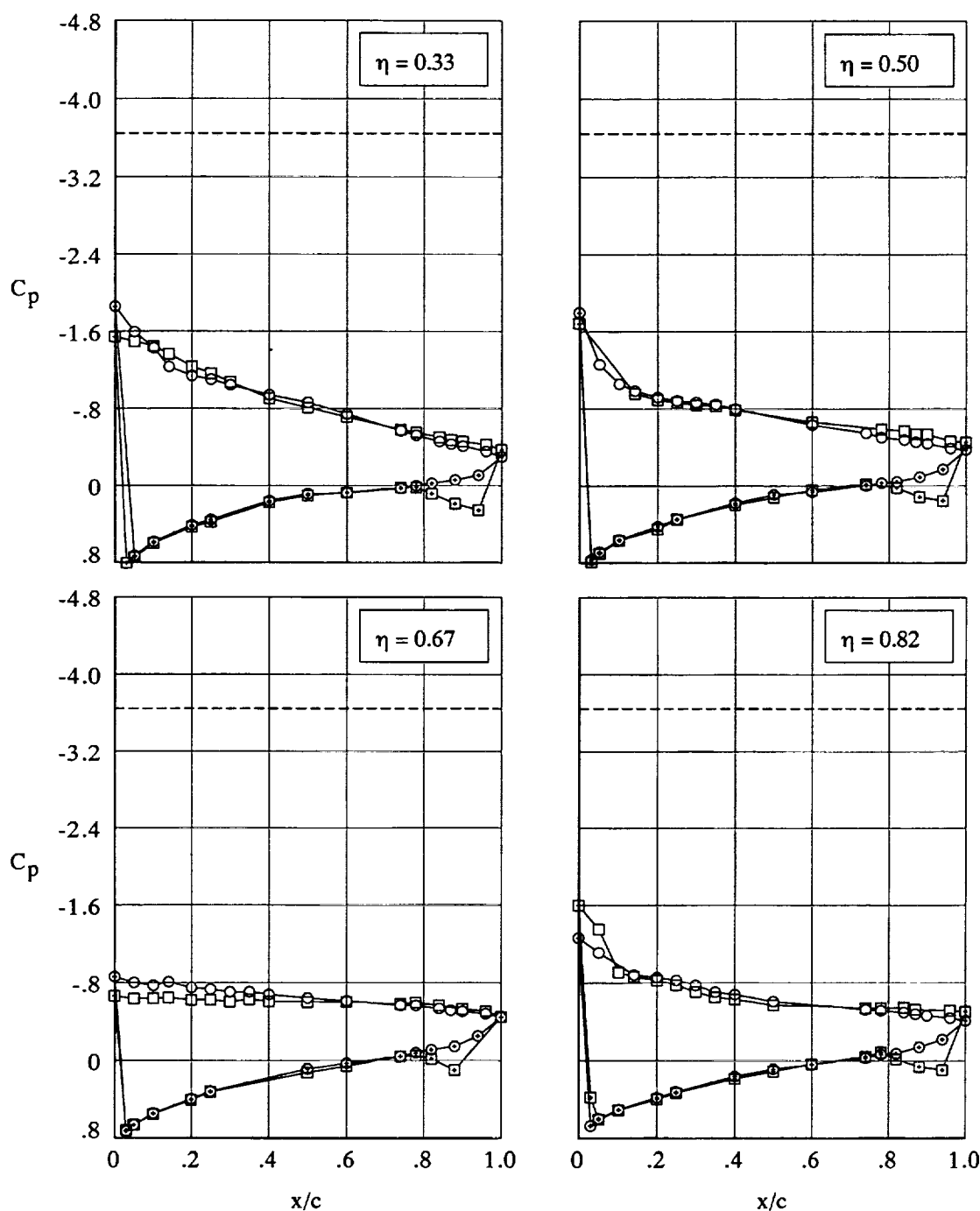


Figure 12. Chordwise pressure distributions measured on EA-6B wing fuselage at  $M_\infty = 0.400$  and  $\alpha = 15.1^\circ$ . Open symbols denote upper surface; + within symbol denotes lower surface. Dashed line indicates sonic  $C_p$ .

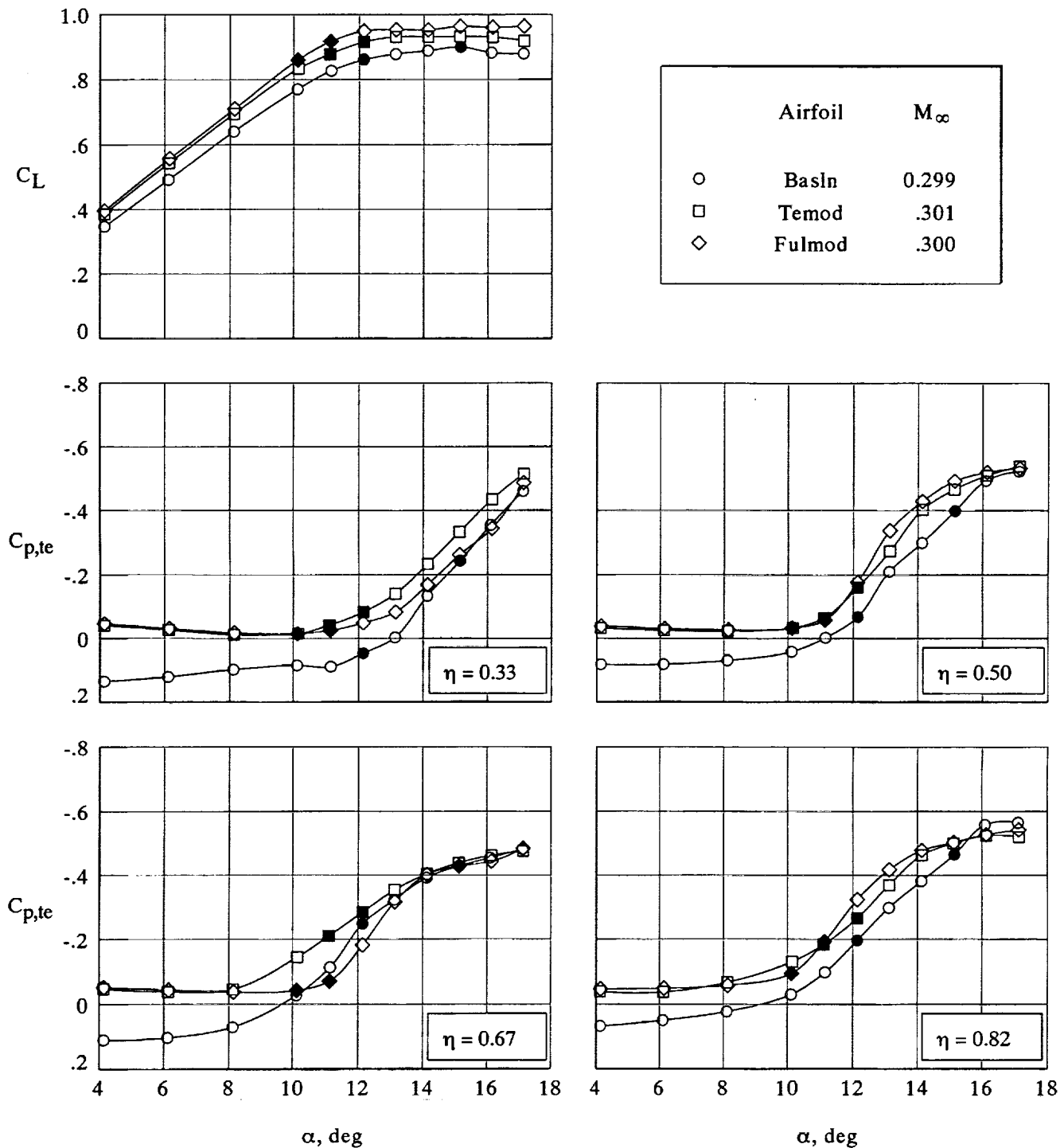


Figure 13. Trailing-edge pressure coefficient measured on EA-6B wing fuselage at  $M_\infty = 0.300$ . Solid symbols correspond to pressure distribution comparisons at similar lift coefficients.

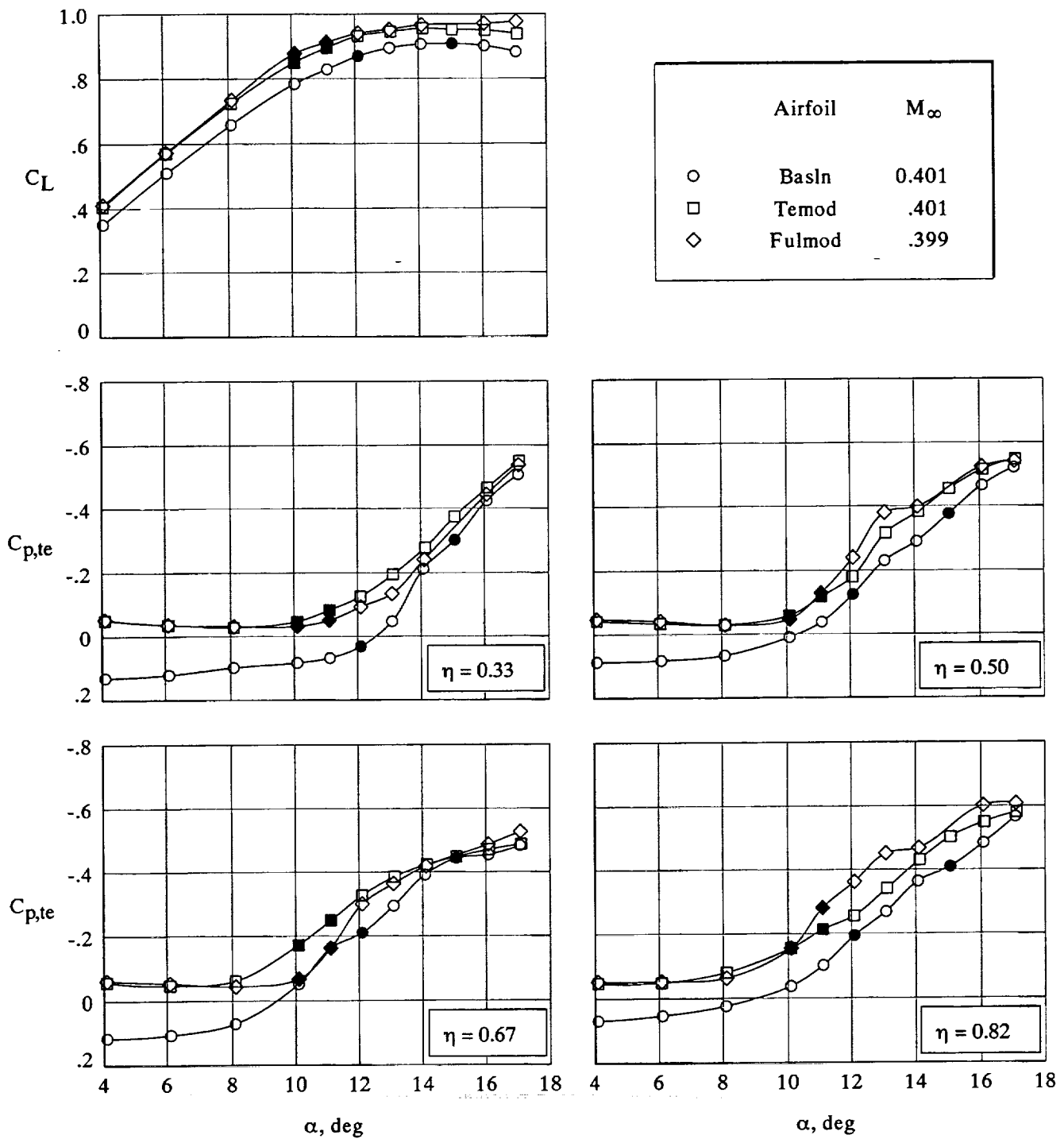
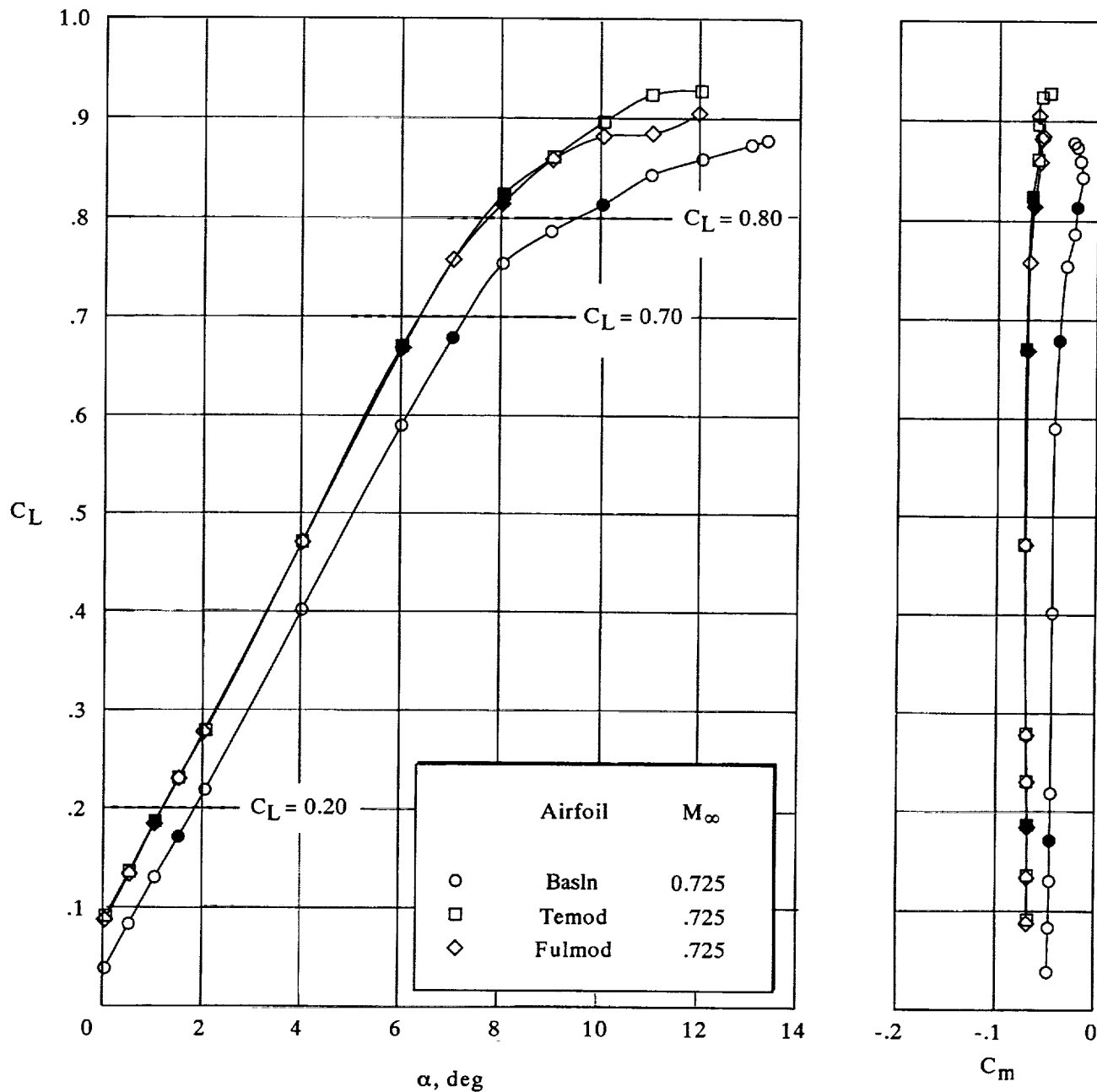
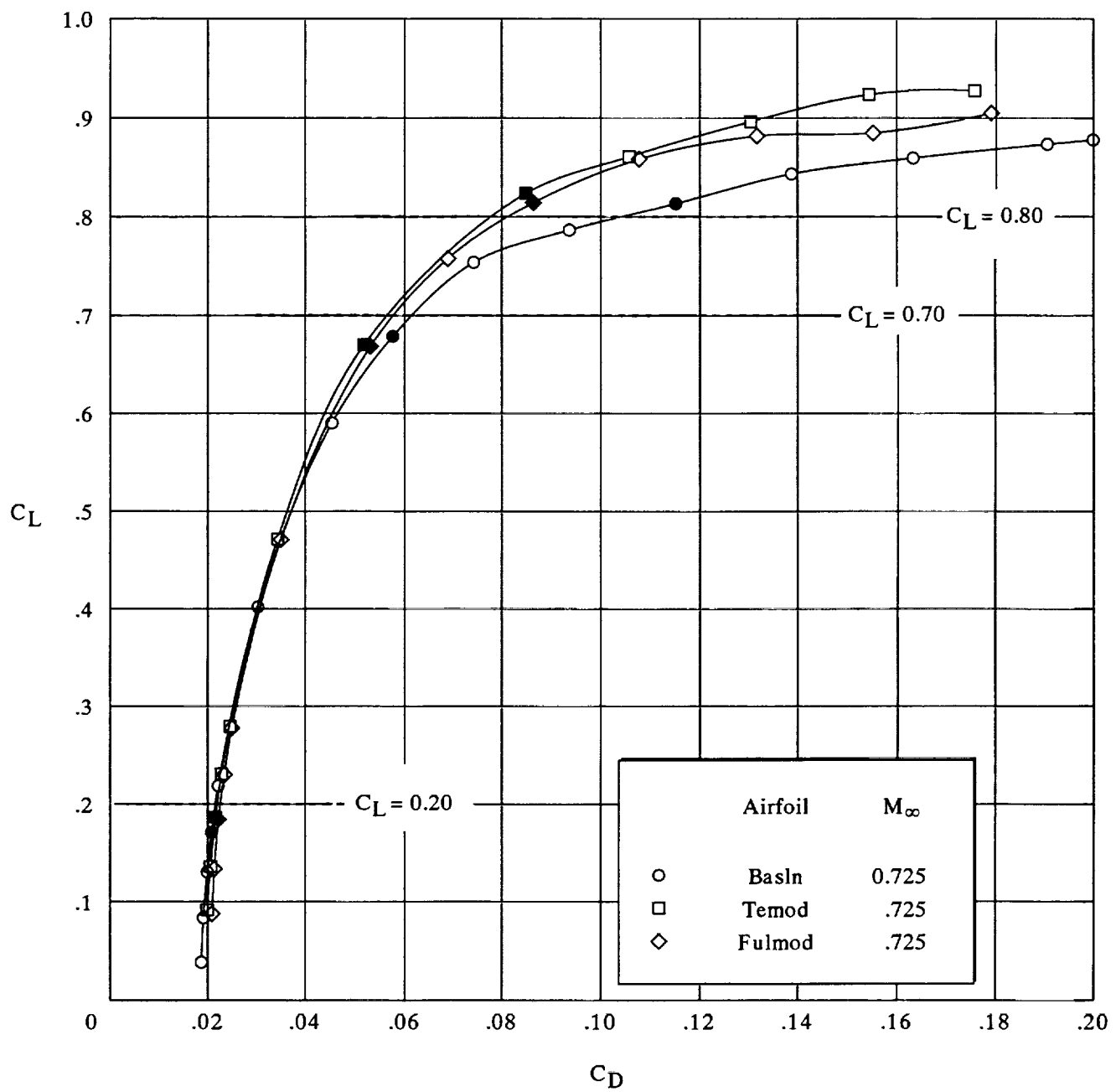


Figure 14. Trailing-edge pressure coefficient measured on EA-6B wing fuselage at  $M_\infty = 0.400$ . Solid symbols correspond to pressure distribution comparisons at similar lift coefficients.



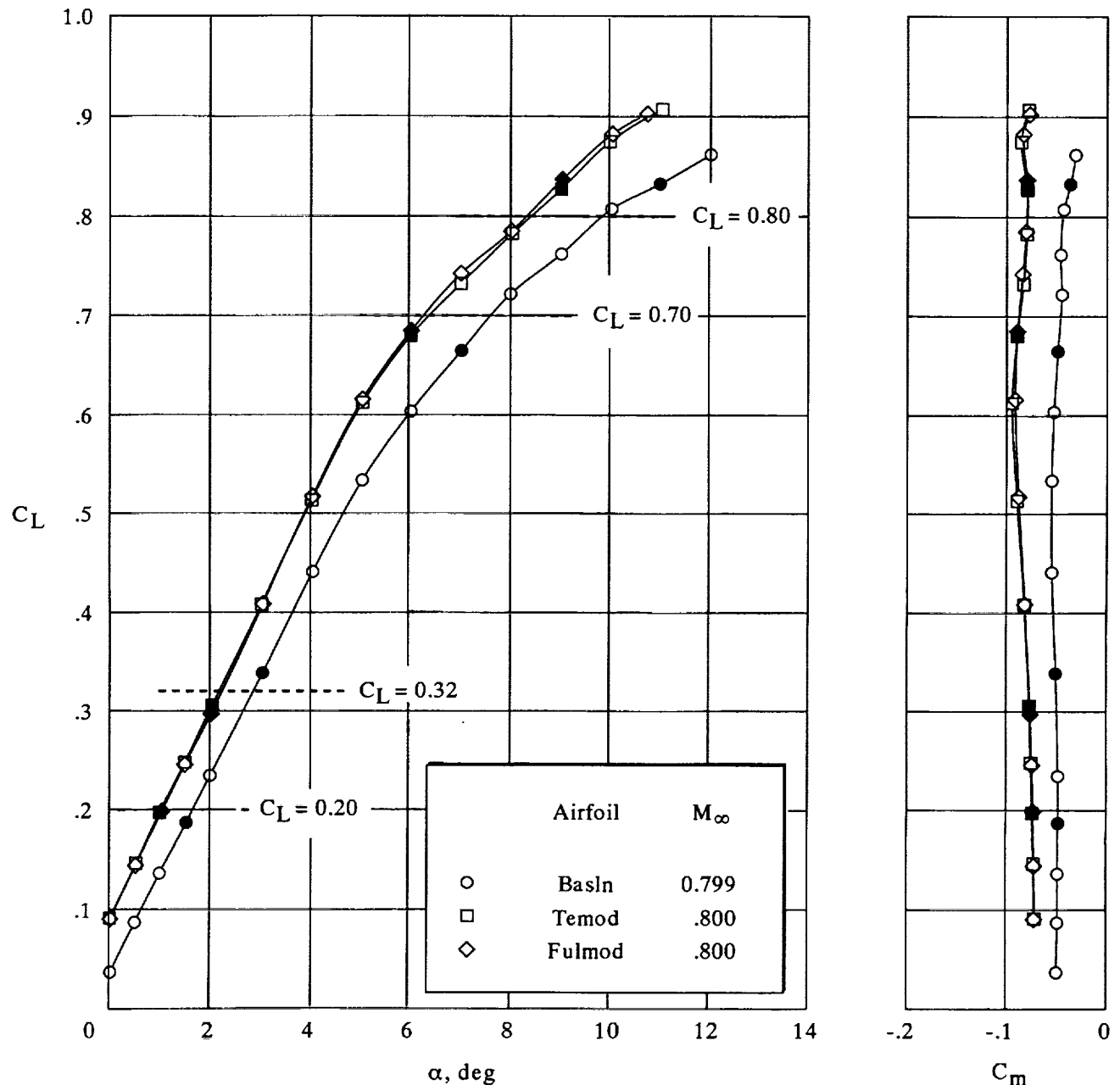
(a) Lift and pitching-moment coefficients.

Figure 15. Airfoil modification effects on longitudinal characteristics measured on EA-6B wing fuselage at  $M_\infty = 0.725$ . Solid symbols correspond to pressure distribution comparisons at similar lift coefficients.



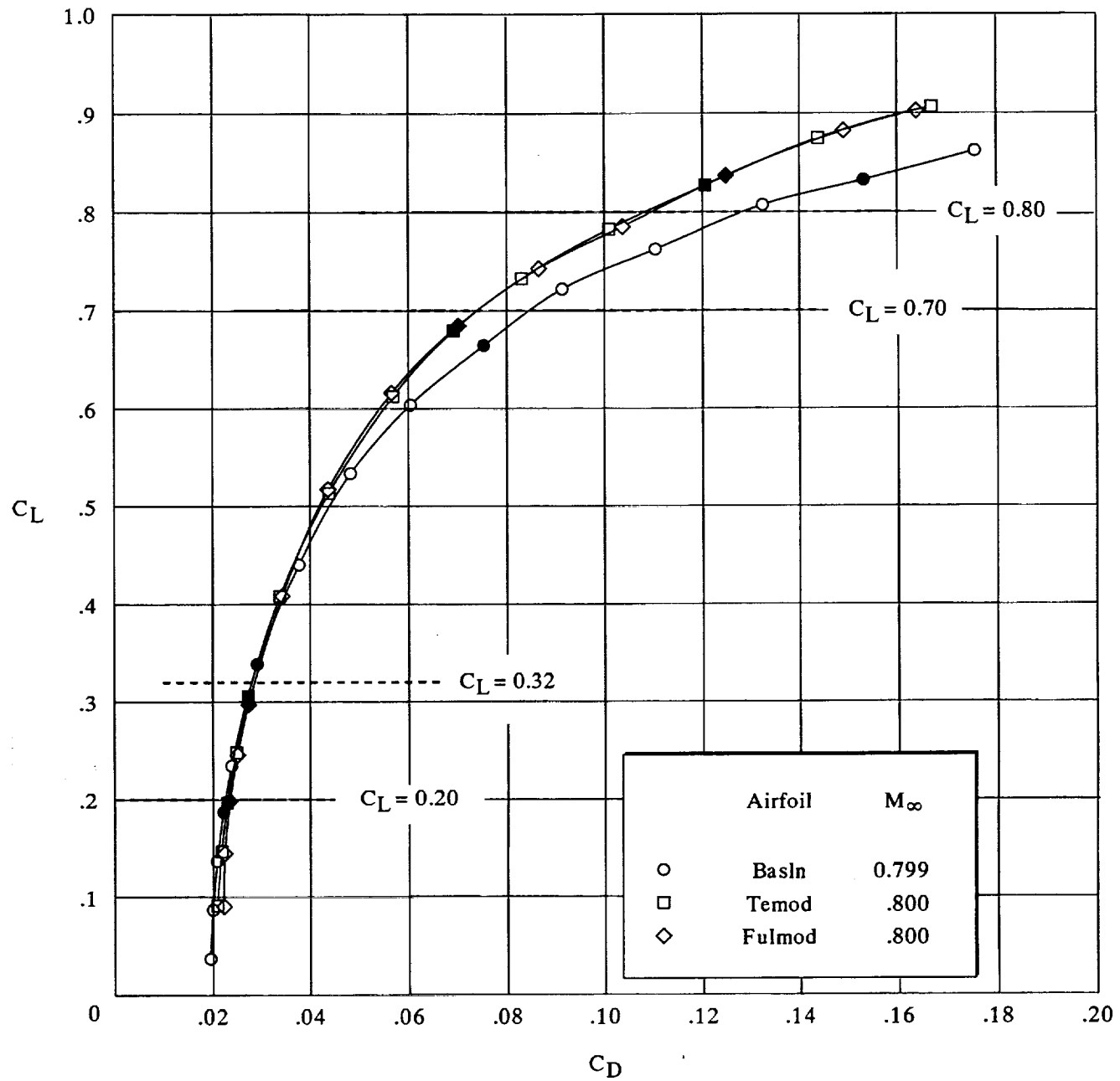
(b) Drag coefficient.

Figure 15. Concluded.



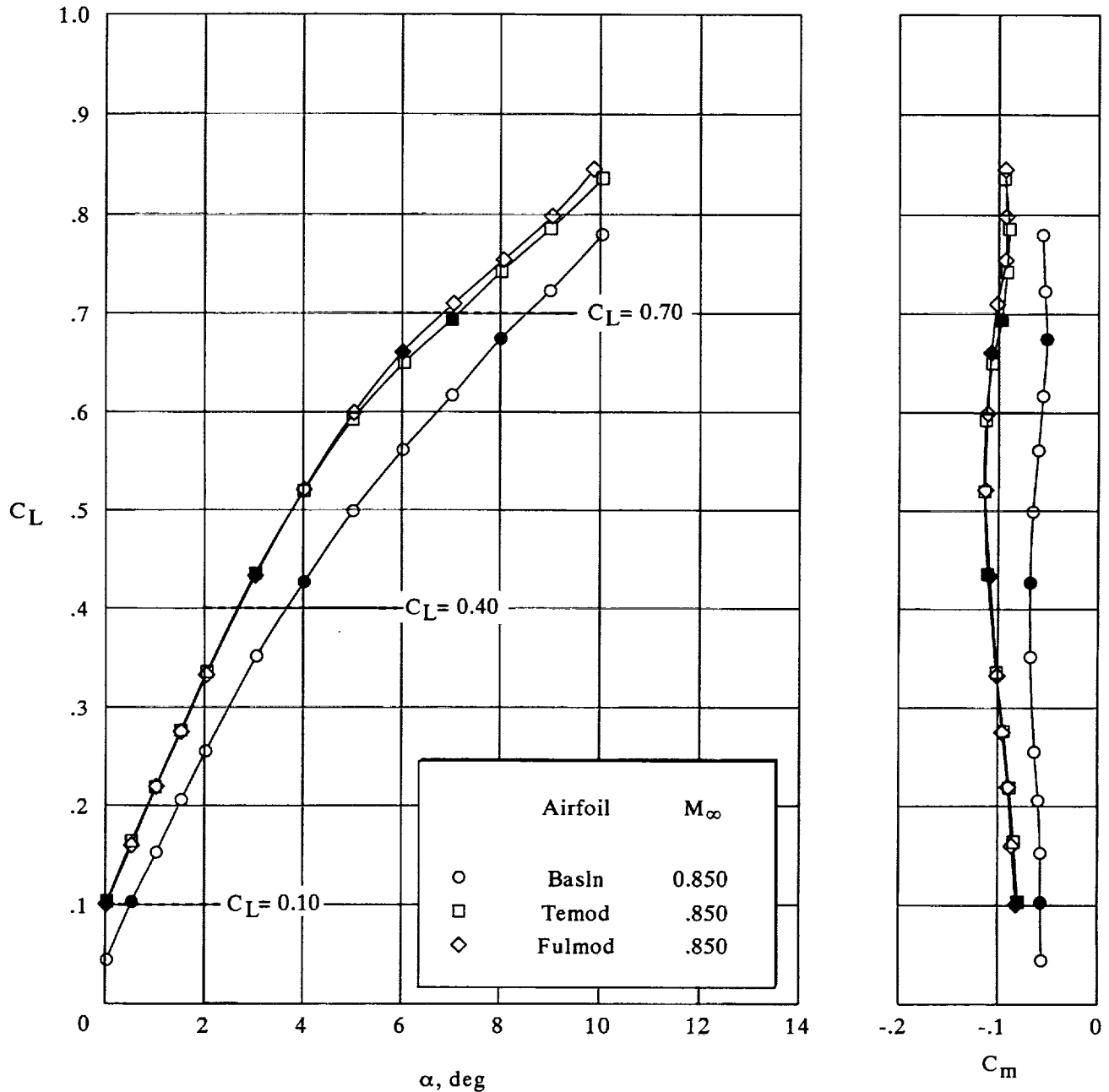
(a) Lift and pitching-moment coefficients.

Figure 16. Airfoil modification effects on longitudinal characteristics measured on EA-6B wing fuselage at  $M_\infty = 0.800$ . Solid symbols correspond to pressure distribution comparisons at similar lift coefficients.



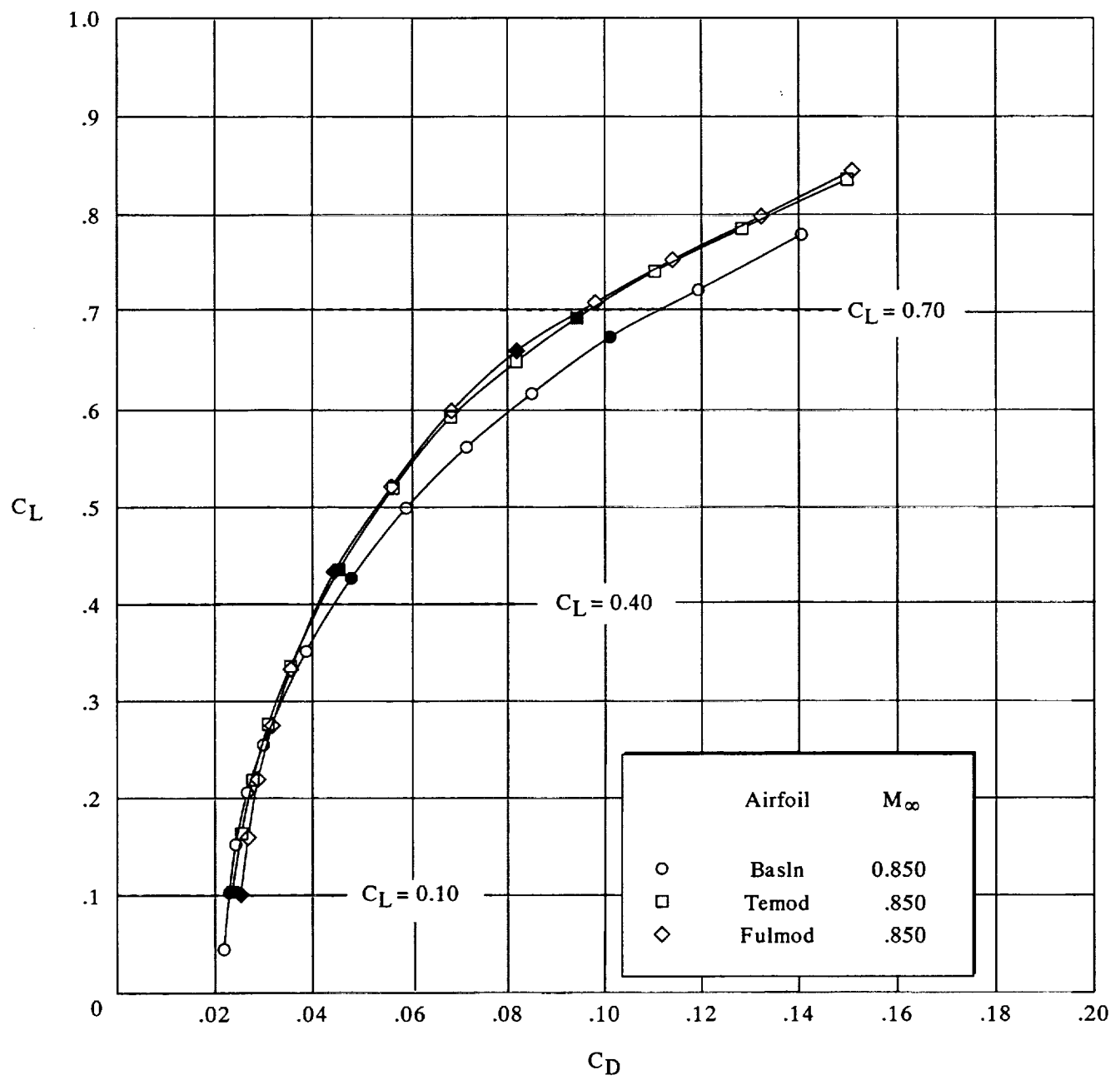
(b) Drag coefficient.

Figure 16. Concluded.



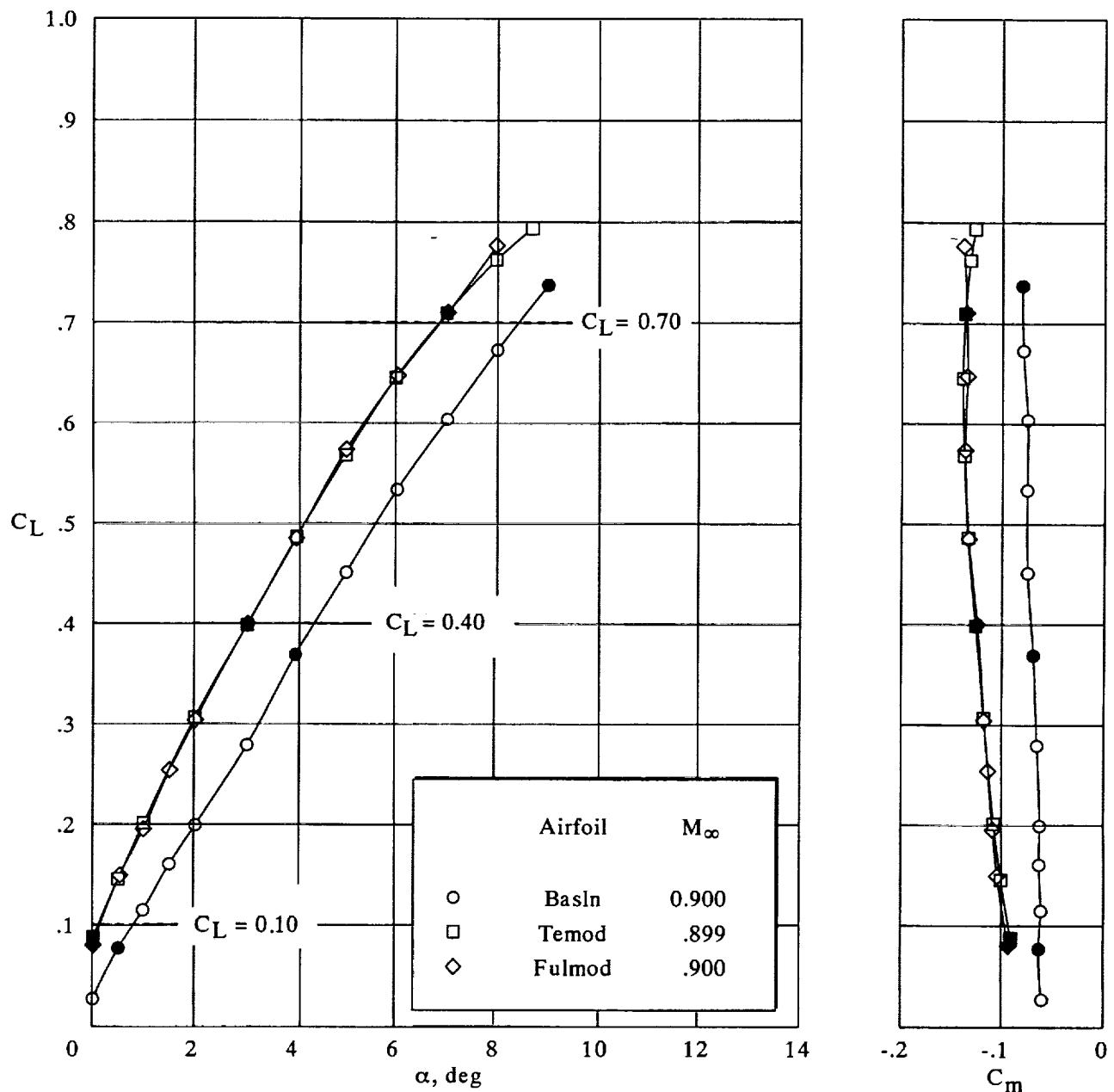
(a) Lift and pitching-moment coefficients.

Figure 17. Airfoil modification effects on longitudinal characteristics measured on EA-6B wing fuselage at  $M_\infty = 0.850$ . Solid symbols correspond to pressure distribution comparisons at similar lift coefficients.



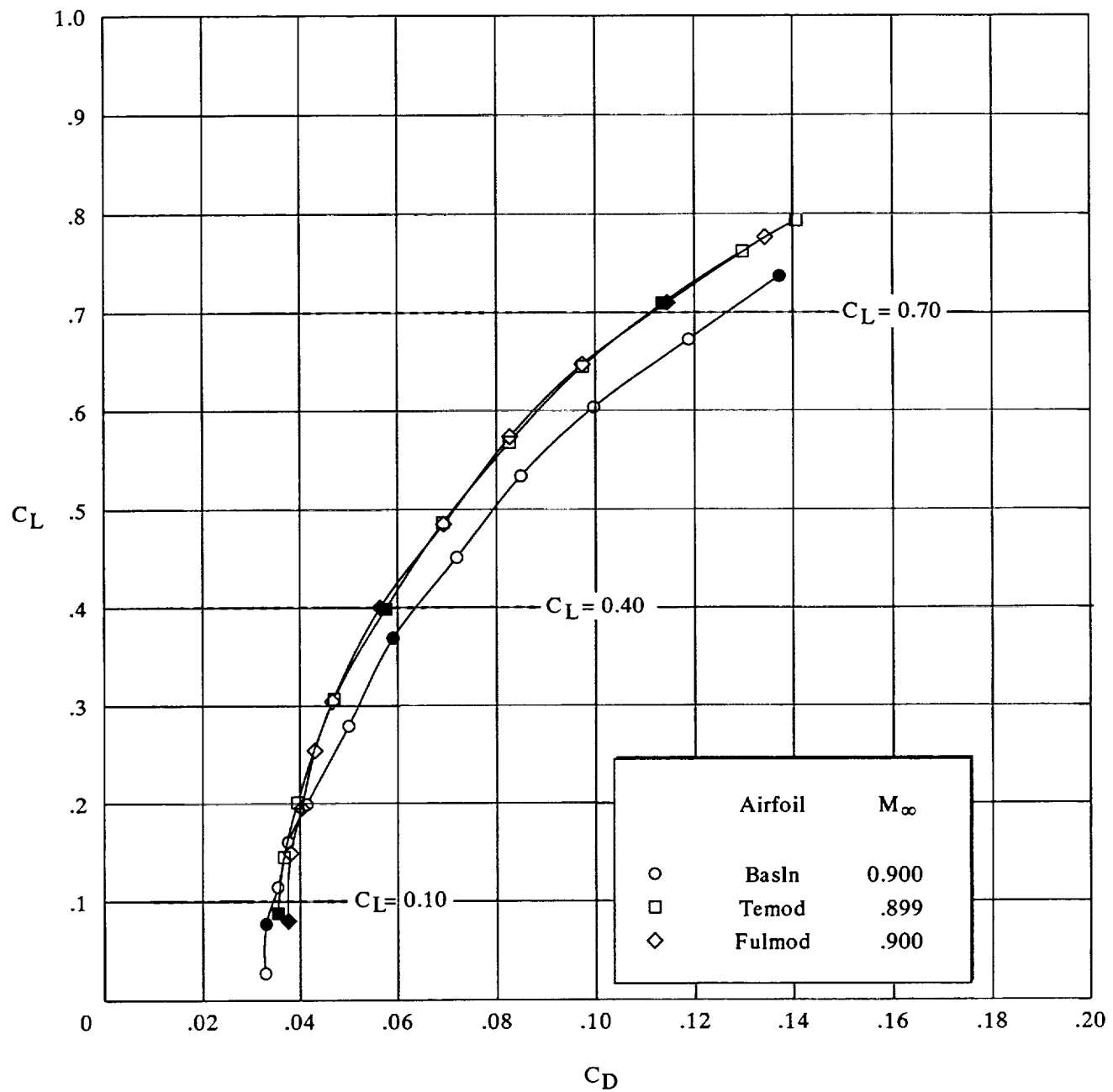
(b) Drag coefficient.

Figure 17. Concluded.



(a) Lift and pitching-moment coefficients.

Figure 18. Airfoil modification effects on longitudinal characteristics measured on EA-6B wing fuselage at  $M_\infty = 0.900$ . Solid symbols correspond to pressure distribution comparisons at similar lift coefficients.



(b) Drag coefficient.

Figure 18. Concluded.

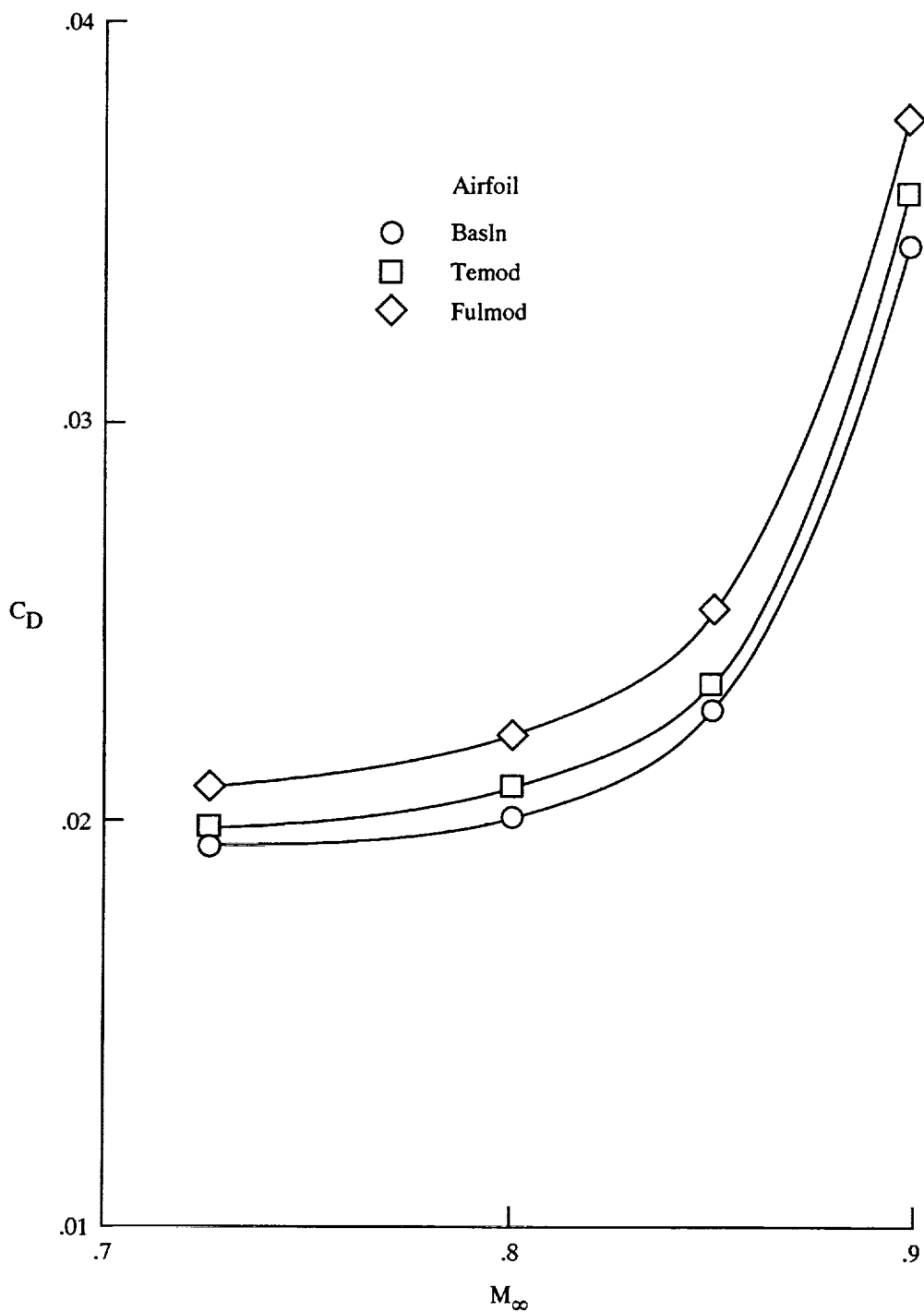


Figure 19. Airfoil modification effects on variation of drag coefficient with free-stream Mach number for EA-6B wing fuselage at  $C_L = 0.10$ .

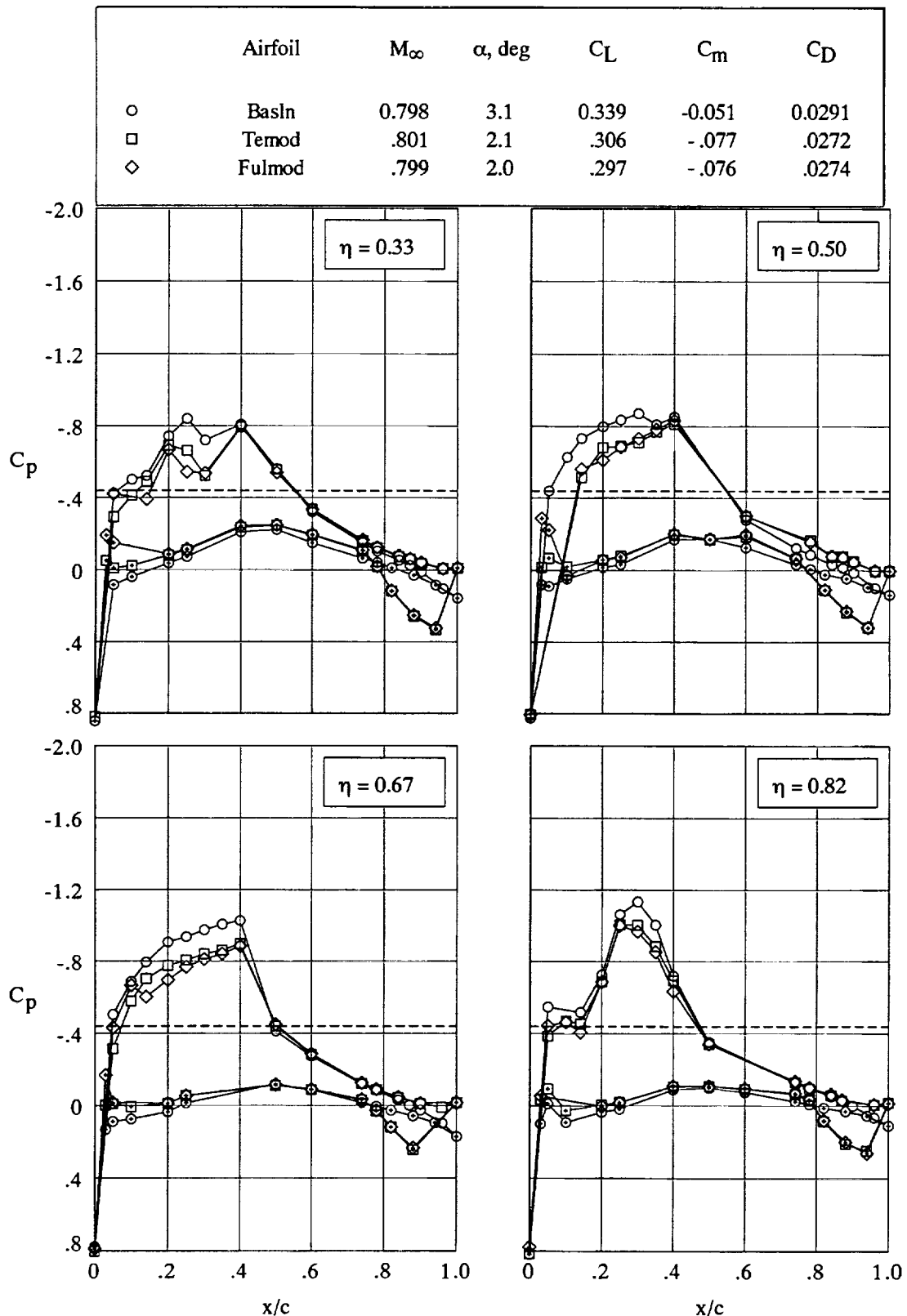


Figure 20. Chordwise pressure distributions measured on EA-6B wing fuselage at  $M_\infty = 0.800$  and  $C_L \approx 0.32$ . Open symbols denote upper surface; + within symbol denotes lower surface. Dashed line indicates sonic  $C_p$ .

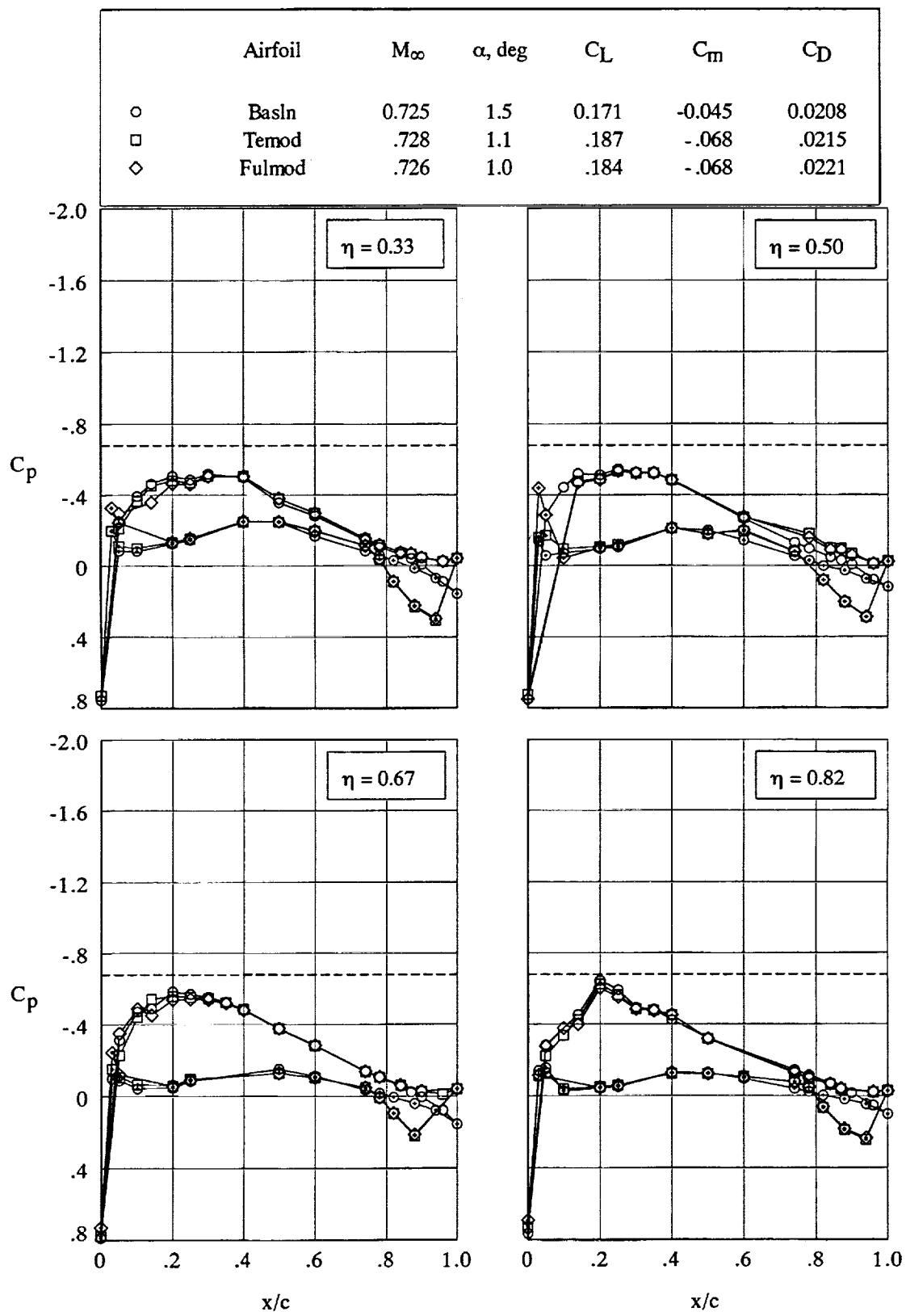


Figure 21. Chordwise pressure distributions measured on EA-6B wing fuselage at  $M_\infty = 0.725$  and  $C_L \approx 0.20$ . Open symbols denote upper surface; + within symbol denotes lower surface. Dashed line indicates sonic  $C_p$ .

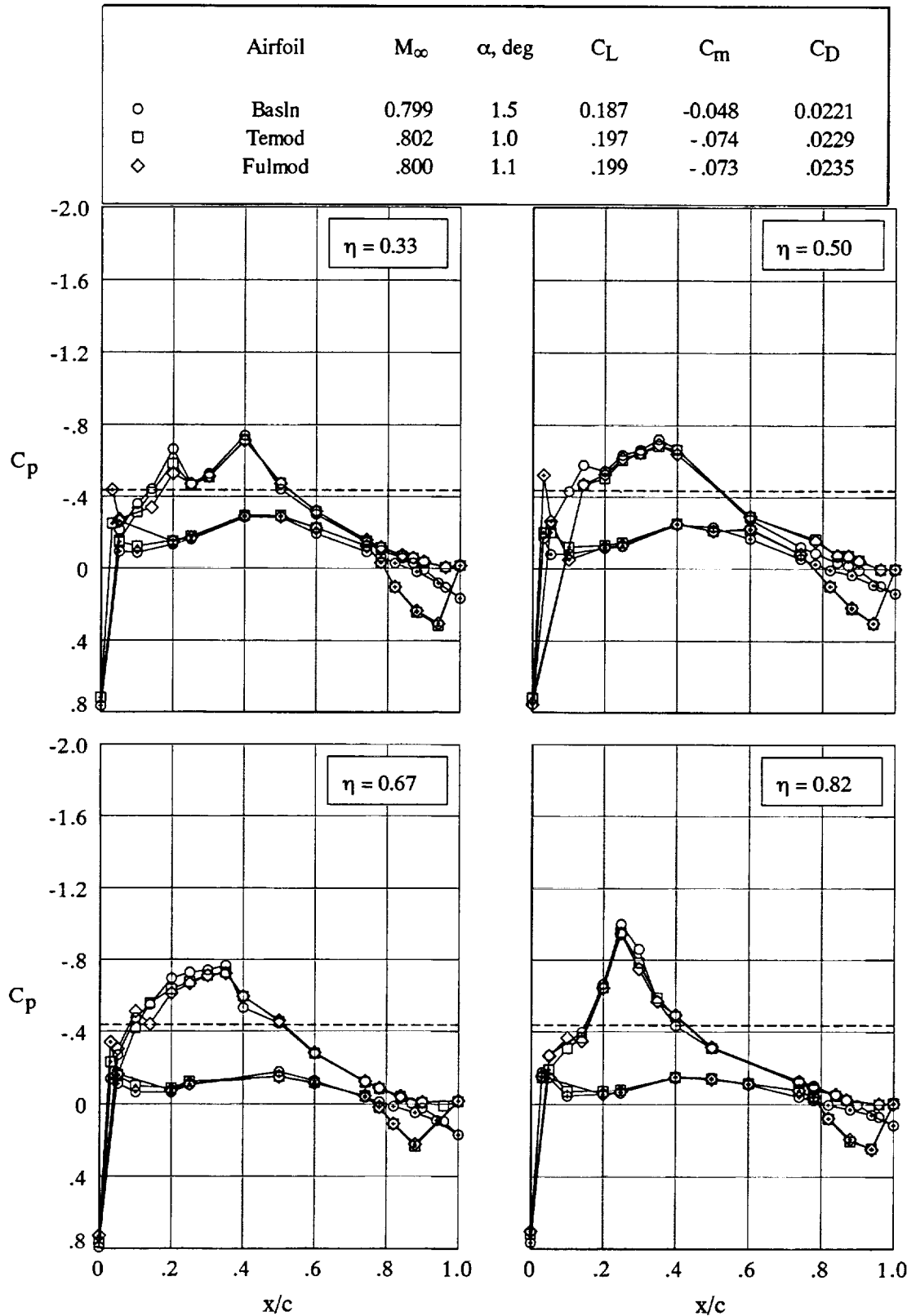


Figure 22. Chordwise pressure distributions measured on EA-6B wing fuselage at  $M_\infty = 0.800$  and  $C_L \approx 0.20$ . Open symbols denote upper surface; + within symbol denotes lower surface. Dashed line indicates sonic  $C_p$ .

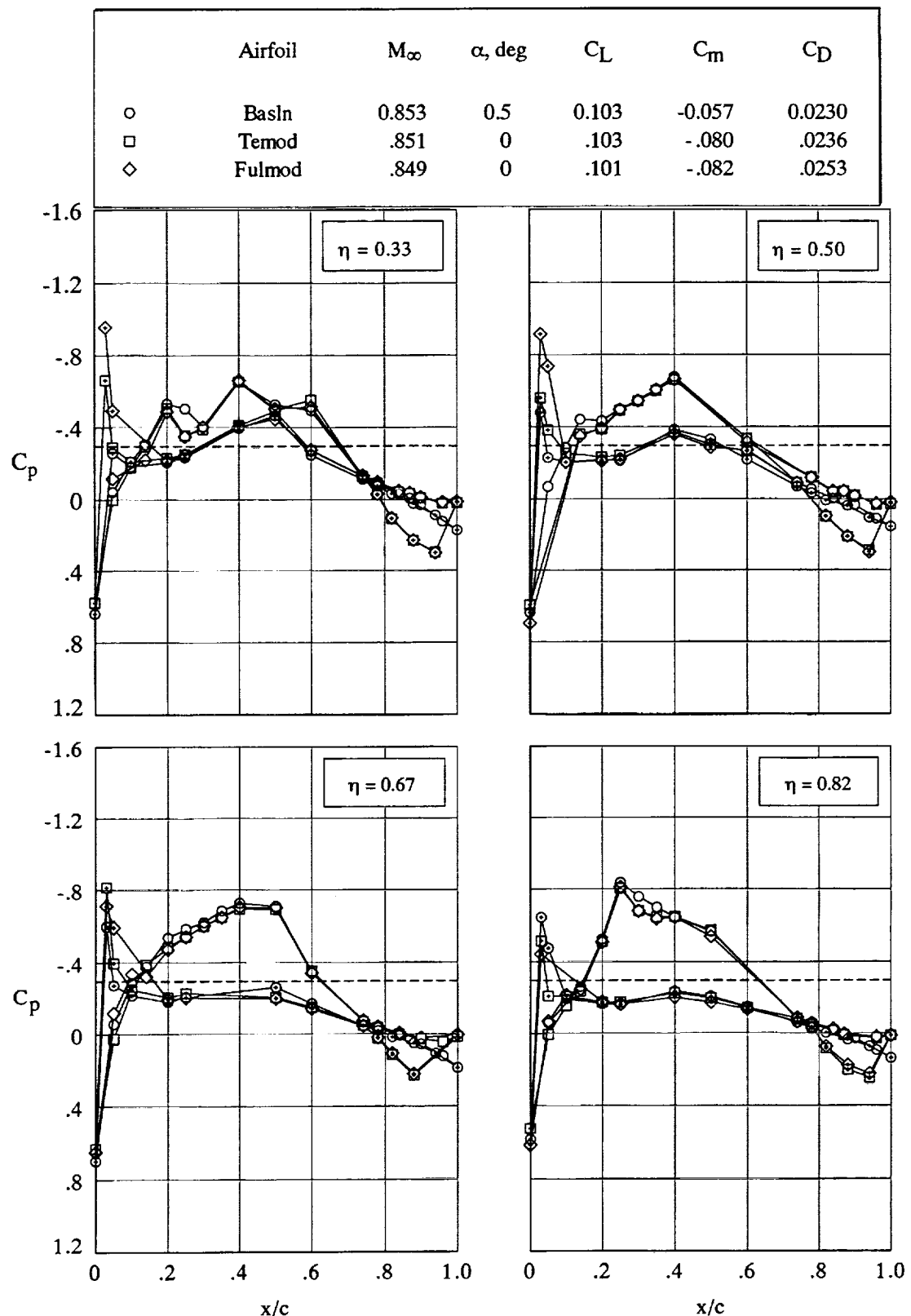


Figure 23. Chordwise pressure distributions measured on EA-6B wing fuselage at  $M_\infty = 0.850$  and  $C_L \approx 0.10$ . Open symbols denote upper surface; + within symbol denotes lower surface. Dashed line indicates sonic  $C_p$ .

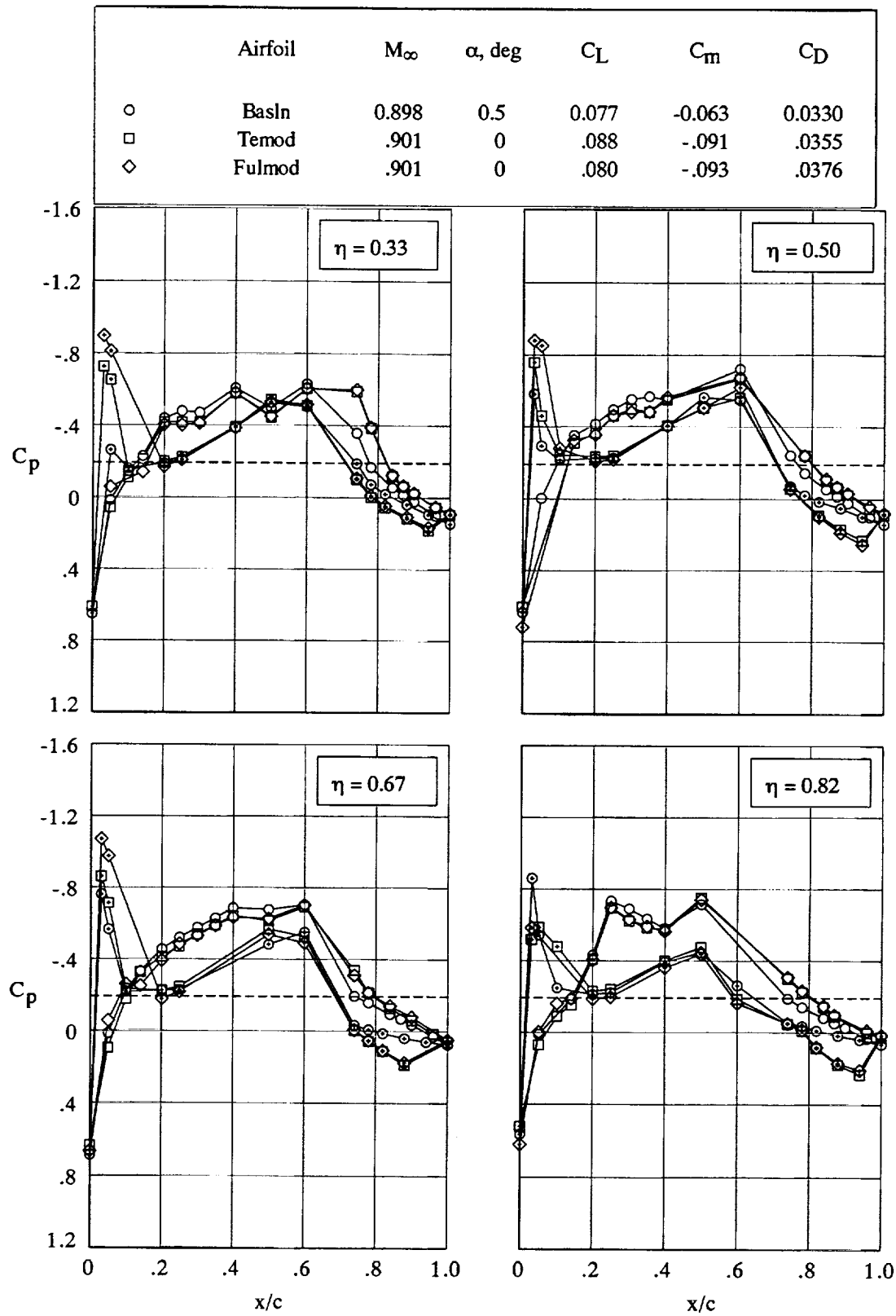


Figure 24. Chordwise pressure distributions measured on EA-6B wing fuselage at  $M_\infty = 0.900$  and  $C_L \approx 0.10$ . Open symbols denote upper surface; + within symbol denotes lower surface. Dashed line indicates sonic  $C_p$ .

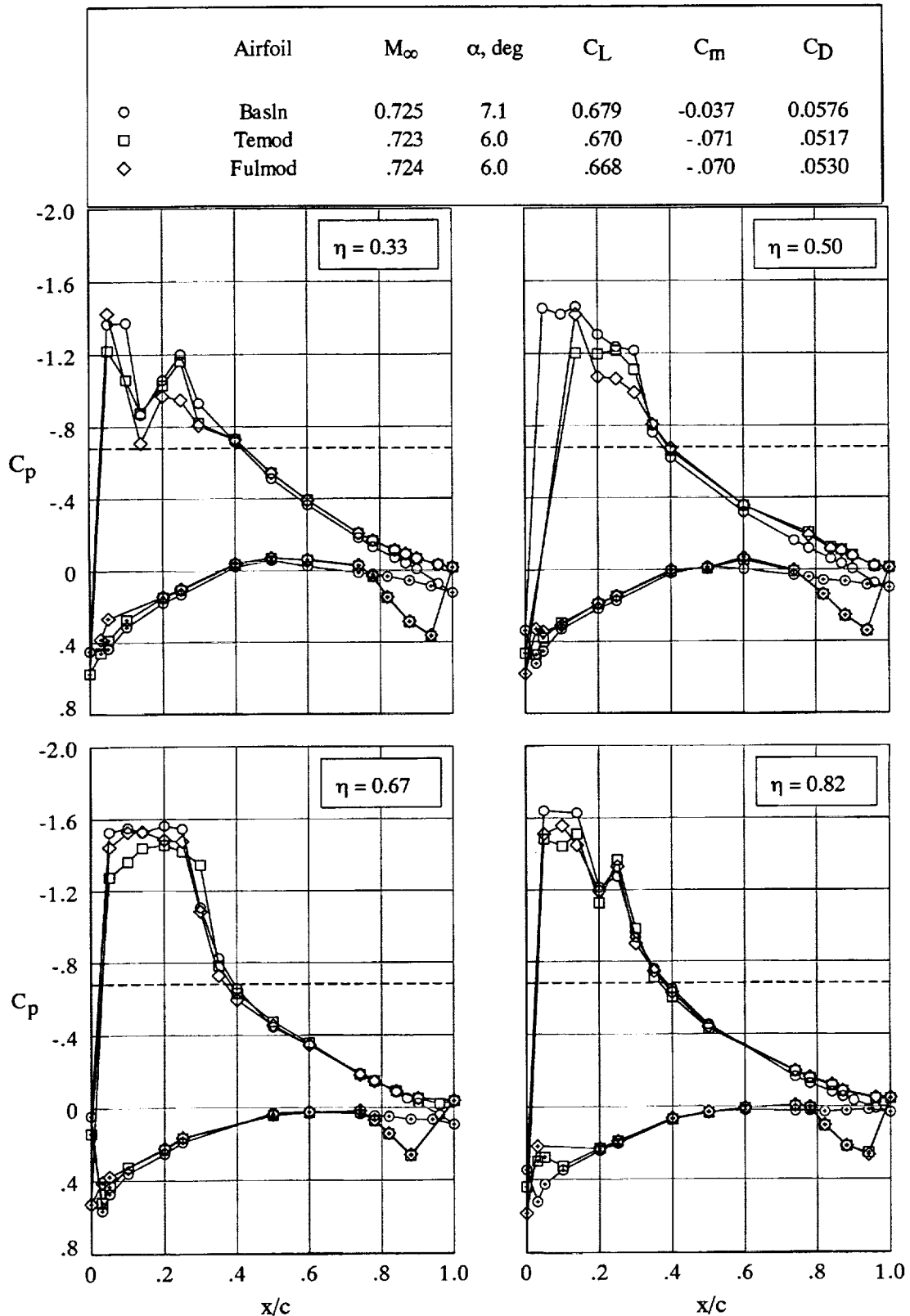


Figure 25. Chordwise pressure distributions measured on EA-6B wing fuselage at  $M_\infty = 0.725$  and  $C_L \approx 0.70$ . Open symbols denote upper surface; + within symbol denotes lower surface. Dashed line indicates sonic  $C_p$ .

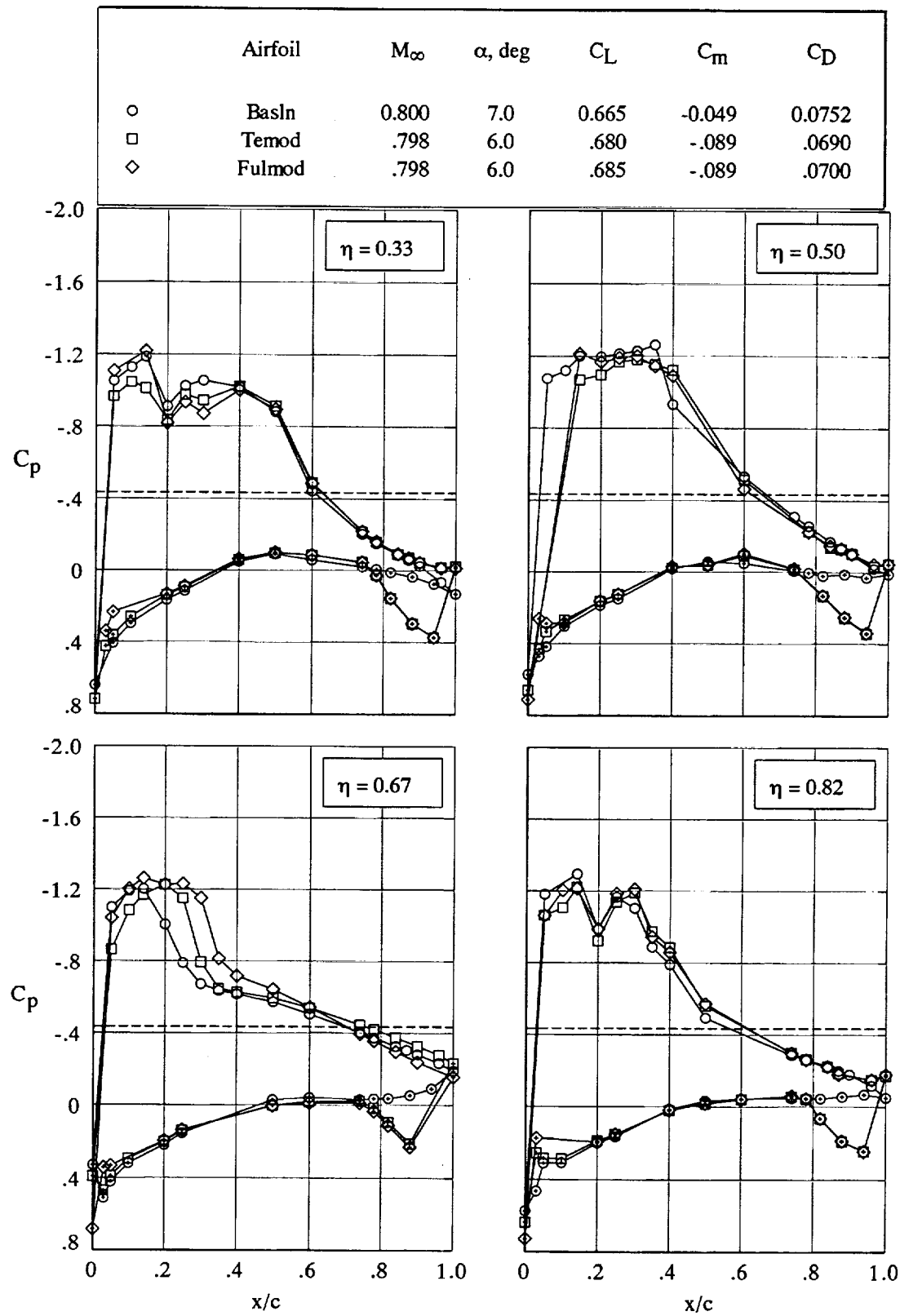


Figure 26. Chordwise pressure distributions measured on EA-6B wing fuselage at  $M_\infty = 0.800$  and  $C_L \approx 0.70$ . Open symbols denote upper surface; + within symbol denotes lower surface. Dashed line indicates sonic  $C_p$ .

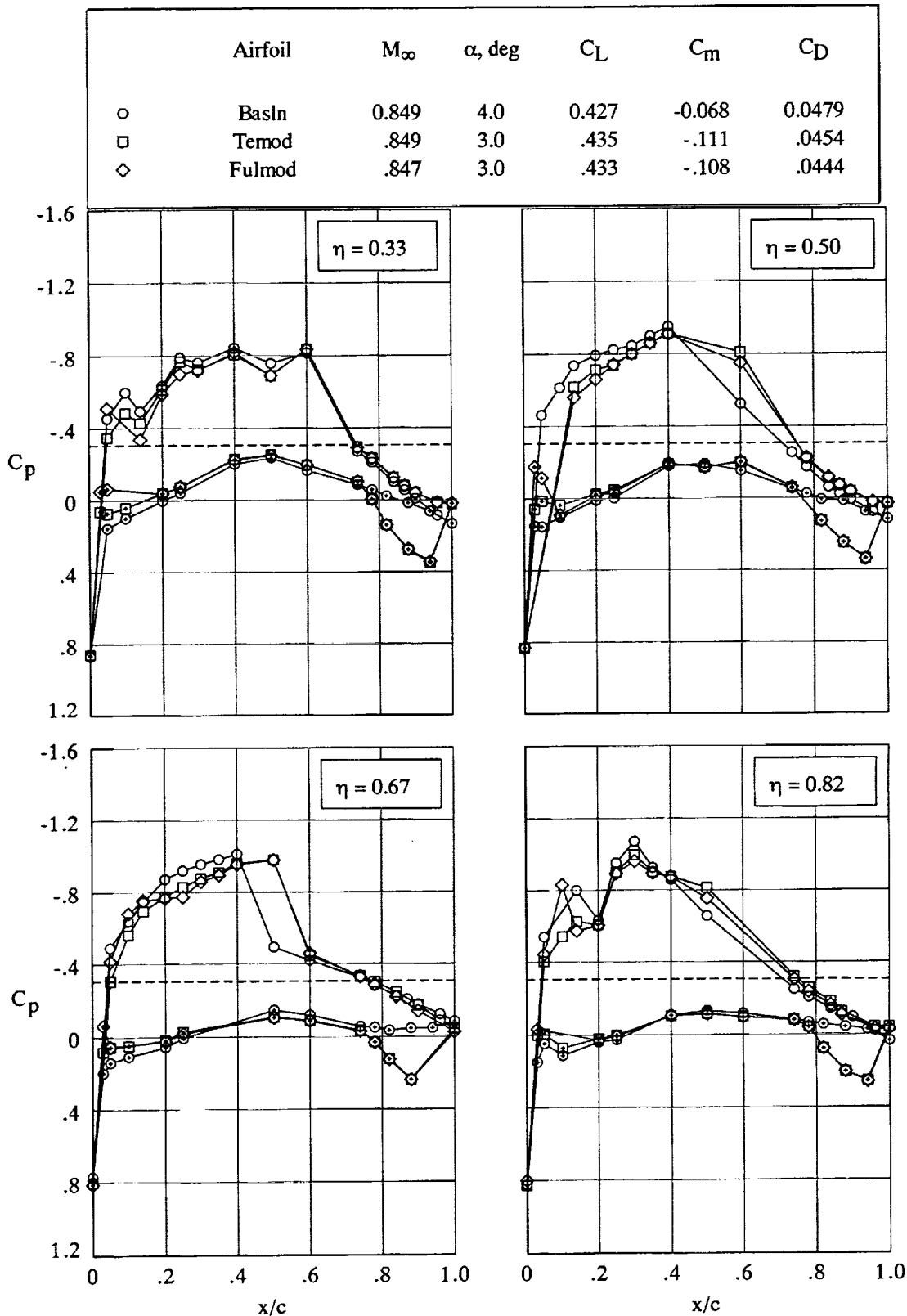


Figure 27. Chordwise pressure distributions measured on EA-6B wing fuselage at  $M_\infty = 0.850$  and  $C_L \approx 0.40$ . Open symbols denote upper surface; + within symbol denotes lower surface. Dashed line indicates sonic  $C_p$ .

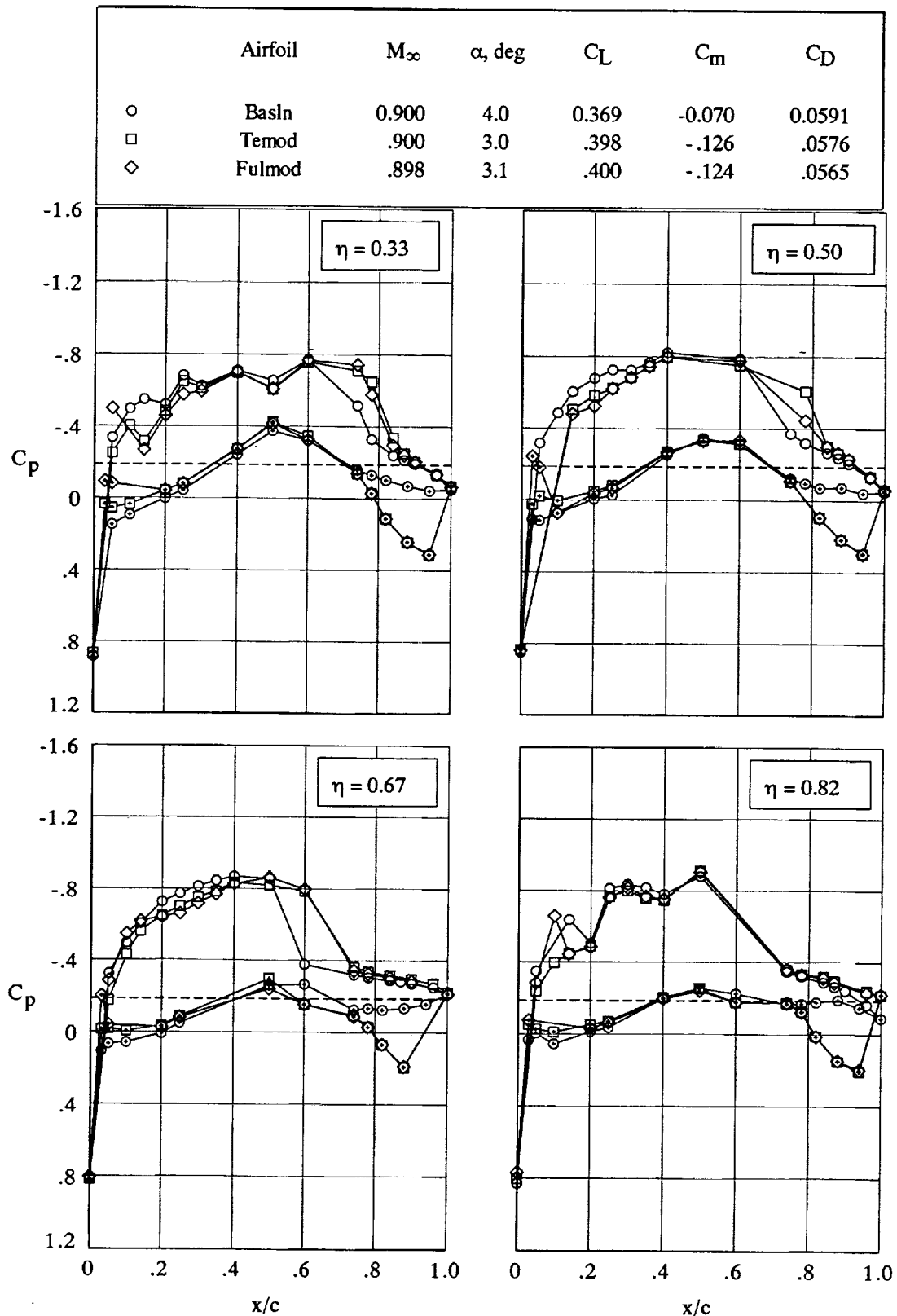


Figure 28. Chordwise pressure distributions measured on EA-6B wing fuselage at  $M_\infty = 0.900$  and  $C_L \approx 0.40$ . Open symbols denote upper surface; + within symbol denotes lower surface. Dashed line indicates sonic  $C_p$ .

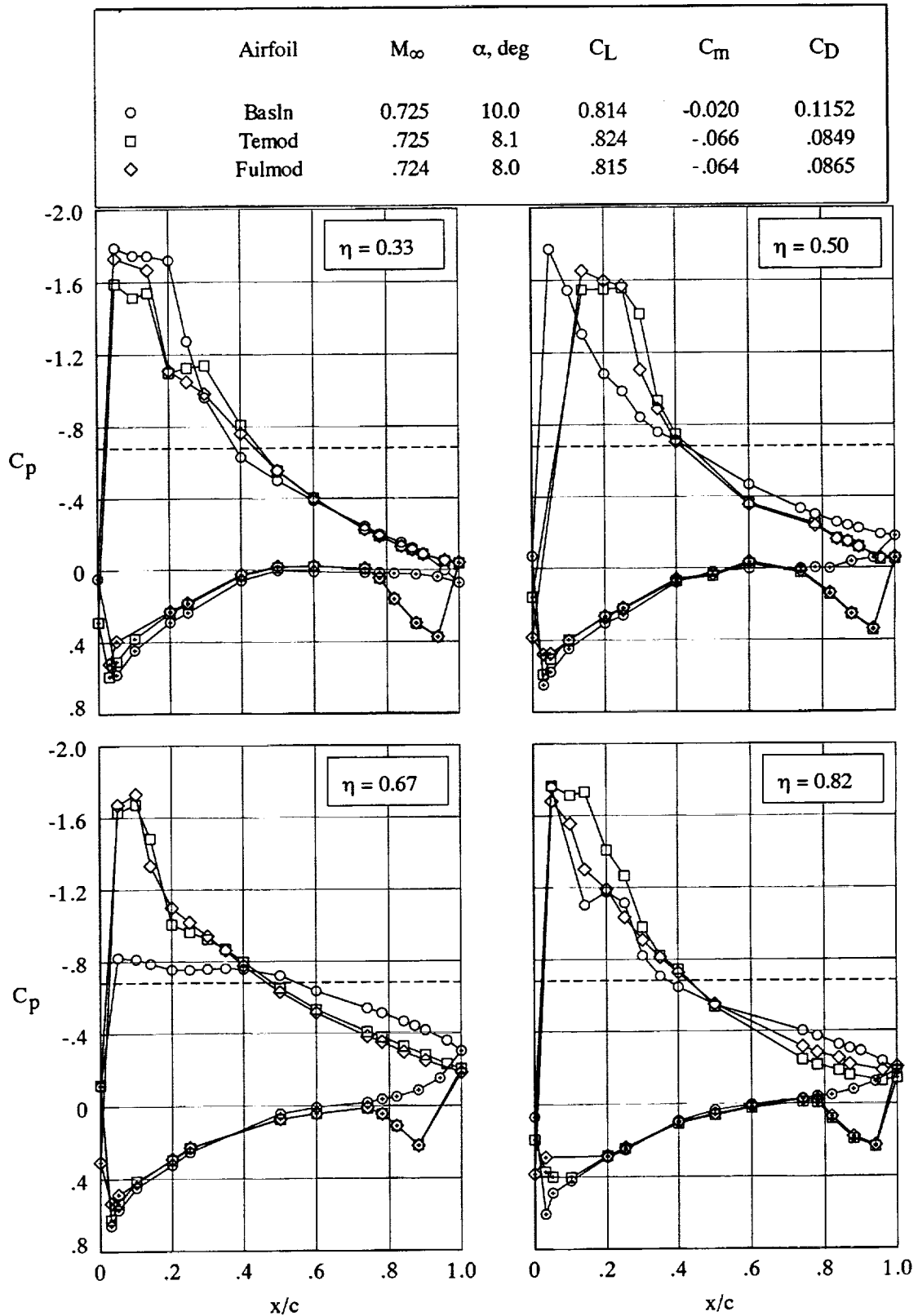


Figure 29. Chordwise pressure distributions measured on EA-6B wing fuselage at  $M_\infty = 0.725$  and  $C_L \approx 0.80$ . Open symbols denote upper surface; + within symbol denotes lower surface. Dashed line indicates sonic  $C_p$ .

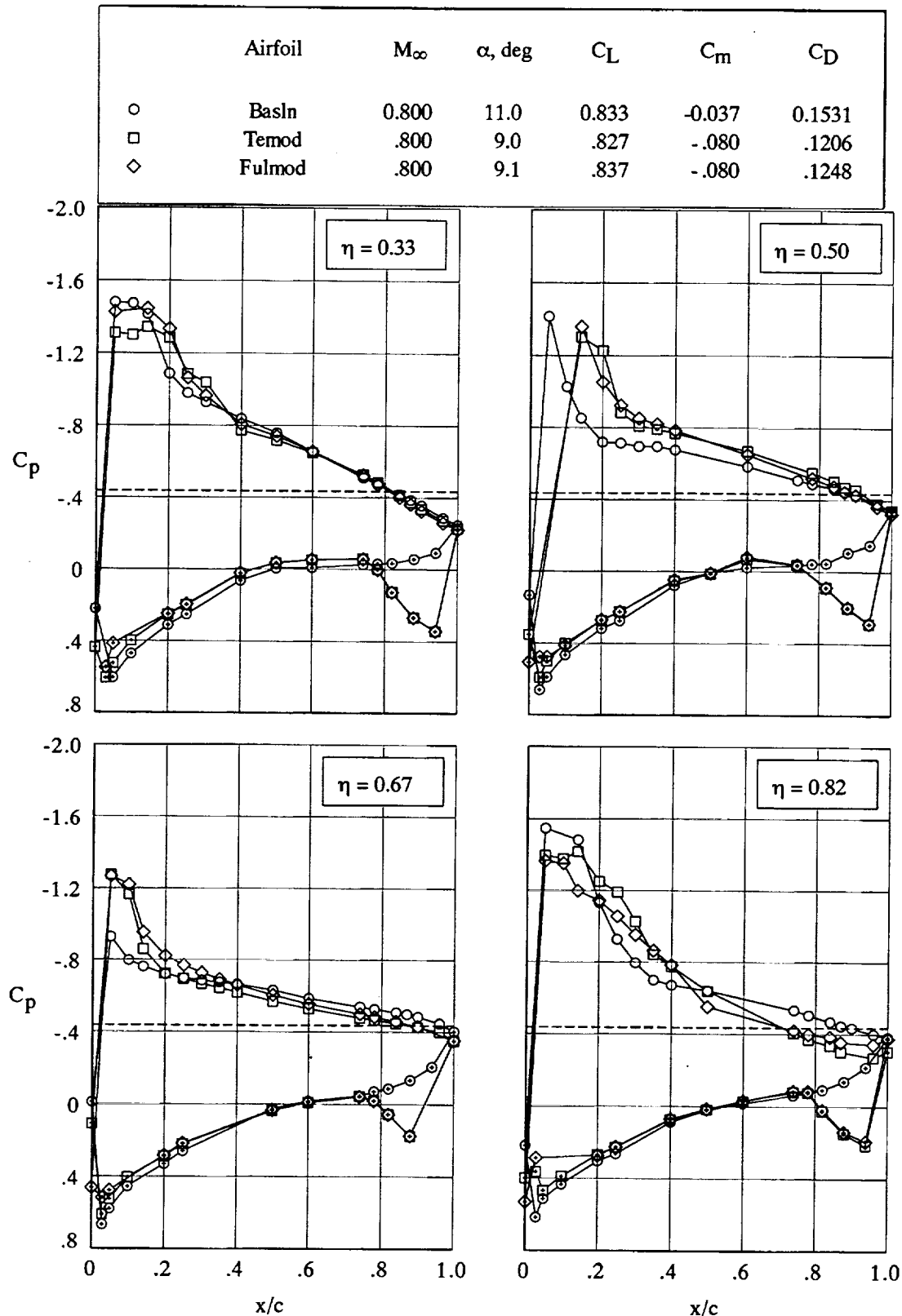


Figure 30. Chordwise pressure distributions measured on EA-6B wing fuselage at  $M_\infty = 0.800$  and  $C_L \approx 0.80$ . Open symbols denote upper surface; + within symbol denotes lower surface. Dashed line indicates sonic  $C_p$ .

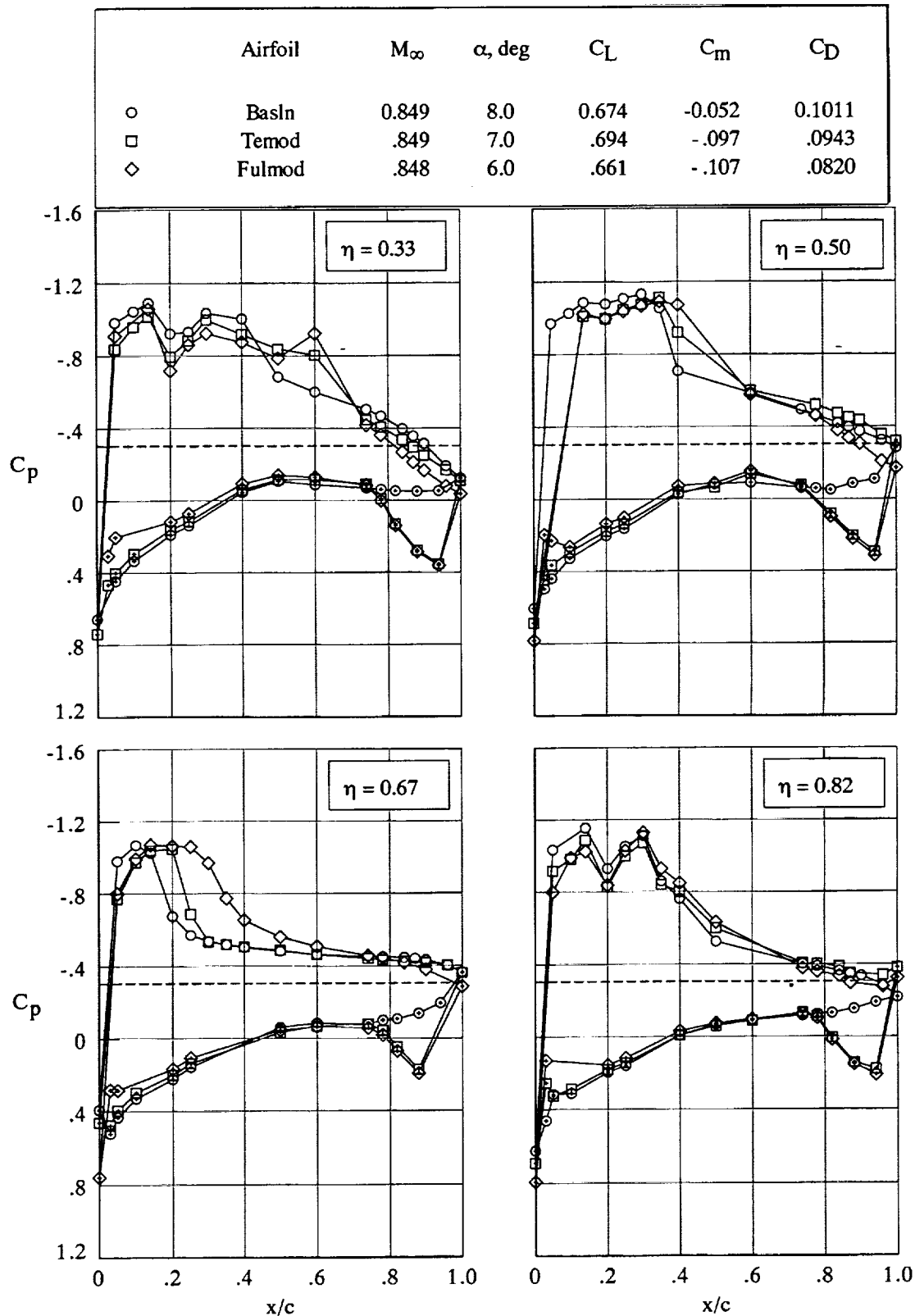


Figure 31. Chordwise pressure distributions measured on EA-6B wing fuselage at  $M_\infty = 0.850$  and  $C_L \approx 0.70$ . Open symbols denote upper surface; + within symbol denotes lower surface. Dashed line indicates sonic  $C_p$ .

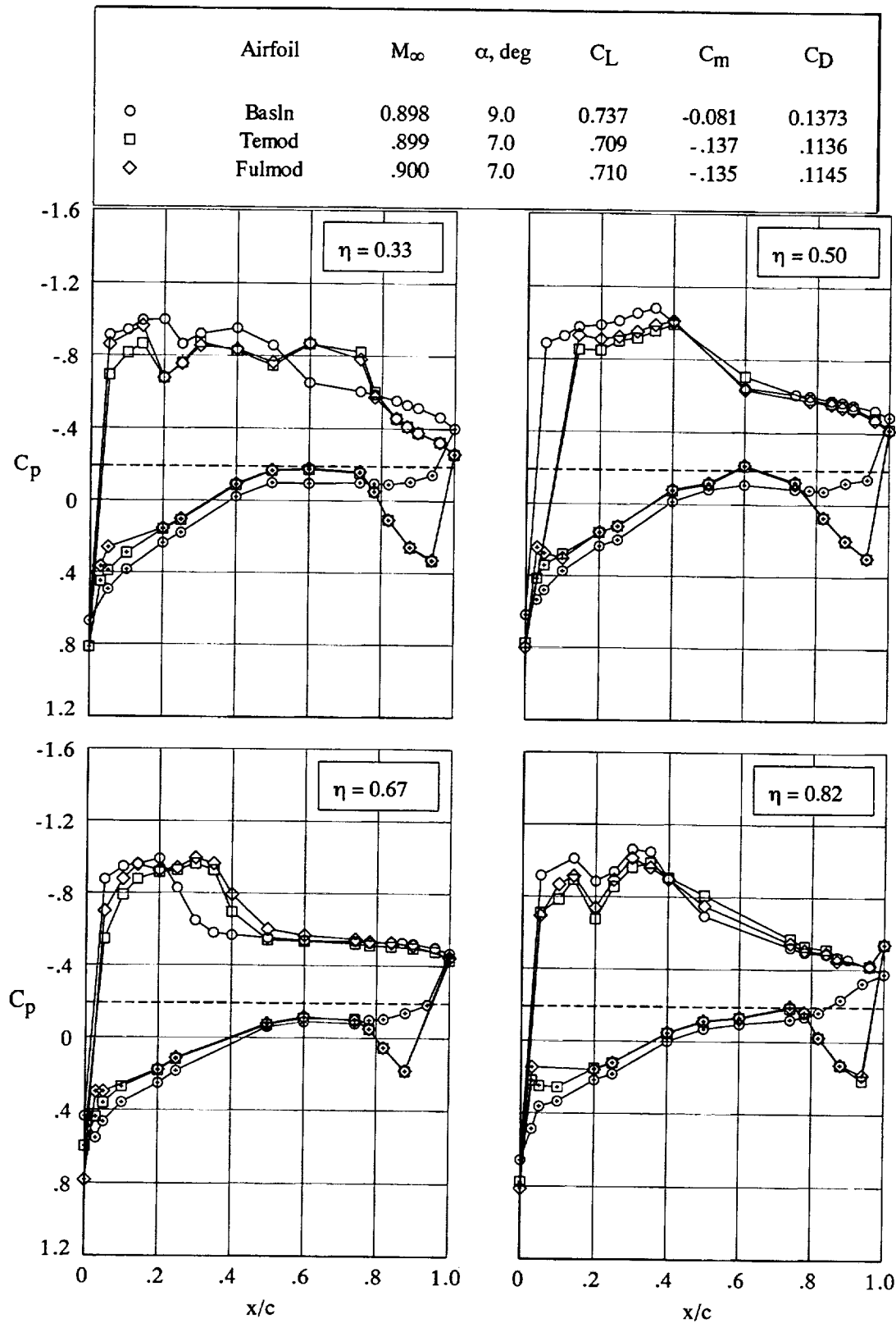


Figure 32. Chordwise pressure distributions measured on EA-6B wing fuselage at  $M_\infty = 0.900$  and  $C_L \approx 0.70$ . Open symbols denote upper surface; + within symbol denotes lower surface. Dashed line indicates sonic  $C_p$ .

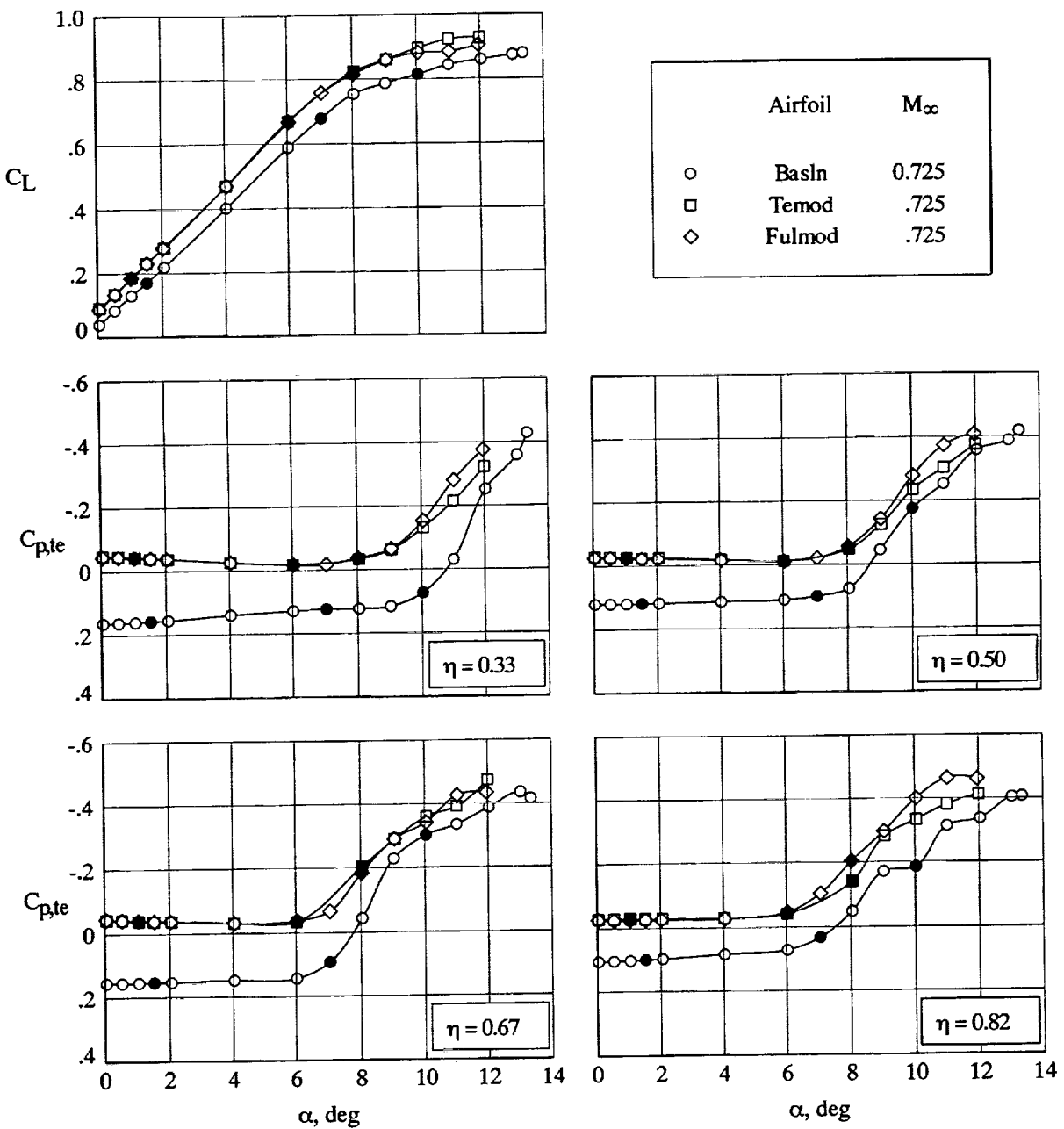


Figure 33. Trailing-edge pressure coefficient measured on EA-6B wing fuselage at  $M_\infty = 0.725$ . Solid symbols correspond to pressure distribution comparisons at similar lift coefficients.

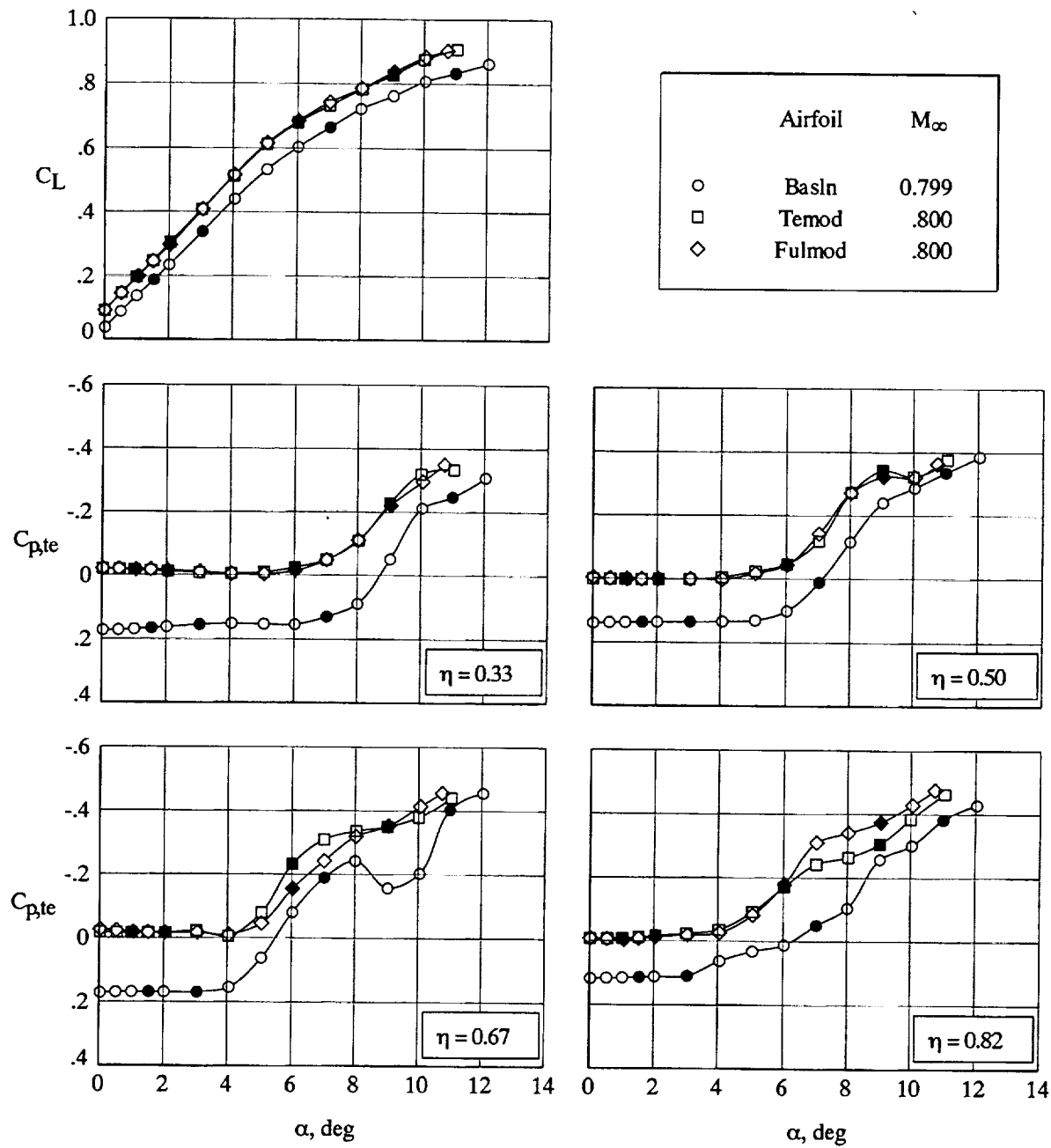


Figure 34. Trailing-edge pressure coefficient measured on EA-6B wing fuselage at  $M_\infty = 0.800$ . Solid symbols correspond to pressure distribution comparisons at similar lift coefficients.

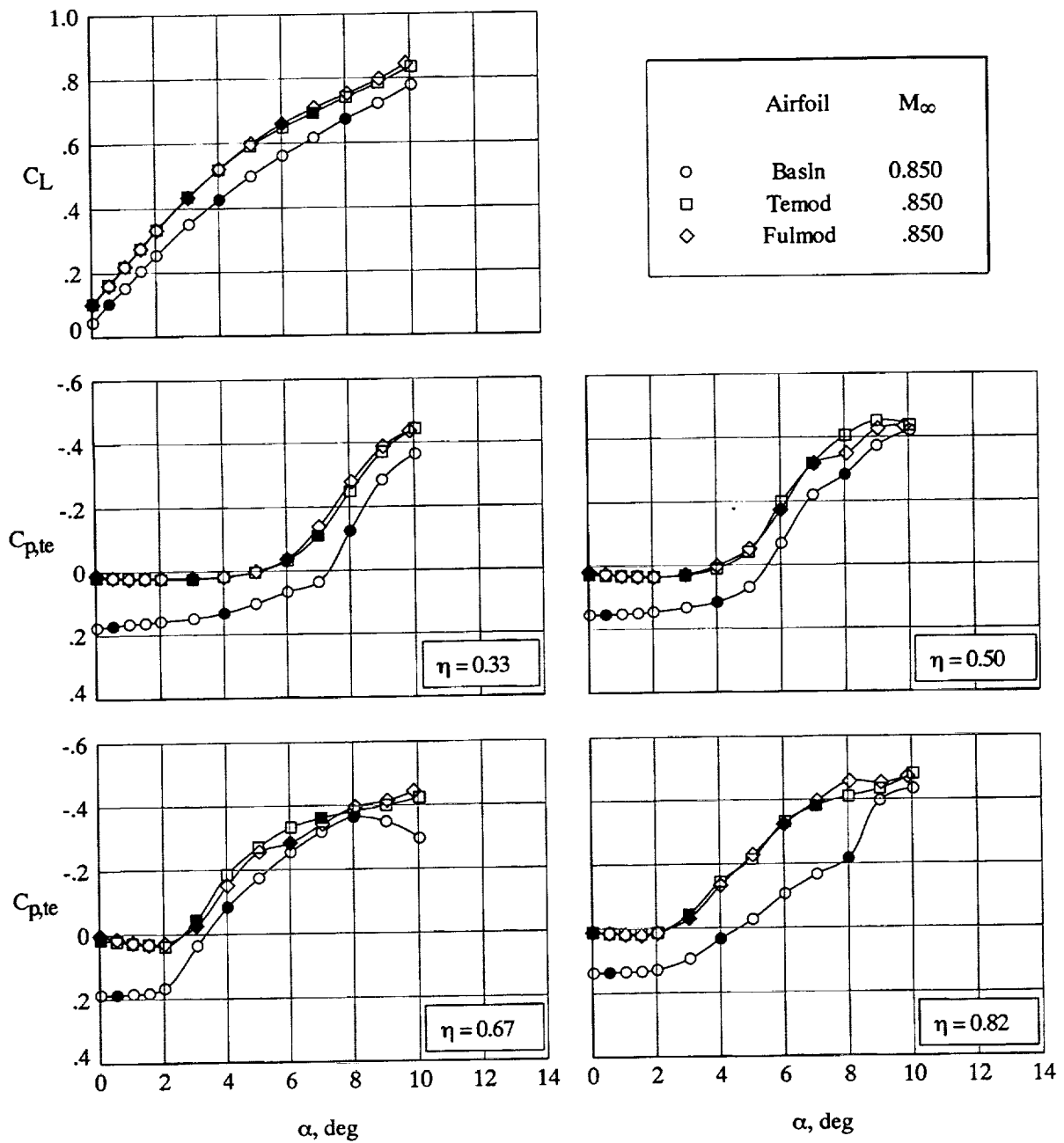


Figure 35. Trailing-edge pressure coefficient measured on EA-6B wing fuselage at  $M_\infty = 0.850$ . Solid symbols correspond to pressure distribution comparisons at similar lift coefficients.

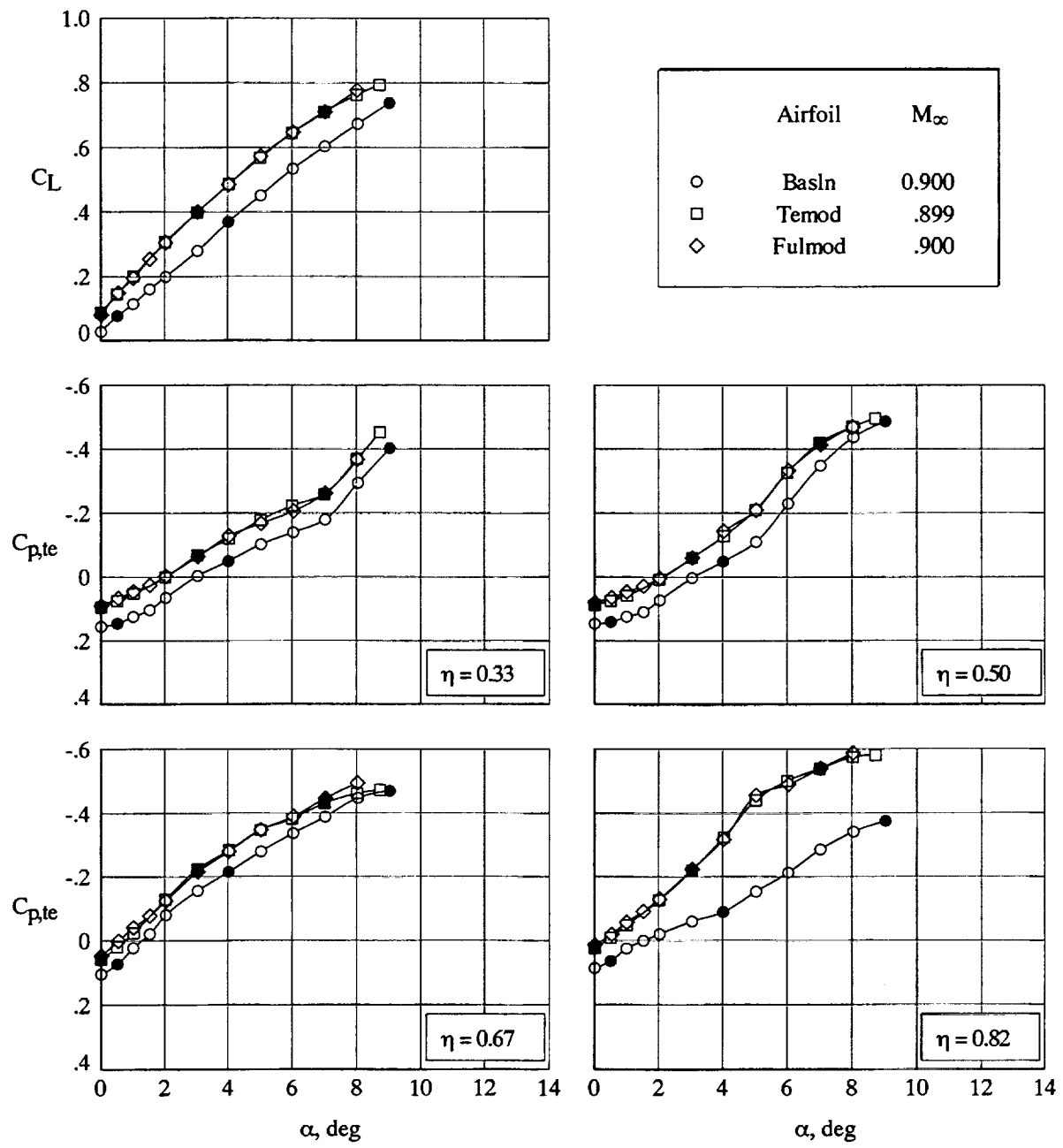
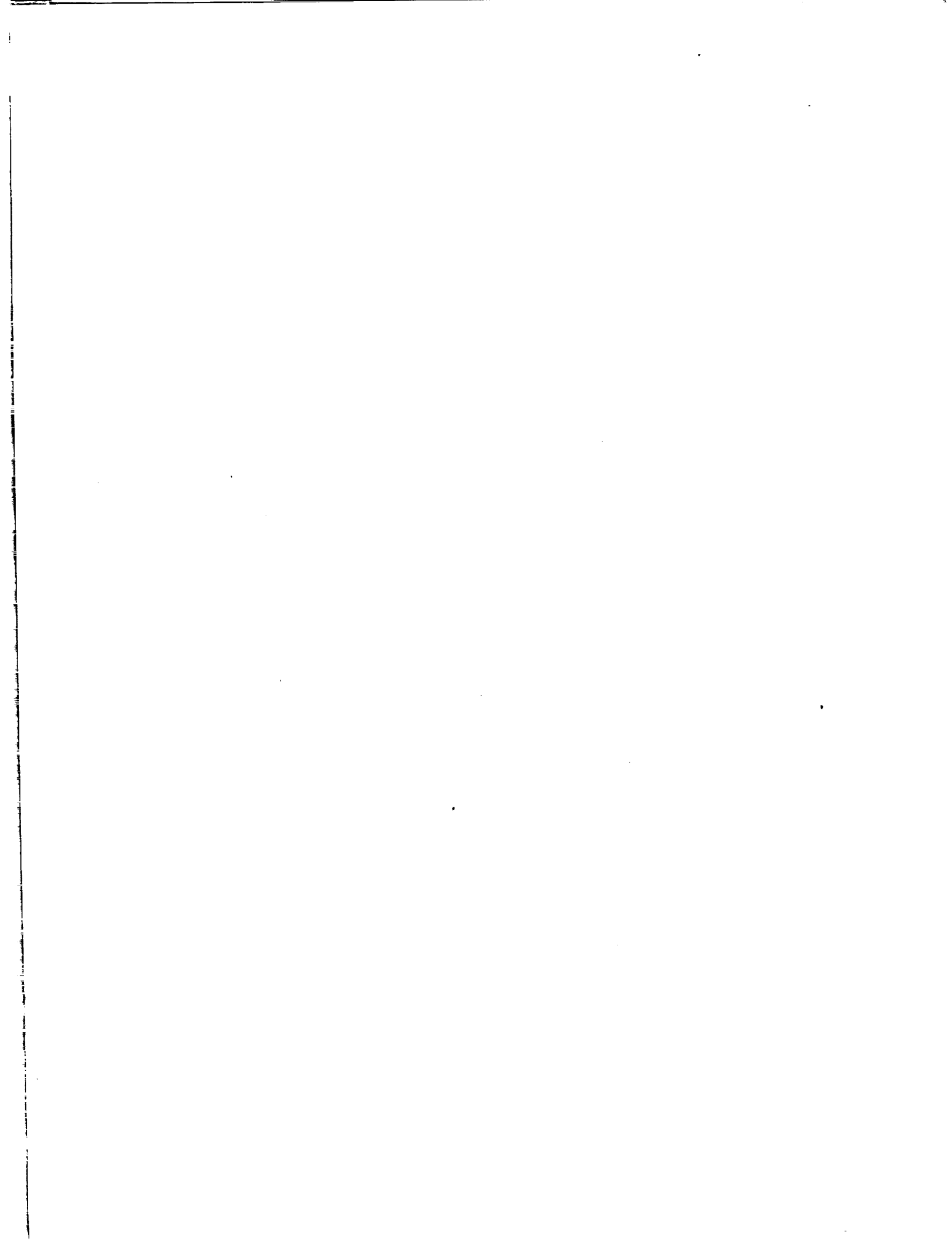


Figure 36. Trailing-edge pressure coefficient measured on EA-6B wing fuselage at  $M_\infty = 0.900$ . Solid symbols correspond to pressure distribution comparisons at similar lift coefficients.

REPORT DOCUMENTATION PAGE			Form Approved OMB No. 0704-0188
<p>Public reporting burden for this collection of information is estimated to average 1 hour per response, including the time for reviewing instructions, searching existing data sources, gathering and maintaining the data needed, and completing and reviewing the collection of information. Send comments regarding this burden estimate or any other aspect of this collection of information, including suggestions for reducing this burden, to Washington Headquarters Services, Directorate for Information Operations and Reports, 1215 Jefferson Davis Highway, Suite 1204, Arlington, VA 22202-4302, and to the Office of Management and Budget, Paperwork Reduction Project (0704-0188), Washington, DC 20503.</p>			
1. AGENCY USE ONLY(Leave blank)	2. REPORT DATE	3. REPORT TYPE AND DATES COVERED	
	May 1995	Technical Paper	
4. TITLE AND SUBTITLE		5. FUNDING NUMBERS	
Airfoil Modification Effects on Subsonic and Transonic Pressure Distributions and Performance for the EA-6B Airplane		WU 505-59-10-30	
6. AUTHOR(S)			
Dennis O. Allison and William G. Sewall			
7. PERFORMING ORGANIZATION NAME(S) AND ADDRESS(ES)		8. PERFORMING ORGANIZATION REPORT NUMBER	
NASA Langley Research Center Hampton, VA 23681-0001		L-17360	
9. SPONSORING/MONITORING AGENCY NAME(S) AND ADDRESS(ES)		10. SPONSORING/MONITORING AGENCY REPORT NUMBER	
National Aeronautics and Space Administration Washington, DC 20546-0001		NASA TP-3516	
11. SUPPLEMENTARY NOTES			
12a. DISTRIBUTION/AVAILABILITY STATEMENT		12b. DISTRIBUTION CODE	
Unclassified-Unlimited Subject Category 02 Availability: NASA CASI (301) 621-0390			
13. ABSTRACT (Maximum 200 words) <p>Longitudinal characteristics and wing-section pressure distributions are compared for the EA-6B airplane with and without airfoil modifications. The airfoil modifications were designed to increase low-speed maximum lift for maneuvering, while having a minimal effect on transonic performance. Section contour changes were confined to the leading-edge slat and trailing-edge flap regions of the wing. Experimental data are analyzed from tests in the Langley 16-Foot Transonic Tunnel on the baseline and two modified wing-fuselage configurations with the slats and flaps in their retracted positions. Wing modification effects on subsonic and transonic performance are seen in wing-section pressure distributions of the various configurations at similar lift coefficients. The modified-wing configurations produced maximum lift coefficients which exceeded those of the baseline configuration at low-speed Mach numbers (0.300 and 0.400). This benefit was related to the behavior of the wing upper surface leading-edge suction peak and the behavior of the trailing-edge pressure. At transonic Mach numbers (0.725 to 0.900), the wing modifications produced a somewhat stronger nose-down pitching moment, a slightly higher drag at low-lift levels, and a lower drag at higher lift levels.</p>			
14. SUBJECT TERMS		15. NUMBER OF PAGES	
Airfoil modifications; Pressure distributions; Maximum lift; Maneuver improvement; Transonic performance		84	
16. PRICE CODE			
A05			
17. SECURITY CLASSIFICATION OF REPORT	18. SECURITY CLASSIFICATION OF THIS PAGE	19. SECURITY CLASSIFICATION OF ABSTRACT	20. LIMITATION OF ABSTRACT
Unclassified	Unclassified	Unclassified	



National Aeronautics and  
Space Administration  
Langley Research Center  
Mail Code 180  
Hampton, VA 23681-0001

Official Business  
Penalty for Private Use, \$300

**BULK RATE**  
**POSTAGE & FEES PAID**  
NASA  
Permit No. G-27